NASA SP-5083

TECHNOLOGY UTILIZATION

ANALYTICAL CHEMISTRY INSTRUMENTATION

A SURVEY

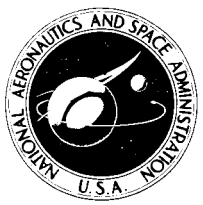

NATIONAL AERONAUTICS AND SPACE ADMINISTRATION

NASA SP-5083

ANALYTICAL CHEMISTRY INSTRUMENTATION

A SURVEY

By J. S. Whittick, R. F. Muraca,
and L. A. Cavanagh

Prepared under
NASA Contract No. NASr-49(10)

Stanford Research Institute
Menlo Park, California
August 1966

Technology Utilization Division
OFFICE OF TECHNOLOGY UTILIZATION
NATIONAL AERONAUTICS AND SPACE ADMINISTRATION
1967
Washington, D.C.

For Sale by the Superintendent of Documents,
U.S. Government Printing Office, Washington, D. C. 20402
Price 60 cents
Library of Congress Catalog Card Number 67-60025

Foreword

The National Aeronautics and Space Administration established its technology utilization program to disseminate information on technological developments "which appear to be useful for general industrial applications." From NASA research centers, NASA contractors, and other sources, space-related technology is collected and screened, and that which has potential industrial use is made generally available.

Chemical analysis is essential for the protection of people's health, the efficient use of natural resources, and the maintenance of high standards of quality in many industries. The analytical chemist's instruments are now highly sophisticated and varied. Further development of such technology has been necessary for the exploration of space. The Stanford Research Institute undertook this survey of that work for the Technology Utilization Division of NASA to help scientists, engineers, and managers in many diverse fields share the fruits of such research and development.

GEORGE J. HOWICK
Director, Technology Utilization Division
National Aeronautics and Space Administration

Contents

Introduction

Nearly all of the satellites launched by the National Aeronautics and Space Administration have carried instrumentation for making analyses of one kind or another: analyses of weather, magnetism, atmospheres, surfaces, temperatures, and radiation. The design of space instrumentation and the interpretation of the results of experiments performed in space are the prime responsibility of geophysicists, chemists, meteorologists, engineers, and other specialists. The analytical experiments performed in space are guided largely by the consensus of scientists and engineers from universities, industry, and Government agencies, as voiced by committees or in colloquia and symposia. Information relayed to Earth by satellites provides insights which lead to a better understanding of Earth and its place in the universe and to an intimate knowledge of planetary bodies and their satellites. The results of space explorations and the work necessary to accomplish them are also contributing to the technological and economic base of the United States and to the welfare of its citizens.

The purpose of this survey is to describe the work in analytical chemistry performed under the sponsorship of NASA from 1959 through 1964 and thus to identify the advances in analytical instrumentation that have come about because of the constraints space and planetary environments place on the performance of instrumentation. The survey also identifies advances that have had to be made in analytical chemistry as preparation for seeking knowledge of planetary surfaces, atmospheres, and life by means of remotely operated instrumentation. Most of this work has been reported in NASA Contractor Reports, NASA Technical Notes, technical journals, and presentations at various symposia. However, this survey is the first to collect under one cover NASA contributions which illustrate the tremendous scope and the painstaking work that is involved in making possible the performance of analytical chemistry in space or on the surface of some distant planet.

Analytical chemistry undoubtedly had its origin with the ancient Greeks and Romans who used the touchstone for assaying mixtures of gold and silver with a speed and accuracy that only recently have been

exceeded. Through the ages, refinements were first made in wet chemical techniques, then electrochemical techniques, and then electronic techniques, until we have today such complex instruments as mass spectrometers that can reveal the structure of molecules. Paradoxically, larger equipment has been developed to cope with smaller things; for example, mile-long accelerators to smash atoms and 2-ton mass spectrometers to determine how atoms are joined in molecules. Since the present state of rocketry restricts the weight and size of an experimental or analytical package, space scientists and engineers have called on their ingenuity to provide the essential characteristics of these large instruments in small packages. One of the earliest examples of such ingenuity was the development of a flyable radiofrequency mass spectrometer to determine the composition of Earth's atmosphere from sounding rockets. Of course, this type of mass spectrometer is no match for the 2-ton variety in overall versatility, capability, and performance; however, it has found a place in the instrumentation market as an analytical tool when fast response is required (as in kinetic studies) and when only low atomic and molecular masses are involved.

Instruments widely used in analytical chemistry and already developed to a high state of application and automation (e.g., the gas chromatograph) are readily miniaturized for use in space exploration. The state of the art even permits programed processing, sensing, recording, and transmitting of data on command by remote control. However, putting a sample (such as Moon dust) into a gas chromatograph when the operator may be 238 000 miles away poses problems that still need to be solved. Perhaps the solutions to some of these problems may be the forerunners of mechanized garbage-handling systems or floor cleaners for use on Earth.

Although the developments discussed in this survey are the results of work preliminary to the exploration of space, the farsighted reader will sense the relationship between many of the concepts and techniques and his own line of endeavor. The broad scope of this survey limits the amount of detail that can be reported; however, it is hoped that sufficient information is given so that the interested reader may be induced to seek amplification by consulting the referenced literature.

The first five chapters of this survey are devoted to analytical instrumentation that either uses or detects energy of various wavelengths in the electromagnetic spectrum; these are followed by chapters on mass spectroscopy and gas chromatography. Simple, single-purpose instruments, many of which are designed for use with vacuum equipment, are the subjects of following chapters, and the survey is concluded with a discussion of life-detection techniques, which are based on the application of many of the foregoing instruments.

References were obtained from a survey of NASA documents, reports, and indexes as well as from technical journals. Additional information was obtained by discussion and correspondence with personnel at NASA research centers. Further developments, of course, occurred while this survey was being made.

CHAPTER 1

Ultraviolet Spectroscopy

Ultraviolet spectroscopy in the region of 1500 to 4000 Å is widely used in analytical chemistry because it provides an insight into the molecular structure of substances and serves as a means for quantitative estimation of small amounts of specific materials or functional groups in complex mixtures. Any substance containing a group of atoms or an atomic configuration that absorbs ultraviolet light (a chromophoric group) or any substance that can be transformed into one which contains a chromophore can be detected by ultraviolet spectroscopy.

Ultraviolet spectroscopy in this region is also referred to as electronic spectroscopy because absorption at these wavelengths is a result of the elevation of an electron to an excited state from a ground state within an atom. In consequence, the chromophoric groups most amenable to detection and interpretation by ultraviolet spectroscopy are electronically resonating structures, such as are found in benzene or naphthalene compounds, ethylenic groups, and in the energetic electronic vibrations characteristic of the configuration of simple diatomic elements. The structure of planetary atmospheres as well as the nature of light emission from stellar sources and the Sun are favorite subjects for study by ultraviolet spectroscopy.

Ultraviolet light in the region of 100 to about 2000 Å is nearly completely absorbed by air; since it is customary to perform experiments in a vacuum, this region of the electromagnetic spectrum is called the vacuum ultraviolet or the far ultraviolet. Vacuum ultraviolet spectroscopy is used for the determination of the ionization potentials of gaseous molecules, the detection and location of energy centers or levels in crystal structures, etc., and it is particularly useful in geophysical and astrophysical research. Vacuum ultraviolet instrumentation has been commercially available only within the last few years.

Experiments performed by NASA in ultraviolet spectroscopy are concerned primarily with studies of energy exchange in the Earth's atmosphere and the determination of the true nature of solar radiation as detected by spectrometers carried in spacecraft. Knowledge of the nature of ultraviolet radiation in space is necessary not only for scientific pursuits but also for practical considerations such as its effect on men and spacecraft materials. NASA is also interested in the use of analytical

ultraviolet spectroscopy for determining the presence of life structures or organic substances on planetary bodies.

NASA DEVELOPMENT CONTRIBUTIONS

A wide variety of instruments, from simple colorimeters to high-resolution, double-beam, automatic-recording equipment, is commercially available. All consist of a source of radiant energy (hydrogen lamp), a monochromator to isolate narrow bands of radiant energy from the source, quartz cells or holders for the sample material, and a photocell detector to measure the transmitted or reflected light energy.

Photodetectors

Spectral response curves for typical middle-ultraviolet detectors (3000 to 2000 Å) investigated up to 1959 are shown in figure 1. A review of more recent spectrally selective ultraviolet photodetectors by Dunkelman (ref. 1) includes a description of the photoionization chambers and multiplier phototubes developed by, or for, NASA.

Several novel techniques for fabrication of photomultiplier tubes were developed at RCA Laboratories for preparation of "solar blind" photodetectors to be used in rocketborne spectrometers by Goddard Space Flight Center. Since alkali tellurides are photoemitters of high-quantum efficiency in the vacuum ultraviolet region and are insensitive to visible light, Sommer (ref. 2) used cesium telluride as the cathode. However, he found that a conductive substrate of vapor-deposited tungsten had to be used in place of the usual thin film of tin oxide in order to provide transmission in the ultraviolet. The ultraviolet-transparent lithium fluoride or calcium fluoride windows were sealed to the tube with silver chloride. To permit bakeout at 300° C, an indium-tellurium alloy bead was used for deposition of tellurium at 500° C on the window after sealoff; this relieved the problem of having to limit bakeout to 200° C because of the high vapor pressure of tellurium when a bead consisting only of tellurium was used.

The ceramic photoionization chamber developed at Goddard Space Flight Center, described by Stober, Scolnik, and Hennes (ref. 3), is now commercially available from the Geophysics Corp. of America and Melpar, Inc. The chambers were used in the 1960 and 1961 rocket experiments to survey the Northern and Southern Hemisphere skies and in 1962 in the Orbiting Solar Observatory. They are also suggested for use as reference standards for laboratory spectroscopy. Basic design suggestions for the chamber and ceramic shell are credited to J. E. Kuperian, Jr., and E. V. Serra of Goddard Space Flight Center. The ceramic shell of the chamber is fabricated of high-density alumina and is plated on the inside with several layers of metallic coatings; a surface

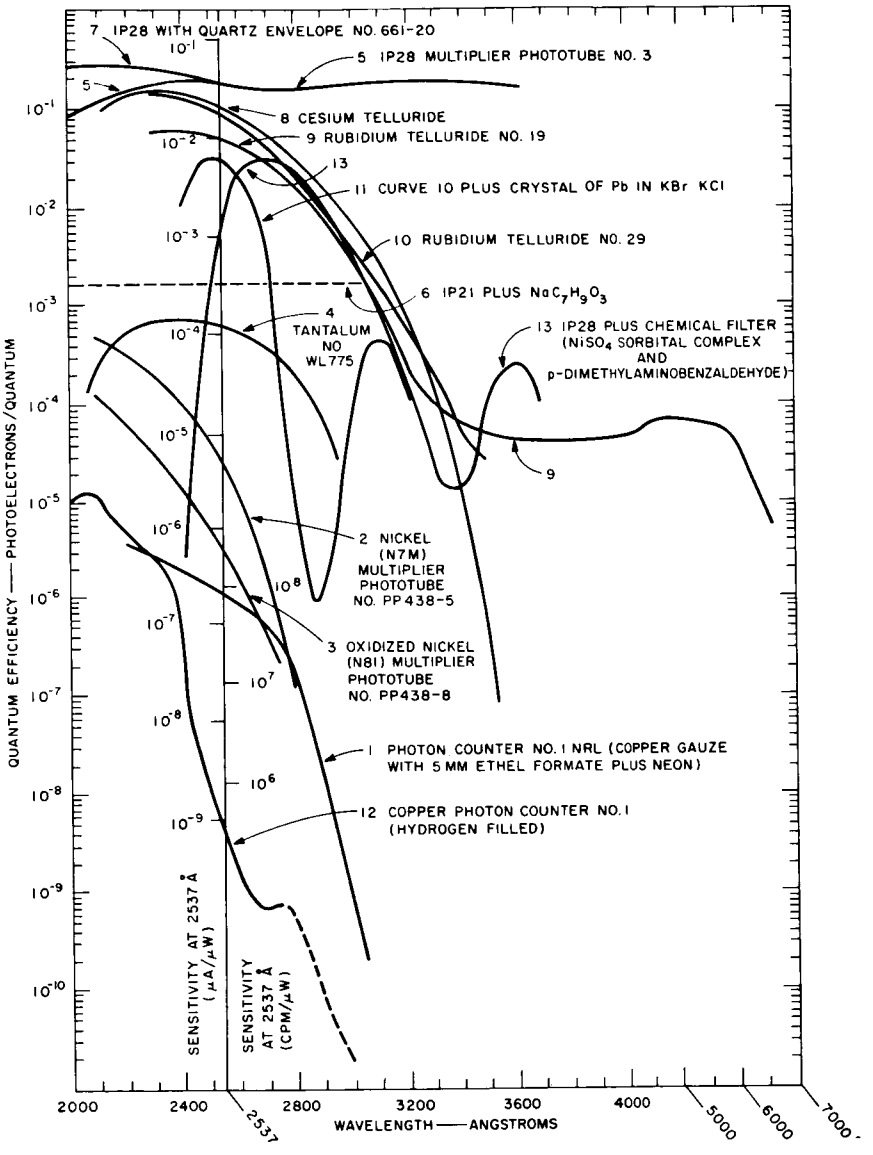

FIGURE 1.—Spectral response curves (photoelectric yield) for some typical middle-ultraviolet detectors.

layer of gold serves as one of the electrodes. The physical configuration of the photoionization chamber is shown in figure 2. The chamber window may be cleaved crystals of LiF, CaF_2, or BaF_2, 1 or 2 millimeters thick, fastened with epoxy cement to a gold-plated silver flange.

The assembled ion chamber is evacuated at 100° C at a pressure of

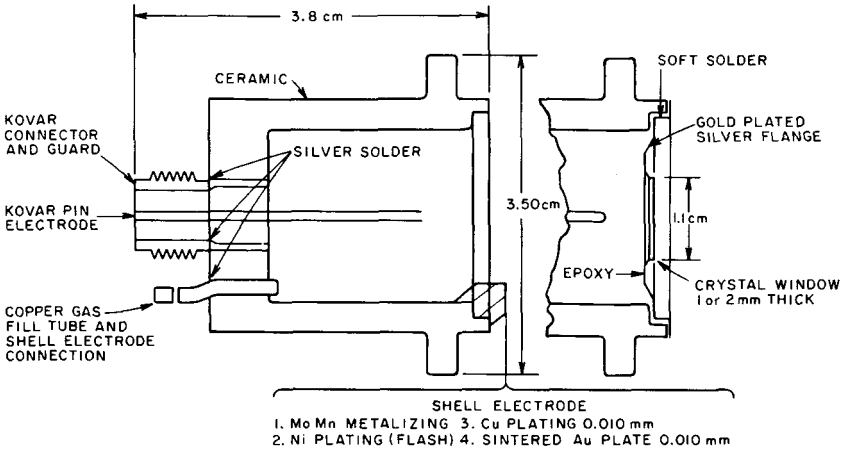

FIGURE 2.—Cross section of NASA ion chamber. The inside diameter of the chamber is 1.9 centimeters and length is 2.3 centimeters. Window materials are generally LiF, CaF_2, or BaF_2 crystals.

1×10^{-6} torr or less, and then a pure fill gas is admitted. The composition and pressure of the fill gas are dictated by the range of spectral response desired; the gas provides the long wavelength cutoff, and the windows provide the short wavelength cutoff. The characteristics of photoionization chambers used with a variety of gases and window materials are summarized in table I, and the spectral response curves of the combinations which have been used in rocket experiments are illustrated in figure 3; the spectral response curves represent smoothed values of quantum yield as measured in a McPherson 1-meter vacuum monochromator operating with a resolution of 3 to 4 Å. The measured quantum yield of any given chamber is a combination of the photoionization yield of the gas, window transmittance, absorption efficiency, and ion-collection efficiency of the chamber.

Information on the development at Goddard Space Flight Center of an ultraviolet detector (photon scintillator) that exhibits very high gain with relatively low noise has been provided by Chin (ref. 4). This detector is a 2-stage device that permits counting of individual incident photons with an overall efficiency of approximately 10 percent. The background count rate of the detector is expected to be 10 counts per second; the maximum average count rate which the detector will develop is approximately 100 000 counts per second.

The first stage of the detector is a 7-stage linear electron accelerator with a cesium iodide photocathode input and a cesium iodide crystal output. The photoelectrons formed at the cathode are field focused into a thin beam and accelerated to about 25 keV. Each of the

TABLE I.—*Typical NASA Ion Chamber Characteristics*

Fill gas	Chemical formula	Gas pressure, torr	Window material	Window thickness, mm	Spectral response region, Å	Typical quantum yields,[a] photoelectrons/photon
Diethyl sulfide	$(C_2H_5)_2S$	5	BaF_2	1	1350–1480	0.10–0.20
Nitric oxide	NO	20	CaF_2	1	1230–1350	0.20–0.30
	NO	20	LiF	1	1050–1350	0.30–0.40
Acetone	CH_3COCH_3	4.5	CaF_2	1	1230–1290	0.08–0.10
Carbon disulfide	CS_2	15	LiF	1	1050–1240	0.50–0.60
Ethylene oxide	$(CH_2)_2O$	4.5	LiF	1	1050–1180	0.10–0.20

[a] Based on an absolute photoionization yield of 0.81 ion pairs/photon for NO at Lyman-alpha.

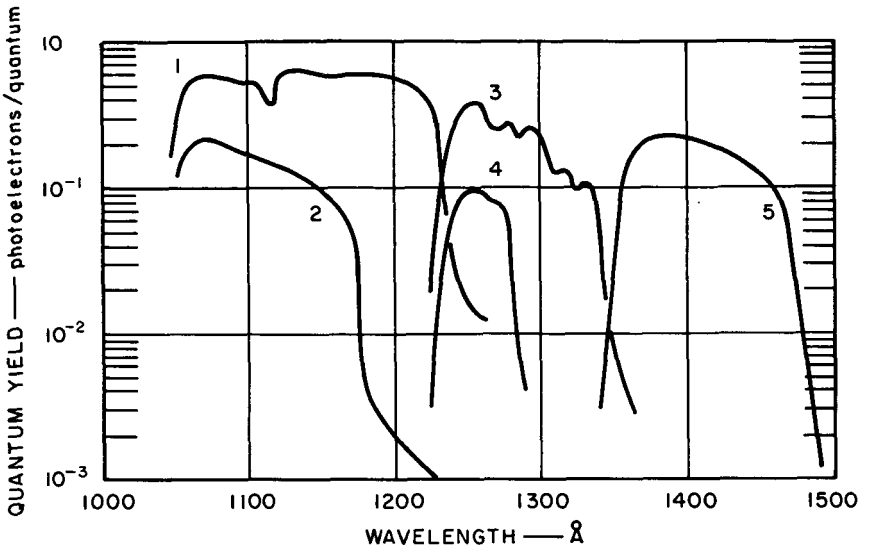

FIGURE 3.—Typical ion-chamber spectral response curves for several gas and window combinations; smoothed curves are shown, although a certain amount of fine structure is obscured: (1) carbon disulfide and LiF window; (2) ethylene oxide with LiF window; (3) nitric oxide with CaF_2 window; (4) acetone with CaF_2 window; (5) diethyl sulfide with BaF_2 window.

25-keV electrons strikes the CsI crystal, yielding a scintillation pulse of approximately 200 photons. The second stage of the detector is a 14-dynode photomultiplier which sees the pulse of photons from the first stage and develops an output charge pulse.

Ultraviolet Polarizer and Analyzer

A pile-of-plates polarizer and analyzer for use in the vacuum ultraviolet spectral region from 1200 to 1600 Å has been fabricated by Walker (ref. 5) at Goddard Space Flight Center. Both the polarizer and analyzer were constructed from cleaved LiF plates, 13 millimeters in diameter and 0.3 to 0.8 millimeter thick, and consist of identical cylinders with 3/16-inch apertures. Eight 1-millimeter slots cut at an angle of 60° to the axis of each cylinder are arranged in two opposing groups of four to give an on-axis emergent beam. Measurements with a 6-plate polarizer gave polarizations of 82 and 65 percent at 1200 and 1600 Å, respectively, with effective transmissions of 4.3 and 21.5 percent at these two wavelengths.

The polarizer has been used to study crystals of the wurtzite structure and may be applied in other solid-state work as well as in techniques of optical pumping.

Vacuum Ultraviolet Attachment

An absorptiometric attachment for a vacuum ultraviolet instrument has been designed by Axelrod (ref. 6) of Goddard Space Flight Center. This device uses the top and bottom halves of the exit slit on a McPherson monochromator to convert the single-beam instrument to double-beam operation. Absorption spectra for two samples may be measured simultaneously, or the absorbance ratio between sample and reference may be measured with the attachment shown schematically in figure 4. Sodium salicylate is used as a phosphor, since its light output is quite constant over the range of 500 to 3000 Å, but other phosphors could be employed. The light pipes are Pyrex glass, coated with vapor-deposited aluminum and sprayed with paint for durability. The output ratio of the photomultipliers (EMI 9256B operated at 940 V) remains constant as a function of wavelength with no sample in either half of the beam. Crosstalk beyond the sample holder is eliminated by the use of a baffle.

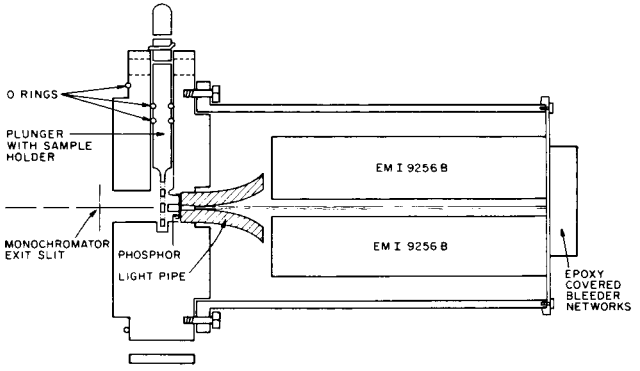

FIGURE 4.—Schematic illustration of the absorptiometric attachment.

Rocket Ultraviolet Spectrometer

Instrumentation for a rocketborne far-ultraviolet spectrometer was developed by Fastie (ref. 7) at Johns Hopkins University for measurement of the dayglow atmospheric emissions with spectral resolution of less than 2 Å. A drawing of the Ebert optical system designed for the flight spectrometer is shown in figure 5. Mechanical developments include the Ebert mirror mount, a double-slit mechanism, and a motor cam-drive assembly.

Dayglow measurements require efficient baffling of both the entrance slit and the photometers when measurements must be made at small angles with respect to the Sun, since atmospheric emissions can be as

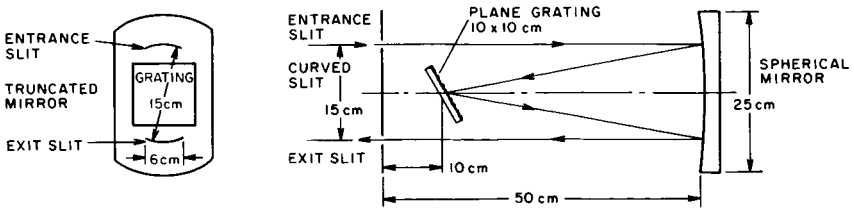

FIGURE 5.—Optical layout of flight spectrometer.

small as 10^{-9} of the total solar flux. To minimize scatter from direct sunlight, the double-angle baffles shown schematically in figure 6 were employed. The entire spectrometer assembly, including detector housing, baffles, and battery power supply, weighs 35 pounds.

Air-Density Meter

The design and fabrication of an air-density meter, based on the measurement of Rayleigh backscatter of ultraviolet light, is described by Van Ornum (ref. 8) of Plasmadyne Corp. The meter was designed to measure the air-density profile during the flight of a sounding rocket at distances up to several meters from the moving vehicle, even in daylight. This semiremote air-density measurement avoids aerodynamic disturbances caused by shock waves, boundary layer ionization, and outgassing. The ultraviolet transmitters developed for this application include an orifice spark transmitter, a pointed electrode transmitter, and a parabolic reflector transmitter. Feasibility of the instrumentation was demonstrated in F–104 flights.

Ultraviolet Microspectrophotometer

Development of a recording ultraviolet microspectrophotometer for the investigation of living cells has been underway at the University of Pittsburgh School of Medicine. As reported by Wolken (ref. 9), the third prototype of such a spectrophotometer includes a front surface mirror

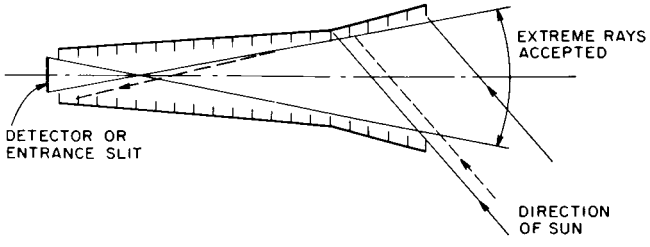

FIGURE 6.—Sketch of double-angle baffle.

that minimizes the wavelength dependency of the focusing action, and a rotating-disk light chopper which alternately passes light to the specimen and the reference; a CdS photodetector is currently used. Absorption spectra have been obtained for chlorophyll, vitamin A, aldehydes in the retinal rods of the frog's eye, screening pigments of insect eyes, and hemoglobin. (See also Appl. Optics, vol. 2, 1963, p. 899.)

NASA APPLICATIONS CONTRIBUTIONS

Life-Detection, Ultraviolet

NASA-sponsored work at Melpar, Inc., on the utility of ultraviolet spectroscopy for detecting life substances is reported by Nelson (ref. 10). Absorption in the ultraviolet region 1850 to 1950 Å (185 to 195 mμ) was studied for compounds such as bovine serum albumin, ribonuclease, phenylalanine, glycine, tyrosine, tryptophan, acetonitrile, serine, pepsin, gelatin, and extracts of local soil.

The ultraviolet absorptivities of compounds containing peptide bonds are markedly affected by changes in pH. Figure 7 shows that the absorption of alanylalanine is a function of pH. The results in figure 7 are typical of compounds containing peptide bonds, but amino acids also exhibit an absorption maximum in the 185- to 195-mμ region. The

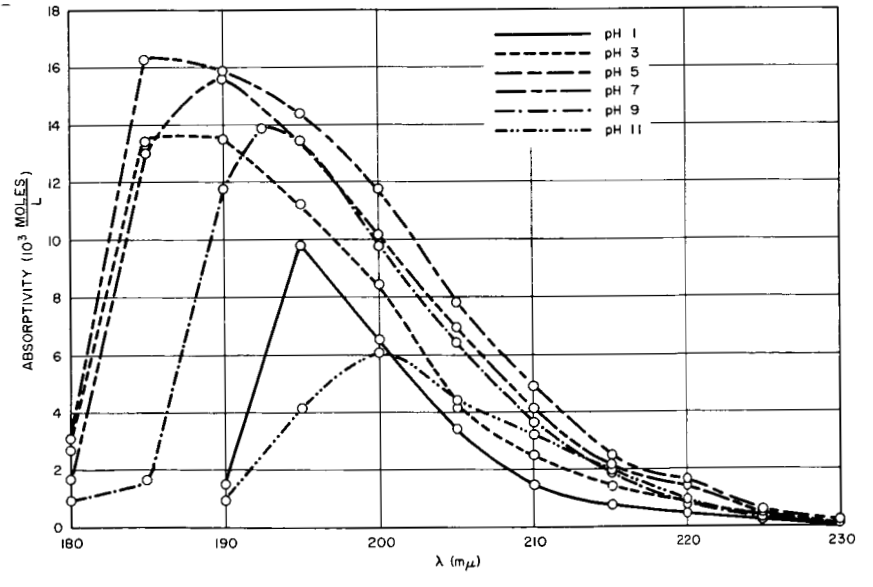

FIGURE 7.—Effect of pH on ultraviolet absorptivity of alanylalanine.

absorptivities of aliphatic amino acids, however, are reduced to zero when the pH is brought to a value of 1.0. Aromatic amino acids absorb in the ultraviolet even when the pH is reduced, as illustrated by the spectrum for phenylalanine in figure 8. Thus, adjustment of pH permits analytical distinction to be made between aliphatic and aromatic amino acids as well as peptides. Quantitative evaluation of the data shown in table II indicates that absorption per peptide bond is quite constant. Polyglutamic acid containing 600 peptide bonds has an absorptivity 600 times greater than alanylalanine or alanylglycine. Polylysine with about 85 peptide bonds has an absorptivity about 110 times that of alanylalanine.

It was found that aqueous extracts of silica, clean glass, and washed, ignited sand all have a relatively narrow absorption band at 177 to 178 mμ as shown in figure 9. The spectrum of a water extract of unwashed sand (source, Potomac River) indicated an absorption peak at 180 mμ, as shown in figure 10. Hydrolysis of the sand extract resulted in a shift of the absorption maximum to longer wavelengths with a decrease in absorbance. Similar experiments were carried out with soil extracts. The absorptions of the soil extracts were affected by hydrolysis in a manner similar to that of sand.

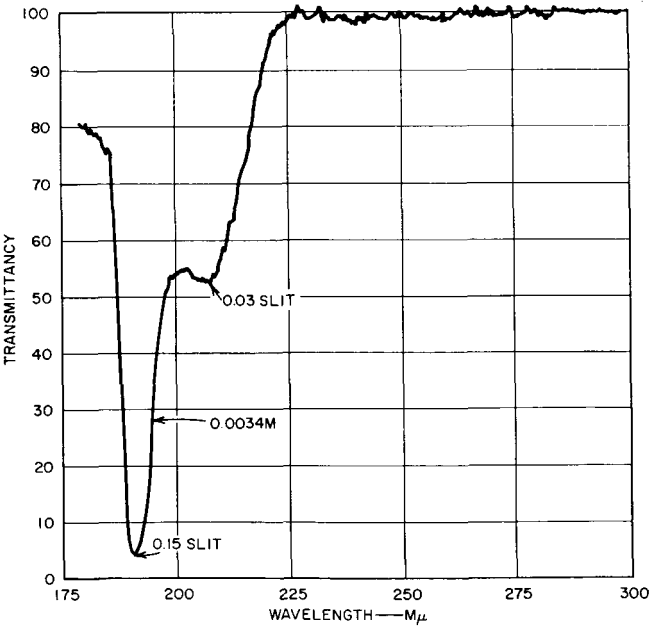

FIGURE 8.—Absorption spectrum—phenylalanine.

TABLE II.—*Absorptivity of Peptides*

Material	Absorptivity					
	pH 1	pH 3	pH 5	pH 7	pH 9	pH 11
DL-alanyl-DL-alanine	1.36×10^3 [a] 9.1×10^3	13.4×10^3	15.8×10^3 [a] 16.4×10^3	15.7×10^3	17.7×10^3 [a] 13.9×10^3	0.71×10^3 [a] 6.1×10^3
DL-alanyl-glycine	1.26×10^3 [a] 10.2×10^3	15.6×10^3	16.4×10^3 [a] 17.2×10^3	16.2×10^3	12.5×10^3 [a] 13.4×10^3	1.01×10^3 [a] 7.9×10^3
DL-alanyl-DL-leucine	2.48×10^3 [a] 17×10^3	30.4×10^3	26×10^3	24.4×10^3	20×10^3 [a] 24.4×10^3	1.21×10^3 [a] 14.4×10^3
DL-leucyl-glycyl-glycine	2.43×10^3 [a] 17.7×10^3	27.5×10^3	27.5×10^3	26×10^3	20.3×10^3 [a] 26×10^3	1.31×10^3 [a] 11.1×10^3
DL-alanyl-glycyl-glycine	1.48×10^3 [a] 15.4×10^3	26.8×10^3	24.4×10^3	23×10^3	16.5×10^3 [a] 20×10^3	1.22×10^3 [a] 9.35×10^3
Poly-L-lysine	1.66×10^5 [a] 15.5×10^5	18.4×10^5	22.4×10^5 [a] 24.2×10^5	16.5×10^5	12.5×10^5 [a] 19×10^5	0.77×10^5 10.4×10^5
Polyglutamic acid				10×10^6		
Polyglycine	[b] 2.9×10^5					
Bovine albumin	1.0×10^6 [a] 6.25×10^6	8.3×10^6	1.8×10^6	7.8×10^6	6.0×10^6 [a] 6.9×10^6	0.66×10^6 [a] 4.9×10^6

[a] Indicates peaks other than at 190 wavelength.
[b] pH was less than 1.

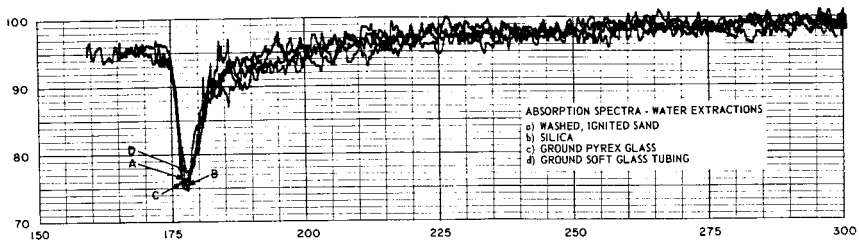

FIGURE 9.—Absorption spectra—aqueous extracts.

The results of the experiments suggest that absorption of far-ultraviolet radiation may be used to detect the presence of the peptide bond since absorption in the 185- to 190-mμ region was observed in all the dipeptides, polypeptides, and proteins that were studied, and Beer's law plots indicate that the results are due to true absorption and not to other processes, such as light scattering. A list of common compounds that would interfere by absorbing at the wavelengths of interest is given by Nelson (ref. 10). None of the interfering compounds will, when hydrolyzed by acid and heat, undergo a shift of absorbance wavelength and a corresponding decrease in absorptivity.

The lower limit of detection depends on the molar absorptivity, the solvent system, and the sensitivity of the photodetectors. Thus, substituting the molar absorptivity for a single bond (10^4 from table II) in the Beer-Lambert equation and assuming a path length of 0.1 centimeter, a peptide-link concentration of 10^{-5} mole/liter would be detectable in an instrument capable of a reliable absorbancy measurement of 0.04. Under these conditions, the minimum detectable quantity in 1.0 milliliter would be of the order of 10^{-8} mole. Based on these conclusions, equipment design is suggested by Melpar for an ultraviolet instrument to be used in the search for life on Mars.

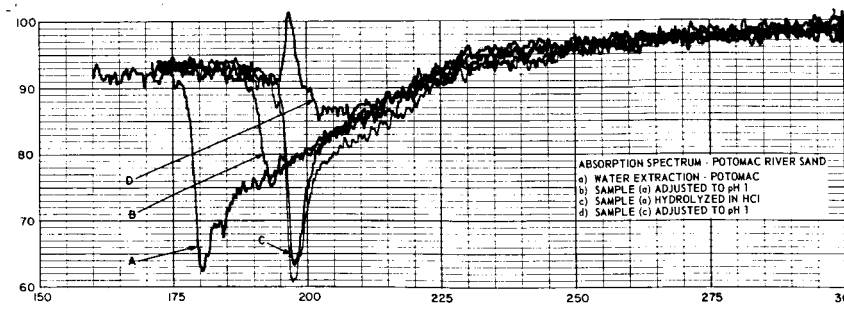

FIGURE 10.—Absorption spectrum—Potomac River sand.

Life-Detection, J-Band

Investigations on the detection of proteins, by the observation of spectral changes due to aggregation of a dibenzothiacarbocyanine dye when it is adsorbed on a macromolecular structure, are reported by Kay (ref. 11) of the Ford Motor Co., Aeronutronic Division. The aggregation of the dye molecules adsorbed on biological materials produces new species with absorption spectra having peaks at shorter wavelengths than the absorption spectrum of the simple dye molecules.

Cyanine dyes are widely used as sensitizing dyes for silver halide emulsions used in the preparation of photographic films; their behavior in solution and as adsorbed films has been studied extensively. In aqueous solutions, aggregation of the dye molecules occurs as their concentration is increased. Most cyanine dyes exhibit new bands at shorter wavelengths when aggregated than when in simpler molecular forms, but the dyes which have a planar structure develop an intense, sharp absorption maximum at longer wavelengths in concentrated aqueous solutions; the new intense absorption band is often referred to as a J-band. Absorption in the J-band appears to be due to interaction of light with large numbers of molecules in an orderly array, and Jelly (ref. 12) concluded that the dye molecules are arranged parallel to each other.

The carbocyanine dyes listed in table III were prepared as aqueous solutions and mixed with equal volumes of aqueous, 0.02 percent deoxyribonucleic acid (DNA), or 0.002 percent gelatin solutions. The absorption spectra of DNA- and gelatin-solution mixtures with dyes were determined and compared with those of the aqueous solutions of the dyes. Dye No. 8 formed the most intense J-band with gelatin and also exhibited the greatest changes in the presence of DNA. Since dye No. 8 appeared to interact most favorably with both DNA and gelatin, it was selected as the test dye for use in subsequent experiments; its structural formula is shown in figure 11.

In aqueous solution, the position of the dye absorption peak varied with the concentration of the dye. The wavelength of the absorption maximum continually increased as the concentration of the dye was

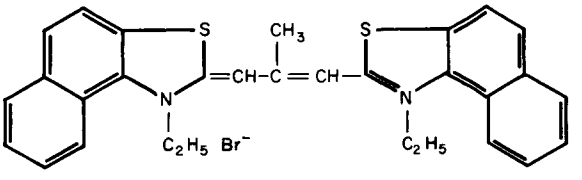

FIGURE 11.—Structural formula of dye No. 8: 3,3′diethyl,4,5-4′,5′dibenzo-9-methyl thiacarbocyanine bromide.

TABLE III.—*Carbocyanine Dyes Tested for Their Interaction with Macromolecules*

[Dilute solutions of each dye were mixed with equal volumes of 0.02 percent DNA, 0.002 percent gelatin, or water, and the absorption spectra of the solutions were determined in a 1-centimeter cell against a water blank]

No.	Dye	Concentration of dye, *M*	Absorption maxima of aqueous dye solution, plus —		
			Water, mμ	0.01 percent DNA, mμ	0.001 percent gelatin, mμ
1	3,3′diethyl-9-ethyl selenocarbocyanine iodide	1×10^{-4}	555	555	555
2	3,3′diethyl-9-ethyl thiacarbocyanine iodide	4×10^{-5}	545 505	545 505	545 505
3	3,3′diethyl-9-ethyl oxacarbocyanine iodide	1×10^{-4}	475	468 490	475
4	3,3′diethyl-9-methyl thiacarbocyanine iodide	4×10^{-5}	503 540	510 545	503 540
5	3,3′diethyl-9-methyl oxacarbocyanine iodide	1×10^{-4}	467	467	467
6	3,3′dimethyl-5,5′-dichloro-9-ethyl thiacarbocyanine chloride	4×10^{-5}	510 550	555	510 550 [a] 650
7	3,3′dimethyl,4,5-4′5′ dibenzo-8-ethyl thiacarbocyanine chloride	4×10^{-5}	506	575	510 656
8	3,3′diethyl,4,5-4′5′dibenzo-9-methyl thiacarbocyanine bromide	4×10^{-5}	510	[b] 575 [a] 535	510 650

[a] Concentration of gelatin must exceed 0.001 percent to induce peak at 650 mu.
[b] Native DNA.
[c] Denatured DNA.

decreased over the range of 1.2×10^{-4} to 5×10^{-7} M. In very dilute solutions, two absorption maxima were evident; one at 530 mμ and the other at 570 mμ. Table IV gives absorption maxima at various dye concentrations in aqueous solution. The addition of some proteins to the dye solution gave rise to the formation of new maxima in the absorption spectra of the dye. The influence of 34 proteins on the absorption spectrum of the dye is summarized in table V; figure 12 illustrates the change in the absorption spectrum of the dye by addition of poly-L-aspartic acid.

The detection of biological macromolecules by their reaction with the dye appears to be feasible. On a weight basis, proteins are far more effective than peptides in producing a significant reaction with the dye, since alterations in the absorption spectrum of the dye take place in the presence of trace amounts of these substances. On Earth, the presence of proteins, polynucleotides, and polysaccharides in the environment appears to be the unique result of the action of living organisms; the primeval form of life is believed to have been protein centered, as is current terrestrial life. Therefore, it is reasonable to base the detection of Martian and Venusian life on the presence of macromolecules which have the same characteristics. From the results of the experiments in the Aeronutronic investigation, it appears that the interaction of the

TABLE IV.—*Effect of 3,3′ Diethyl, 4, 5-4′5′ Dibenzo-9-Methyl Thiacarbocyanine Bromide on the Position of the Absorption Maximum in an Aqueous Dye Solution*

[Aqueous solutions having the indicated dye concentrations were prepared by diluting a 1.2×10^{-5} solution of the dye. The absorption spectra of these solutions were determined at 25° C, and the wavelengths of the absorption maxima were obtained by inspection of the absorption curves. Measurements were made against water in cells having path lengths of 0.1 to 10 centimeters. All solutions were buffered at pH 7.0 with 0.017 M cacodylic acid buffer]

Dye concentration, M	Absorption maximum, mμ
1.2×10^{-4}	500
8×10^{-5}	502
6×10^{-5}	505
4×10^{-5}	506
2×10^{-5}	509
1×10^{-5}	510
5×10^{-6}	527
1×10^{-6}	528 and 570
5×10^{-7}	530 and 570

TABLE V.—*New Absorption Maxima Formed by the Dye in the Presence of Trace Amounts of Protein*

[The absorption spectrum of a 2×10^{-5} *M* solution of 3,3′diethyl,4,5-4′5′dibenzo-9-methyl thiacarbocyanine bromide in the presence of 0.002 percent protein was determined using a 2×10^{-5} *M* solution of the dye as a blank. All solutions were buffered in 0.001 *M* tris-buffer, pH 8.8, and measurements were made in 1.0-centimeter cells]

Protein	Commercial source [a]	Wavelengths of new maxima, mμ
Ribonuclease, oxidized, bovine pancreas	Mann	650
Oxytocin, pituitary (heterogeneous sources)	Calbio	620
Fibrinogen, bovine [b]	NBCo.	643, 600
Urease, jack bean meal [b]	Calbio	626, 570
Alpha globulin, bovine fraction IV	NBCo.	650, 570
Beta globulin, bovine fraction III	NBCo.	650, 570
Acetylcholine esterase, bovine erythrocytes	Mann	637, 570
Carbonic anhydrase	Calbio	642, 580
Casein	Calbio	646, 560
Plasminogen, bovine fraction III	NBCo.	642, 570
Gelatin	Knox	650, 580
Pepsin, swine gastric mucosa	Worth	615, 559
Pepsinogen, swine gastric mucosa	Worth	620, 558, 480
Alpha lipoprotein, bovine	Calbio	637, 570, 480
Beta lipoprotein, bovine fraction III-O	Calbio	630, 560, 480
Beta lactoglobulin, bovine	NBCo.	646, 560, 480
Myoglobin, horse heart	NBCo.	640, 600, 570
Glycoprotein, bovine fraction VI	NBCo.	650, 600, 570
Deoxyribonuclease, bovine pancreas	Calbio	650, 600, 570, 450
Cellulase, fungal [b]	Calbio	600, 570
Pectinase, fungal [b]	Calbio	600, 570
Follicle stimulating hormone, porcine	Calbio	600, 570
Beta glucuronidase, bovine liver	Mann	600, 556
Glutenin [b]	NBCo.	600, 570
Insulin, bovine pancreas [b]	Calbio	600, 555, 480
Trypsin, bovine pancreas [b]	Worth	570
Albumin, bovine	NBCo.	480
Albumin, human fraction V	Calbio	480
Albumin, egg [b]	NBCo.	480
Alpha chymotrypsin, bovine pancreas	Worth	480
Hemoglobin, human	NBCo.	480
Somatotrophic hormone, porcine	Calbio	480
Ribonuclease, native, bovine pancreas	Mann	None
Carboxypeptidase, pancreas	Calbio	None

[a] Abbreviations used in the table are as follows: Mann, Mann Research Laboratories, Inc.; Calbio, California Corp. for Biochemical Research; NBCo., Nutritional Biochemicals Corp.; Worth, Worthington Biochemical Corp.

[b] Solutions were saturated and contained considerably less than 0.012 percent protein.

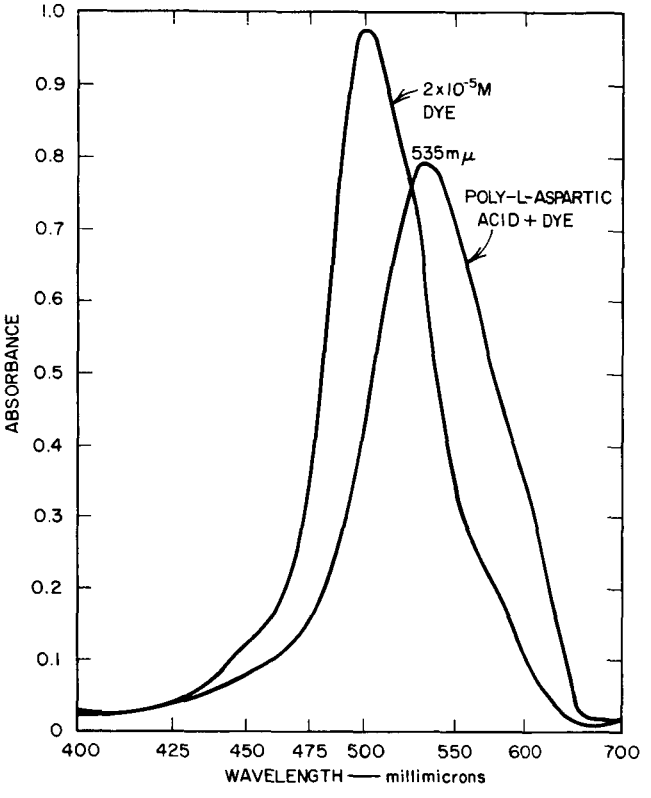

FIGURE 12.—Effect of poly-L-aspartic acid on the absorption spectrum of the dye. The dye was 2×10^{-5} *M* and the poly-L-aspartic acid, 0.0002 percent. The mixture was buffered at pH 7.0 in a 0.017-centimeter cell against a water blank. The aqueous dye spectrum is shown for comparison.

dye 3,3′diethyl,4,5-4′,5′dibenzo-9-methyl thiacarbocyanine bromide with proteins, polynucleotides, and substituted polysaccharides can provide a means for the detection of a large number of these substances in trace amounts. The minimum detectable macromolecule concentration is of the order of 0.0005 to 0.00005 percent, depending on the macromolecule tested. There appear to be no environmental factors that will seriously handicap the use of the dye; the deleterious effects of high temperature, exposure to high light intensity, and large changes in pH can be avoided.

CHAPTER 2

Infrared Spectroscopy

The extensive work of W. W. Coblentz about 1905 in the field of infrared spectroscopy was attractive to many workers when he published his studies of the infrared absorption spectra of organic liquids as well as the infrared absorption and reflectance spectra of inorganic materials. However, infrared spectrophotometers did not become commercially available until 1945, at which time they were adopted widely for chemical analysis, particularly for the determination of the molecular structure of compounds and the identification of unknown materials by matching reference "infrared fingerprints." Commercial instruments were developed in response to the needs of petroleum refineries and the synthetic-rubber industries during World War II.

Infrared spectrophotometers are routinely used for the absorptiometric determination of impurities, quantitative estimations, determination of reflectance, and automatic process control. Infrared spectroscopes are used to detect infrared radiation; their uses include measuring temperature, tracking missiles, and detecting malfunctioning organs in the human body.

The infrared range of typical laboratory instruments is generally from 2 to 15 μ (NaCl optics); prism interchanges of potassium bromide have extended the region to 25 μ, and, more recently, grating instruments that permit study in the far infrared, i.e., to 300 or 400 μ, have become available. An analytical infrared instrument consists of five basic components:

(1) A source of infrared, such as the Globar (a bonded silicon carbide rod) or the Nernst glower (a bonded mixture of rare earths in rod form), heated to 1000° to 1200° K by passage of an electric current.

(2) An infrared energy disperser which may be a prism or a grating. Selection of prisms or gratings is made according to the desired resolution and range of transmission. Combinations of prisms and gratings are also available (double monochromator).

(3) An infrared detector, generally a thermocouple (bolometer), photoconductive cell, Golay detector, or thermistor.

(4) An amplifier for the small signals which arise from the various detectors, often preceded by a preamplifier.

(5) A scanning and beam-splitting system to provide smooth transition across the wavelength range and to permit double-beam operation.

Infrared spectroscopy has played a prominent role in the NASA program for analyses requiring use of infrared sources (monitoring of gases in life-support systems) as well as for analyses requiring detection of infrared radiation (temperature of planets). Thus, it is not surprising that NASA will sponsor additional work on extending the state of the art of infrared spectroscopy for increased utility in space exploration.

NASA DEVELOPMENT CONTRIBUTIONS

Infrared Detectors

A theoretical study by Hanel (ref. 13) at Goddard Space Flight Center indicated the advantages to be gained in the detection of infrared radiation by using certain ferroelectric materials that show a drastic change of dielectric constant with temperature. Hanel proposed the design of a dielectric bolometer, and his computations indicated that such bolometers should have very low noise levels and should approach the ultimate sensitivity of thermal detectors currently in use. Experimental measurements later demonstrated the feasibility of this concept.

The dielectric material useful for such bolometers must have high mechanical strength (to permit cutting small, thin sections), chemical stability, and a large temperature coefficient of dielectric constant at ambient temperature. Rochelle salt exhibits drastic variations in dielectric constant in the range of $-18°$ to $+25°$ C, but it is not stable enough for use in bolometers. Consideration of various ferroelectric materials led to the selection of barium titanate which has excellent mechanical properties but a curie point at $+120°$ C; however, it was found that additions of strontium titanate permitted alteration of the curie point to room temperature or below.

In the dielectric bolometer, Johnson noise, caused by velocity fluctuations of electrons in the conduction band, is negligible compared with thermal noise, and current noise is absent in this type of detector circuit. Other sources of noise, such as flicker noise in the amplifier, shot noise in tubes, and generator noise, can be curtailed by proper circuit design. The possible interferences of dielectric noise may require the use of antiferromagnetic materials.

Another concept for a radiometer, also described by Hanel (ref. 14), uses coated thermistors mounted in highly reflective cones as detectors. As a low-resolution unchopped radiometer, such a detector would have a wide-angle field of view and would permit simultaneous measurement of both a blackbody temperature and the albedo of Earth and other planets.

Flight Spectrometer

A joint effort (to which Kaplan (ref. 15) contributed) by the U.S. Weather Bureau and the Barnes Engineering Co. led to the design and construction of a laboratory model of a satellite-borne infrared spectrometer which could provide information on the vertical temperature structure of the atmosphere from measurements of infrared radiation in narrow spectral intervals. The instrument as finally constructed permits measurements in four carbon dioxide-band intervals to allow inference of temperatures between 1- and 500-millibar levels; surface temperatures were deduced from measurements at an interval near 11.1 μ. As described by Dreyfus and Hilleary (ref. 16), optical and sensor design and assembly of the instrument were performed at Barnes, while the Weather Bureau provided counsel on the atmospheric radiation and instrument problems posed by Kaplan's experiment.

The field of view of the spectrometer corresponds to a square on Earth of about 120 miles on a side as seen from a satellite at a distance of about 600 miles. Spectral intensities of 25 to 180 ergs/sec-cm^2-sr-cm^{-1} are expected to be measured as well as changes as small as ¼ erg/sec-cm^2-

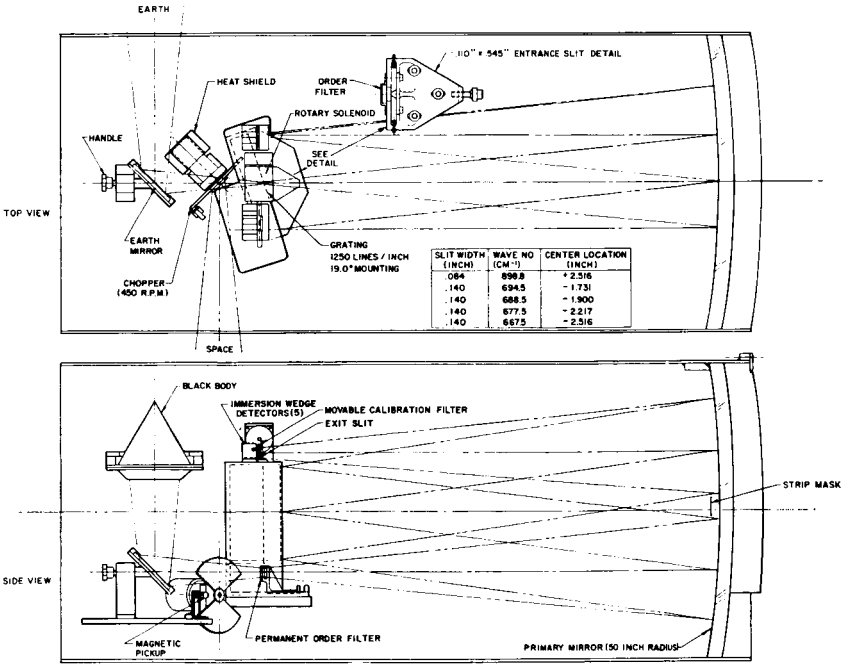

FIGURE 13.—Layout of satellite meteorological spectrometer.

sr-cm^{-1} with a response to changes with a 6-second time constant as the satellite travels at 4 miles a second. A 25-inch focal length, 16-inch-diameter spherical mirror and a 5-inch-square diffraction grating are used in a Fastie-Ebert (refs. 17 and 18) type of arrangement as shown in figure 13.

By turning the Earth mirror inward toward a built-in blackbody source in the instrument, a convenient means of intensity calibration is made available. At the same time, wavelength calibration can be checked by placing an interference filter in the beams and observing the attenuation it produces. The transmittance of the calibration filter used in the laboratory instrument is shown in figure 14, superimposed on four bandpass brackets indicating the spectral intervals used in the 15-μ carbon dioxide band.

The sensitivity of the thermistor bolometers is improved by mounting a wedge-immersed detector behind each spectrometer exit slit; the spherical lens face and optical funnel shown in figure 15 serve to minimize the size of the image of the diffraction-grating area which the immersed detector flake intercepts.

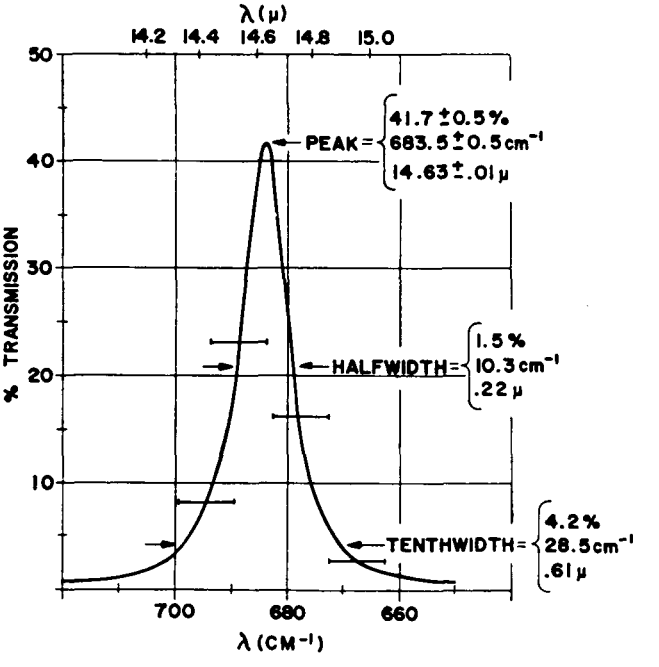

FIGURE 14.—Narrow bandpass calibration filter, No. 4648-103-1. (Drawn from infrared-7 spectrometer data taken with 0.4 cm^{-1} effective ½ intensity bandwidth.)

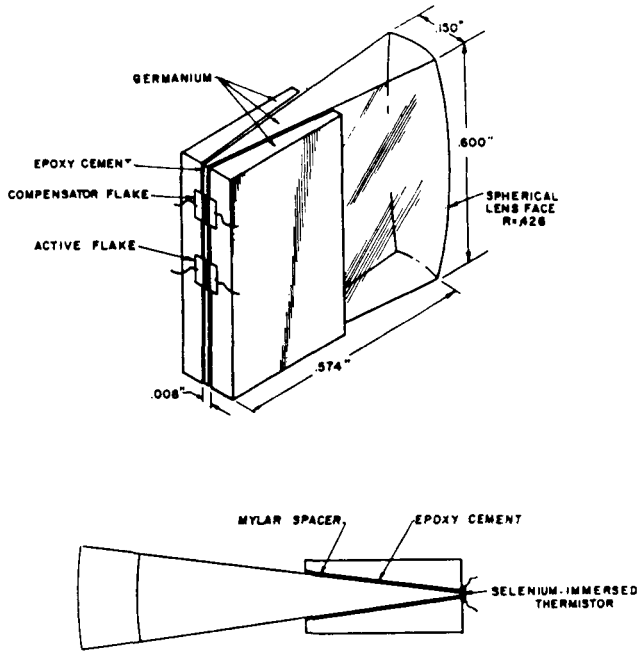

FIGURE 15.—Wedge-immersed thermistor detector construction.

Infrared Instrumentation

Westphal, Murray, and Martz (ref. 19) at the California Institute of Technology have developed an infrared telescope and photometer which will measure on Earth the emission from extraterrestrial objects in a "window" of the range of 8 to 14 μ. All mirrors in the telescope system are coated with vapor-deposited gold, which has the lowest emissivity of any common metal at the ambient temperatures employed; windows and a Fabry lens are made of barium fluoride. The working component of the photometer is a rotating chopper mounted at a 45° angle to the incoming beam. Quantum detectors of mercury-doped germanium are used because the cutoff wavelength for this detector coincides closely with the useful upper limit of the 8- to 14-μ atmospheric window and because adequate cell resistance and cell sensitivity are achieved at liquid-hydrogen temperatures rather than at the liquid-helium temperatures that are necessary for broadband infrared detectors of high sensitivity. Radiation measurements have been made of the Moon, Alpha-Orionis, and Jupiter; photographic resolution is about equivalent to a circular area of 50 kilometers in diameter at the surface of the Moon.

The design and coupling optics for a calibration monochromator for quantitative measurement of the performance of infrared spectrometers to be used in space applications were studied by Beckman Instruments, Inc., for the Jet Propulsion Laboratory (JPL). According to Henderson and Zerucha (ref. 20), the techniques for coupling optics will be applicable for use with monochromators of various optical configurations.

Submillimeter Interference Spectrometer

An experimental submillimeter interference spectrometer for providing information about the power-density spectrum of radiation from a broadband source (e.g., nightglow) has been designed and constructed for NASA at the Georgia Institute of Technology. The instrument, as described by Rivers (ref. 21), uses a wavefront-dividing interferometer and has demonstrated a resolving power of 1 part in 250 to 500 over the wavelength range of 4 millimeters to 100 μ (i.e., low microwave to far infrared); corresponding spectral resolution is about 0.01 cm^{-1}. A 15-gigacycle noise source was used for testing; output was detected with a phase-sensitive bolometer. The optical elements of the instrument include 10 flat mirrors, two 12-inch f/1 paraboloids, two 2½-inch-aperture prolate spheroidal reflectors, and waveguide feed horns. The experimental spectrometer bridges the gap between commercially available instruments in the far infrared (400 μ) and the microwave region (about 5 mm).

Fast-Scan Infrared Microscope

The design of a fast-scan infrared microscope for NASA was made possible by developments in optics, in scan systems, and in the uses of detectors at the Raytheon Co. (ref. 22). The optical system for the microscope, using a Pfund pierced mirror, was designed near the diffraction resolution limit which insures uniformity of radiance over the field at a magnification ratio of 7.62 to 1.0. To accommodate the wide range of applications for this infrared microscope, two detectors were recommended: copper-doped germanium (requiring liquid-helium cooling) for detecting the smallest spot size, and mercury-doped germanium (cooled by closed-cycle refrigeration systems) for detecting larger spot sizes.

Patent rights on behalf of NASA have been sought for the scanning system; that is, "how to move an optical field in a sawtooth pattern avoiding alternating motion and return losses." The scanning system is comprised of two flat mirrors rigidly tied together at a 90° angle; a horizontal motion of the mirrors by one unit in length produces a two-unit displacement of the outgoing ray without change in optical path. To achieve a linear scan speed from the motion of mirrors and to eliminate time loss for their return motion, two rotating wheels with heli-

coidal surfaces at the outer rims are used; the height of a single step of the surfaces equals the pitch. The two wheels rotate in synchronism and are phased to face each other at every turn. For every turn, the displacement of the reflecting surfaces passing through the axes of rotation of both wheels moves in the X direction at uniform speed and then flies back to the starting position at the end of a 360° revolution of the wheels.

NASA APPLICATIONS CONTRIBUTIONS TO ANALYSIS OF SOIL COMPOSITION BY INFRARED TECHNIQUES

An evaluation of the applications of infrared spectroscopy to the analysis of lunar and planetary soils was conducted for NASA by Lyon (ref. 23) at Stanford Research Institute. It was determined that infrared techniques can be used for distinguishing four major groups of minerals:

(1) Minerals of relatively constant chemical composition (e.g., quartz).

(2) Minerals that exhibit marked differences in composition (e.g., plagioclase feldspars and olivines, or pyroxenes and amphiboles).

(3) Minerals of constant chemical composition which differ in crystal structure (e.g., SiO_2 as quartz, cristobalite, trydimite, or coesite).

(4) Minerals which exhibit differing composition and structure (soda-plagioclase with high- and low-temperature forms, ranging from An_0 to An_{20} in composition).

The infrared spectra of the inorganic anions found in minerals are relatively simple with strong absorption peaks as shown in figure 16; the positions of the absorption peaks are summarized in table VI. A

TABLE VI.—*Position of Principal Anion Absorptions*

Group	Absorption peak	
	cm^{-1}	Microns
CO_3^{2-}	1450–1410	6.90– 7.09
	880– 800	11.36–12.50
NO_2^-	1400–1300	7.14– 7.69
	840– 800	11.90–12.50
NO_3^-	1410–1340	7.09– 7.46
	860– 800	11.63–12.50
PO_4^{3-}	1100– 950	9.09–10.53
SO_4^{2-}	1130–1080	8.85– 9.26
	680– 610	14.71–16.40
All silicates	1100– 900	9.09–11.11

strong absorption at one of the bands indicates the anion is present; weaker absorption bands elsewhere in the spectrum indicate the cation to which the anion group is bonded.

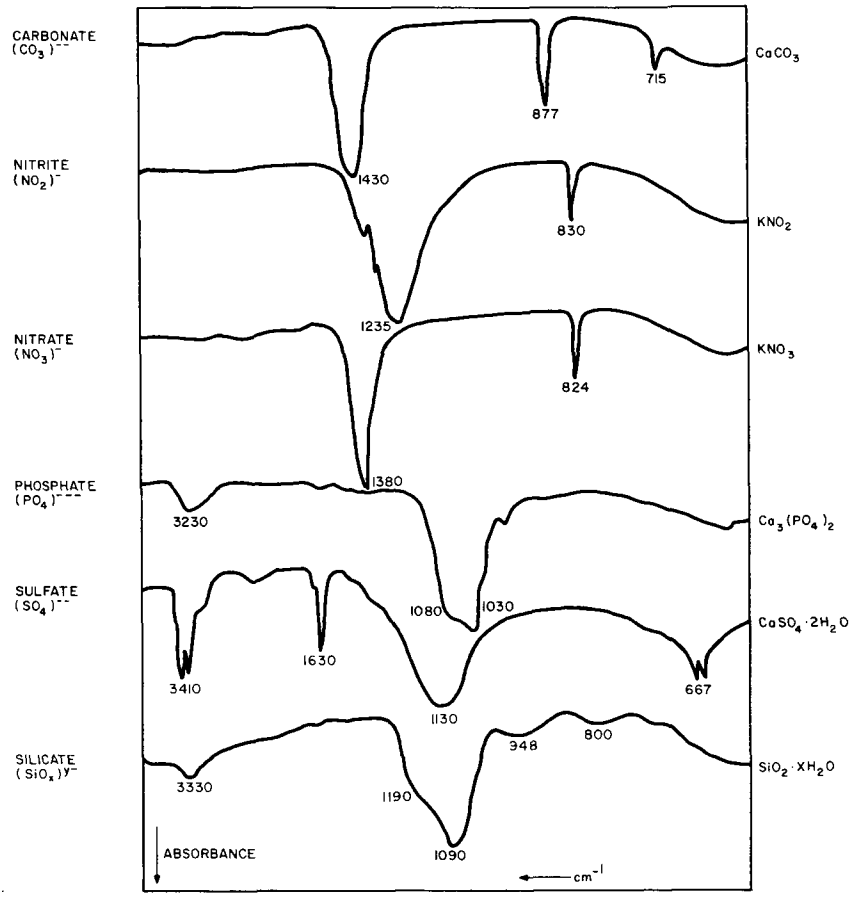

FIGURE 16.—Infrared spectra of the principal inorganic anion absorption peaks (after Miller and Wilkins, Anal. Chem., vol. 24, 1952, p. 1253).

As shown in figure 17, the spectrum of a mixture of minerals is the sum of their spectra. Figure 18 illustrates the differences in absorption strengths and peak locations created by varying the ratio of augite to olivine in a mixture. The change in infrared absorption of minerals of

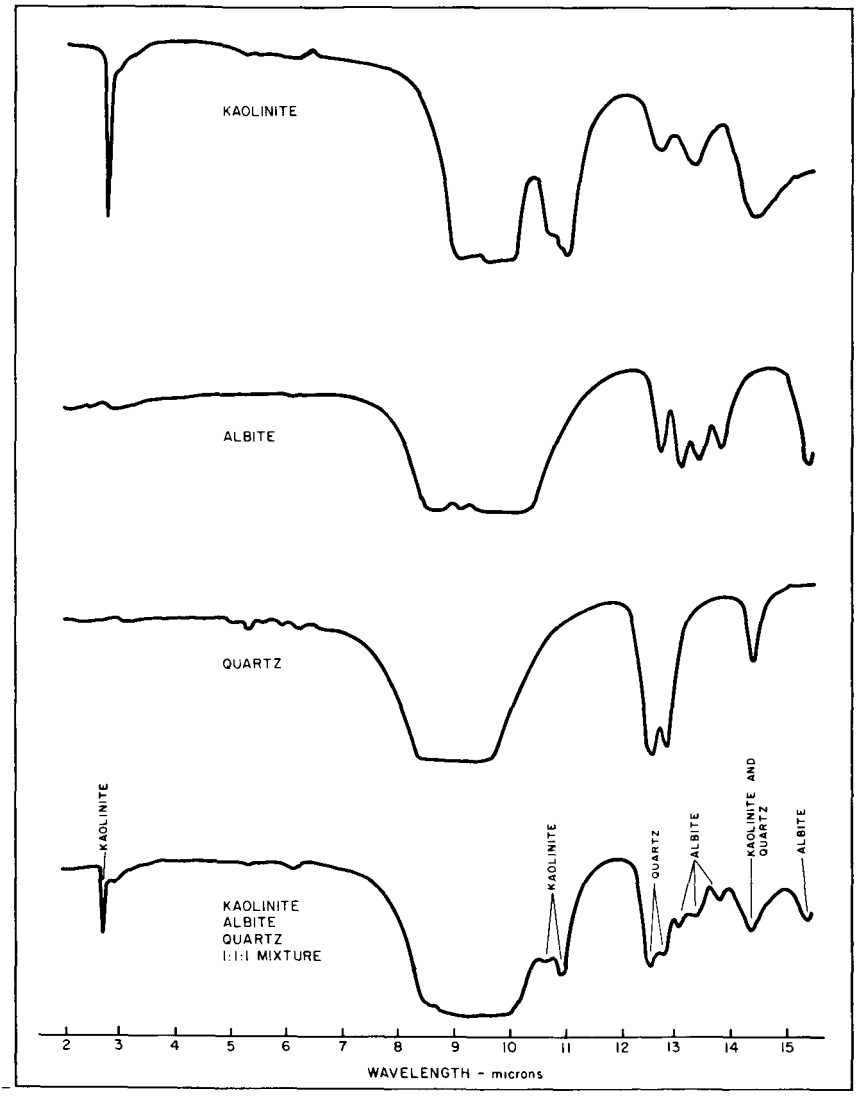

FIGURE 17.—Mineral identification in mixtures by infrared absorption analysis.

the same elemental composition but with differing structures is illustrated in figure 19 for magnesium silicates.

Most of the 370 minerals and mixtures used for the absorption spectra were powdered and pressed into potassium bromide pellets. The feasibility of using this technique for quantitative work was studied for

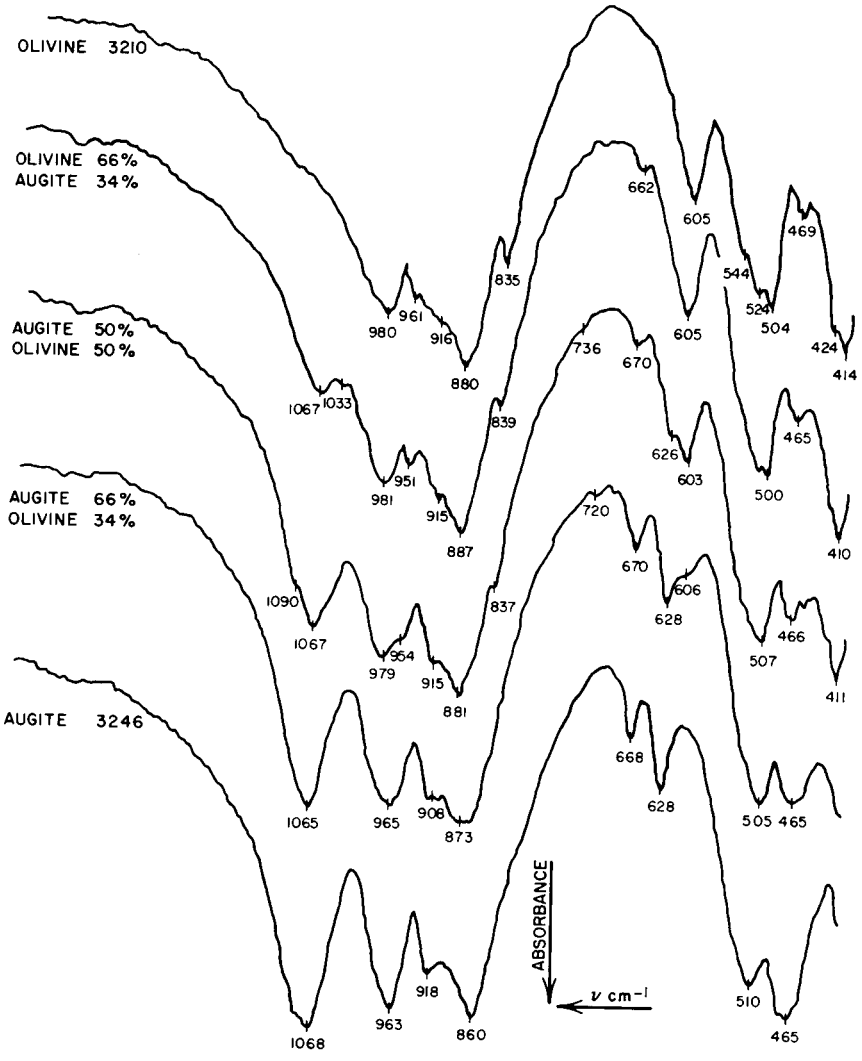

FIGURE 18.—Absorption spectra for augite and olivine mixtures.

quartz, calcite, and some clays; typical calibration curves are given in figure 20.

Infrared reflection spectra were obtained from minerals with highly polished surfaces or from mineral powders which had been formed into briquets with infrared-transparent Lucite and then polished. The reflection spectra for a series of granites are given in figure 21. As shown by

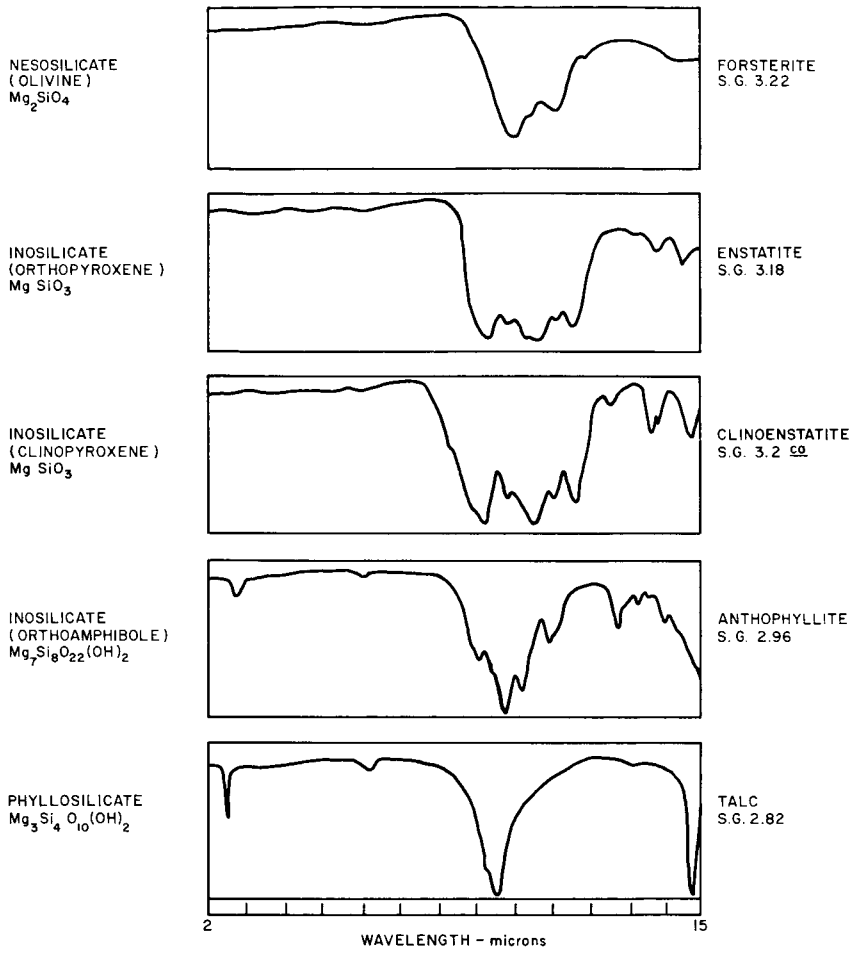

FIGURE 19.—Infrared spectra changing with structure within a single chemical group —the magnesium silicates.

a comparison of the curves in figure 22, a general similarity of curve shapes is indicated for both absorption and reflection spectra. Differences in the depths of particular peaks (e.g., the quartz doublets at 794 and 775 cm^{-1}) are probably due to differences in the mechanisms of reflection and absorption rather than to differences in the sample preparation as a pelletized powder (absorption) or a polished surface (reflection). In general, however, a mineral will have similar absorption and reflection spectra. Experimental data suggest that analysis of solar reflections must be used to determine the mineral content of surfaces

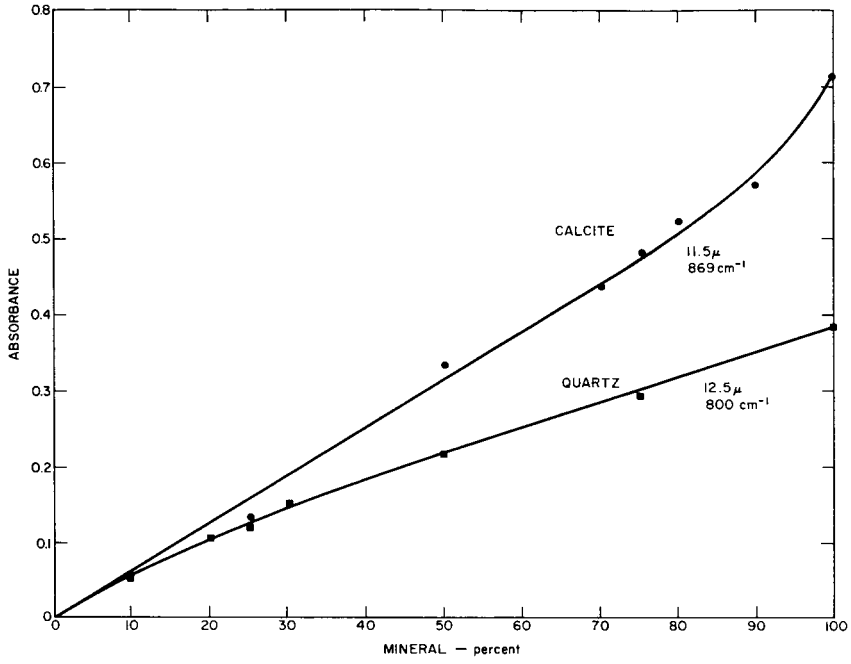

FIGURE 20.—Calibration curves obtained with mixtures of quartz and calcite for use with infrared absorption spectra.

once a catalog of reference data is established. However, the application of this method of analysis to planetary surfaces is complicated by many factors, such as the loss of spectral characteristics by multiple reflections from powdered surfaces.

A comprehensive bibliography (to 1962) of the examination of minerals by infrared spectroscopy has been prepared by Lyon (ref. 24).

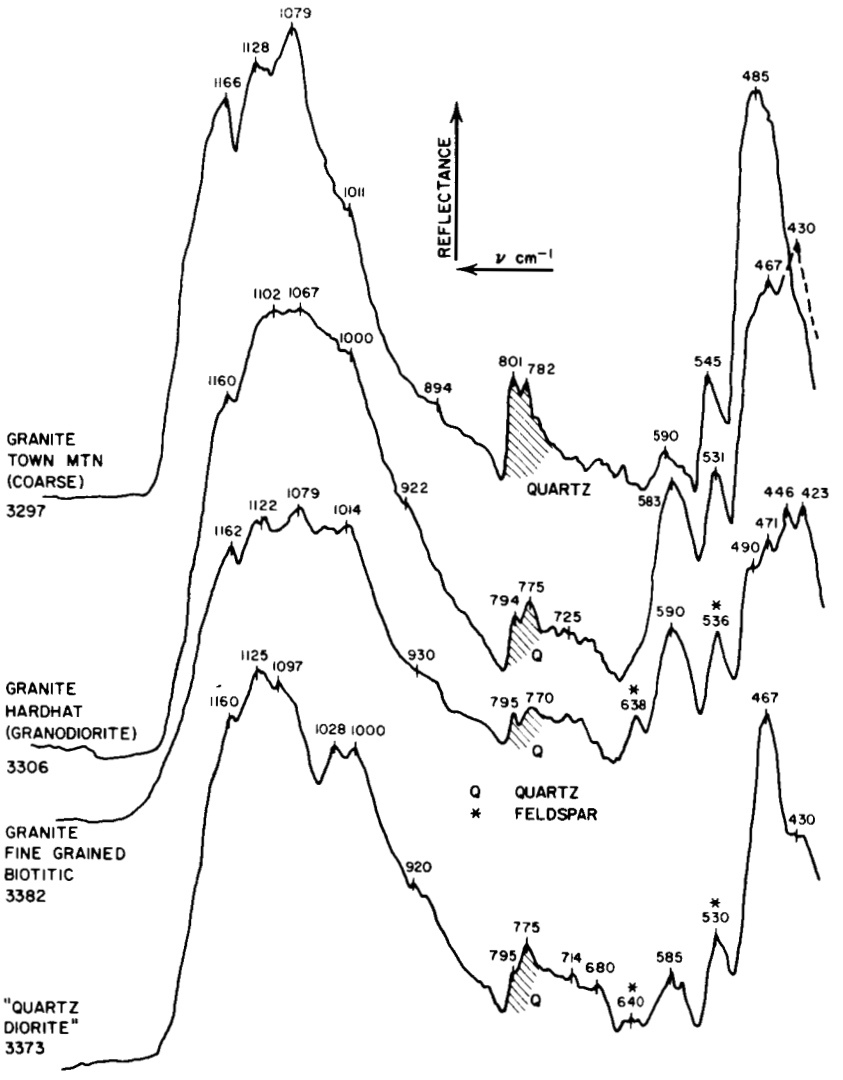

FIGURE 21.—Reflection spectra for granites. Note the quartz doublets at approximately 800 and 775 cm^{-1}.

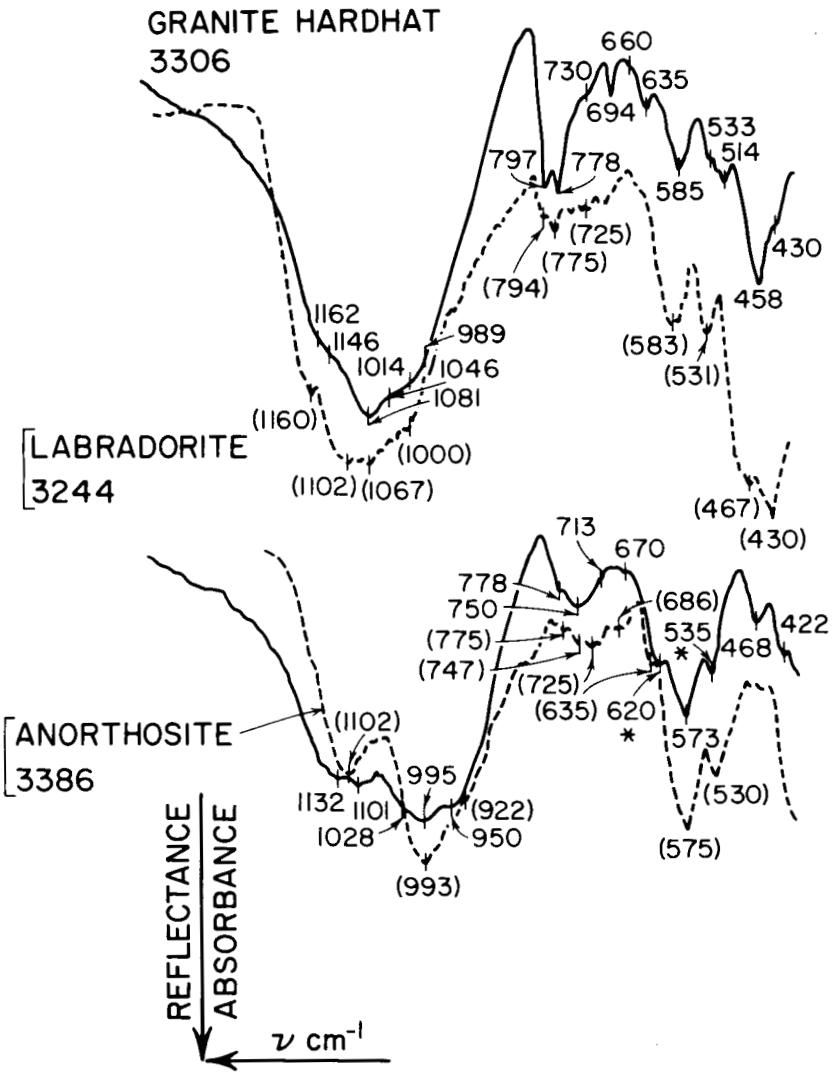

FIGURE 22.—Comparison between absorption (solid line) and reflection (dashed line) spectra for granite from the test site, Mercury, Nev., and anorthosite and labradorite. The anorthosite is from the San Gabriel Mountains, Calif. The reflection spectra have been inverted for comparison.

CHAPTER 3

X-Ray Spectrometry

X-rays were discovered in 1895 by W. Roentgen during his experiments with a Crookes tube; they are produced by the rapid deceleration of a high-velocity stream of electrons, usually by collision with a metal surface. X-rays (or gamma rays) are not deflected by electric or magnetic fields. X-rays have wavelengths from 100 to 0.1 Å, but they are often loosely classified as "hard" or "soft," depending on their penetrating power; the soft rays are of the longer wavelengths.

X-ray generators are high-vacuum devices containing an electron-emitting cathode (a tungsten filament), a heavy-metal target or anticathode (such as tungsten or copper) from which the X-rays emanate, and a window through which the X-rays pass. Since the predominant X-ray wavelength is characteristic of the element used as an anticathode (H. G. J. Moseley, 1913), X-ray emission may be used to determine the atomic numbers of elements.

The use of crystals as diffraction gratings for X-rays, suggested by W. von Laue in 1913, opened a new field of analysis of crystal structure. The diffraction of a collimated beam of X-rays passing through a crystal and falling on a photographic plate forms a characteristic circular "Laue pattern"; the diffracted X-ray flux may also be detected and measured electrically. Techniques for X-ray diffraction analysis and identification of crystalline materials were developed by P. Debye and P. Scherrer (1916) and A. W. Hull (1917). The most widely applicable technique for X-ray diffraction analysis is the rotating crystal method, but a technique using powder is more generally used for identifying materials such as nonmetals (diamond, silicon, sulfur, and iodine), metals, simple inorganic compounds (salts), and organic compounds. Other techniques for analysis involve the measurement of the X-ray fluorescence which may be given off by a material in the path of hard X-rays and the measurement of the absorption of X-rays.

X-ray instrumentation has been given primary consideration as a means for remote elemental analysis of lunar and planetary surfaces, principally because the equipment required is simple and the results are easily interpreted.

NASA DEVELOPMENT CONTRIBUTIONS

Lunar X-Ray Diffractometer

Three prototype models of an X-ray diffractometer for compositional analysis of lunar soils were designed and constructed by Philips Electronic Instruments (ref. 25) to meet JPL specifications. The diffractometer is designed to receive samples from a processor aboard the spacecraft which will compact a powdered sample into a curved specimen holder. A miniaturized 25-kV X-ray tube in the diffractometer head provides a divergent Cu $K\alpha$ X-ray beam for irradiation of the sample; the diffracted beam is detected with a side-window proportional counter.

The instrument consists of the diffractometer head, compartment B electronics, and a power supply as shown in block-diagram form in figure 23; it weighs 25 pounds, occupies a space of 0.6 ft^3, and requires 65 watts of continuous power. The compartment B electronics are logic circuitry for execution of ground commands to control the direction and speed of the goniometer drive motor and logic circuitry to generate goniometer angular position signals for telemetry. The 25-kV power supply (fig. 24) is a direct-current-to-direct-current converter which generates 25 000 Vdc, 2000 Vdc, 5-V to 7-V peak-to-peak alternating current square wave, 6 Vdc, and 28 Vdc. The anode current of 1 milliampere is regulated to 0.1 percent over the temperature range of $-50°$ to $+100°$ C at an input power supply variation of ± 5 percent.

The results of the acceptance tests for the X-ray diffractometer Models P–4/P–5 are summarized in table VII.

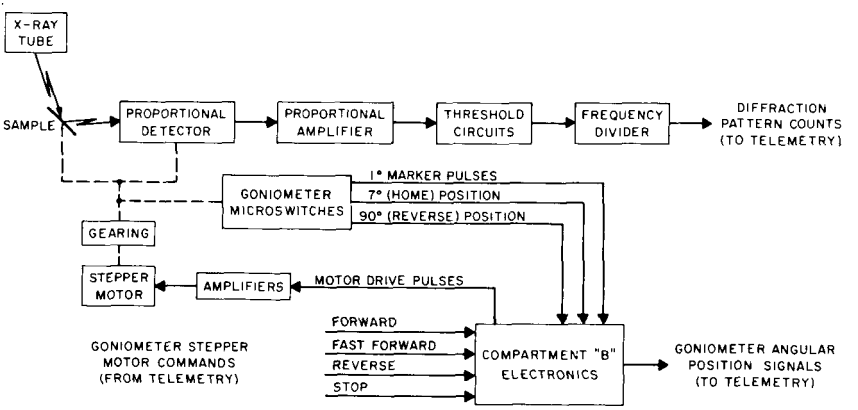

FIGURE 23.—X-ray diffractometer block diagram.

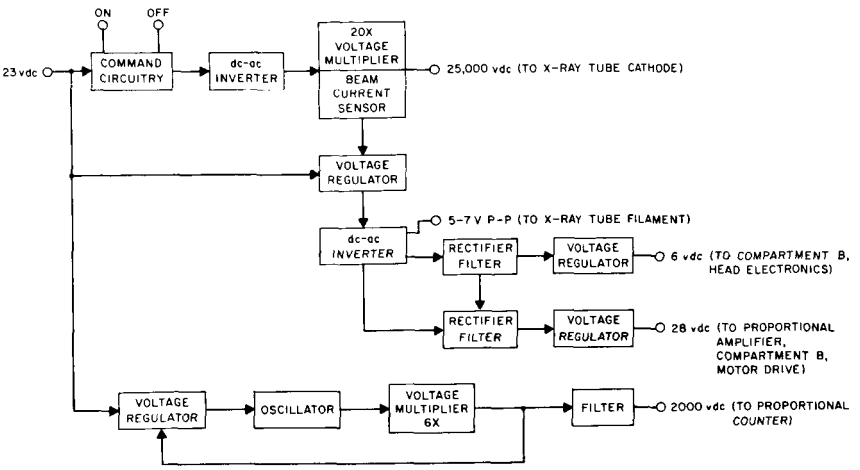

FIGURE 24.—Diffractometer power supply block diagram.

TABLE VII.—*X-Ray Diffractometer Model P–4/P–5 Typical Performance Data*

	Performance	Required
Peak intensity at 26° line of quartz	Over 4000 cps	2300 cps min
Signal-to-background	90	27
Goniometer speed accuracy, percent	0.5	1
Peak width at half height, deg	0.17	0.22 max
Symmetry	1.07	1.12
Reproducibility, deg	0.03	0.05
Maximum deviation from peak count rate, percent	2	3

Lunar X-Ray Spectrograph

Subsequent to a proposal by Philips Electronic Instruments to use X-ray fluorescence as a means of performing compositional analysis on the lunar surface, a prototype breadboard model of an X-ray spectrograph was delivered to JPL for evaluation. The instrument requires less power to generate characteristic X-rays than the operation of an X-ray tube and is based on electron-beam excitation of materials. Analyzing crystals and collimators are used as the primary means of wavelength discrimination since the resolving capability of a dispersive system is an order of magnitude greater than that of a nondispersive system consisting of a proportional counter and pulse-height analyzer. A multiple fixed-channel system is used because of its many advantages (such as simplicity, speed, and sensitivity) over a scanning system.

A schematic drawing of the breadboard X-ray spectrograph is shown in figure 25. The electron gun consists of a heated tungsten filament biased to high negative voltage, a control grid operated at 50 to 100 volts positive with respect to the filament, and an anode at ground potential. It accelerates a beam of electrons through a hole in the anode onto a sample target surface in the shape of a slightly elliptical spot.

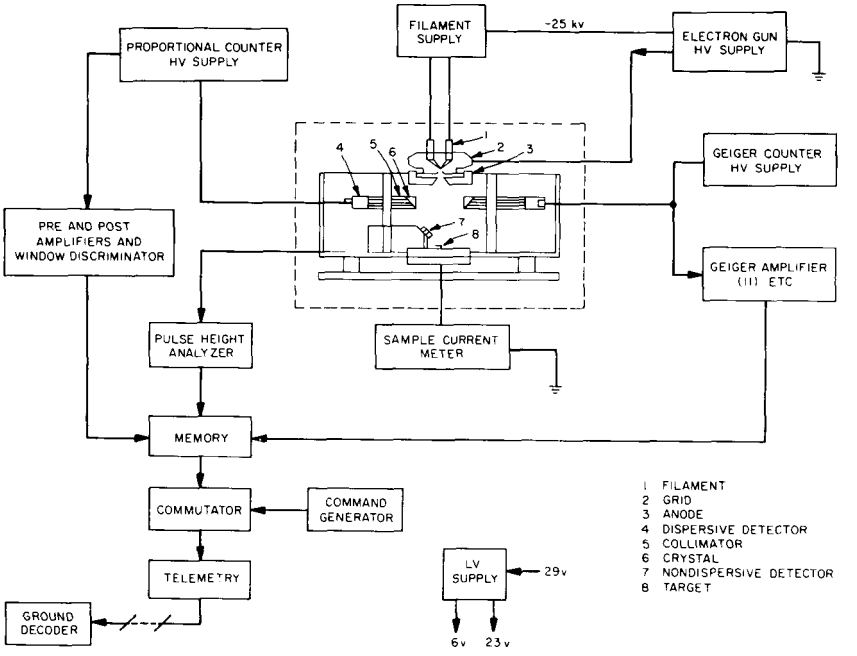

FIGURE 25.—Schematic drawing of the lunar X-ray spectrograph.

Thirteen dispersive channels, each corresponding to one of the elements summarized in table VIII, receive the fluorescent radiation from the excited sample. Each dispersive channel consists of a crystal, positioned at the reflection angle for the required wavelength; a flat blade collimator stack; and a radiation detector. A nondispersive pulse-height analyzer system provides a backup to the dispersive channels for elements of major abundance or elements not provided for in the 13 channels.

At JPL, Metzger (ref. 26) examined the use of this instrument for lunar compositional analysis from the following viewpoints: sample conductivity, sample presentation, sample heterogeneity, analytic sensi-

tivity, and interelemental effects. Analyses were performed for four mineral samples: a sulfide, a syenite, a gabbro, and a granite. Results were comparable to those obtained with a standard laboratory X-ray spectrometer.

TABLE VIII.—*Lunar X-ray Spectrograph Dispersive-Channel Capability*

Atomic number, Z	Element	Atomic number, Z	Element
11	Sodium	22	Titanium
12	Magnesium	23	Vanadium [a]
13	Aluminum	24	Chromium
14	Silicon	25	Manganese
16	Sulfur	26	Iron
19	Potassium	28	Nickel
20	Calcium		

[a] To be replaced by a chlorine channel.

Other Instrument Developments

The design and experimental testing of a nondispersive X-ray spectrometer for extraterrestrial mineral analysis is discussed by Metzger (ref. 27). The instrument employs the X-ray tube and electron gun designed by Philips (ref. 25) and includes a proportional counting system. It is designed to be compact, fast, and deployable with low power consumption. It is suggested primarily for use by astronauts or by roving planetary vehicles.

To increase the intensity of the weak X-ray fluorescence emanating from the lighter elements when irradiated by hard X-rays, Wyckoff and Davidson (ref. 28) at the University of Arizona developed a demountable, windowless X-ray tube. The demountable tube is connected to an evacuated sample housing in such a way that the sample "sees" the target through a ¼-inch aperture and the X-ray output of the sample is passed through a Mylar window into an X-ray spectrometer. Intensity and peak-to-background ratios are increased sevenfold to tenfold for a number of light elements, such as aluminum, in the mineral clevelandite. This system of X-ray analysis is particularly attractive for lunar analyses (no atmosphere) and does not have the disadvantages of contamination, sample decomposition, or disruptive accumulation of charge common to the analytical techniques for direct generation of X-rays from the sample by electron bombardment.

NASA APPLICATIONS CONTRIBUTIONS

Silicate Concentration in Rock Glasses

The linear relationship between silicon dioxide and the 2θ position of the X-ray diffraction maxima for rock glasses has been demonstrated at JPL (ref. 29). Powdered samples of 19 analyzed rocks and 5 plagioclase mineral specimens were fused and then repowdered for analysis by a standard laboratory X-ray diffractometer. As shown in figure 26, where the 2θ position of each maximum is plotted as a function of SiO_2 content, most of the points fall approximately on two straight lines representing (1) glasses with less than 16 percent Al_2O_3 and (2) high-alumina glasses of the plagioclase feldspar series. Data points for rock glasses containing more than 16 percent Al_2O_3 fall near the plagioclase curve at lower 2θ values.

The SiO_2 content of the following materials can be determined rapidly with an accuracy of ± 2.5 percent with the curves shown in figure 26: low-alumina natural glasses, such as obsidian and tektites; low-alumina rocks, by fusing the rock powder to glass; plagioclase minerals, by fusing; natural glass in volcanic rocks when the glass content is greater than 10 percent.

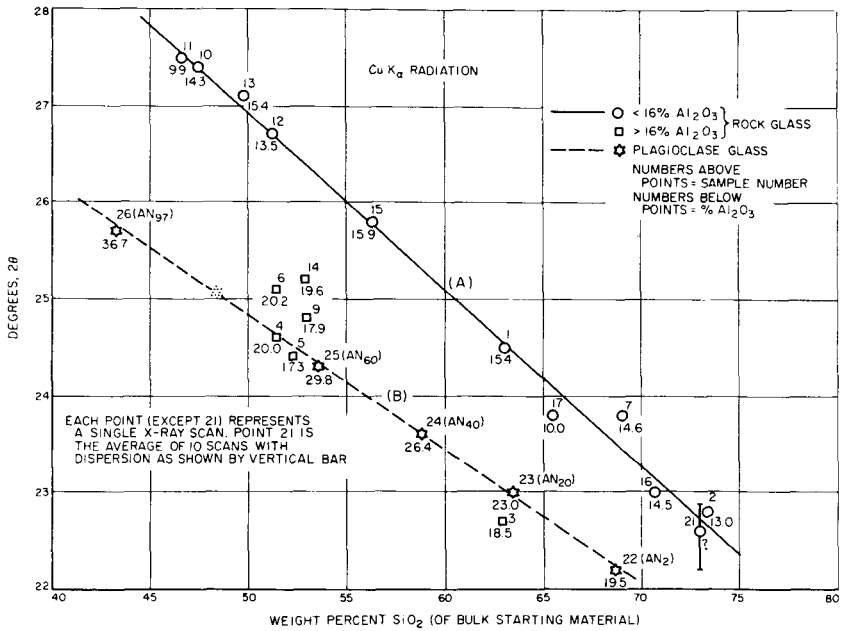

FIGURE 26.—Relation between SiO_2 content and position of diffraction maxima of synthetic and natural rock and mineral glasses.

Analysis of Proton-Irradiated Rock Powders

The results of X-ray diffraction analysis of proton-irradiated rock powders at JPL are described by Nash (ref. 30). The purpose of the analysis was to determine the effects of low-energy proton irradiation on minerals so as to evaluate the significance of the results obtained from X-ray analysis of lunar minerals which have suffered solar-wind damage.

The X-ray diffractometer patterns obtained for original material and the darkened crusts formed by 0.5-keV proton irradiation of various types of 2- to 10-particle-size rock powders such as greenstone (a basaltic mineral) and hematite (an iron oxide) showed that moderate to radical changes had occurred in both chemical and mineralogical composition as a result of the irradiation. The results of the analysis showed the extent of differential sputtering of minerals in silicate rocks and the reduction of iron oxides, but there was nothing in the patterns which indicated that irradiation had taken place; hence, it would be impossible to tell from them whether the lunar surface consists of minerals such as are formed on Earth or whether it consists of new species.

CHAPTER 4

Alpha-Particle Scattering

Alpha-particle scattering is a technique which has been investigated for use as a method of nondestructive analysis. When a material is bombarded by a collimated beam of α-particles, the particles are scattered by interaction with the atoms in the material at various angles and energies as a function of the atomic number of the target elements. The particles scattered by each element have a characteristic energy spectrum which can be detected and counted by a scintillation counter and scaled by a pulse-height analyzer; typically, the pulse-height analyzer uses 250 (energy) channels. The level of response from a sample is governed by the α-particle source strength, the fraction of the beam which is collimated, the area of the detector, the scatterer-to-detector distance, and the mean scattering angle.

One of the earliest reports of investigations with α-particle scattering for surface analysis was published by Snyder et al. (ref. 31), and the technique has been proposed for analysis of elements on the surface (depth to less than 100 μ) of rock materials, glass surfaces, and metals (ref. 32). A logical extension of the technique is the analysis of thin films (ref. 33). Ionization by α-particles has been used for the analysis of gaseous mixtures in flowing or static systems (ref. 34), including gas chromatographic effluents (ref. 35).

The rapid advances in the technology of solid-state devices and the development of techniques for particle measurement and interpretation have helped make α-particle-scattering analysis a suitable candidate for space exploration, especially since the equipment can be contained in a relatively simple, lightweight, and rugged package.

NASA DEVELOPMENT CONTRIBUTIONS

Lunar Surface Analyzer

Modification of the exceedingly bulky experimental α-particle-scattering instrumentation to a miniaturized, solid-state device for the compositional analyses of lunar and planetary materials was proposed to NASA in 1960 by Turkevich of the University of Chicago and later described in the open literature (ref. 36). Figures 27 and 28 illustrate the apparatus described by Patterson, Turkevich, and Franzgrote (ref. 37).

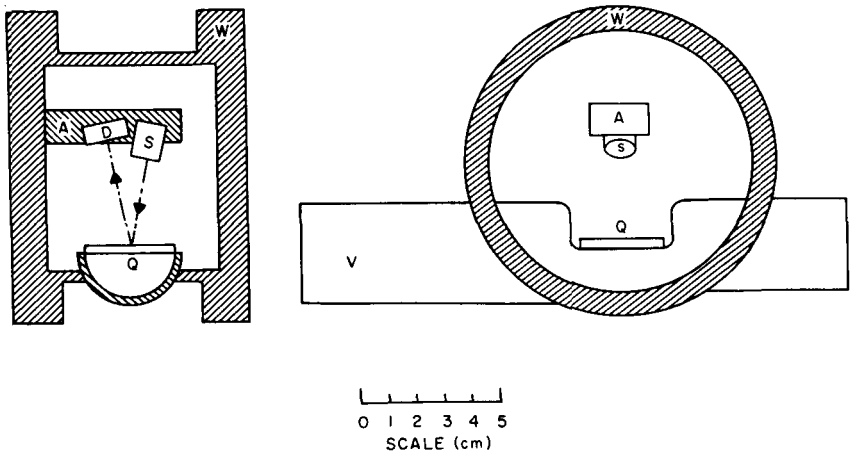

FIGURE 27.—Research apparatus used at Argonne National Laboratory and the Enrico Fermi Institute for Nuclear Studies of the University of Chicago to study α-particle scattering. Two perpendicular sections are shown. (*D*) detector housing; (*S*) source housing; (*Q*) sample position; (*W*) vacuum box; (*V*) vacuum lock for introducing samples; and (*A*) adjustable arm to control sample-to-source and detector distance.

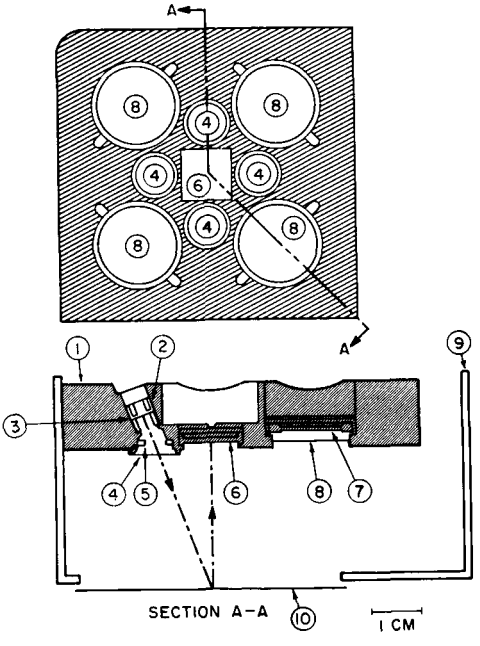

FIGURE 28.—Construction details of breadboard instrument for chemical analysis using α-particle interactions. (1) head block; (2) source holder assembly; (3) source position; (4) VYNS film for containing recoils from source; (5) source collimator; (6) detector; (7) proton detector; (8) α-particle detector; (9) instrument case; and (10) sample position. The breadboard instrument, including case and transistorized amplifiers and mixing circuit, weighs about 0.3 kilogram.

Neutron irradiated americium 241 was purified to prepare curium 242 sources ($T_{1/2} = 163$ days, $T_2 = 6.11$ MeV) which were electrodeposited onto platinum disks. (Sources were also deposited on stainless steel by evaporation.) The disks were mounted in source holders which provided collimation. Freshly prepared sources were monoenergetic, but with time, plutonium 238 was accumulated and impurities of Cm^{244} became apparent.

The detectors were made of surface-barrier silicon, and applied reverse biases were selected to give appropriate depletion layers for the detection of α-particles ($\sim$50 μ) or protons (200 to 300 μ). Transistorized charge-sensitive amplifiers were used in most of the experimental instruments, and the stability of the system was checked frequently with monochromatic sources. (Small amounts of contamination present in the instrument were used to monitor detection stability.) Detection was linear in energy response to better than 5 percent.

The data shown in figure 29, obtained from analyses of flat pieces of metal or powdered material in trays, indicate that for elements of atomic number, Z, greater than 20 the spectra are nearly rectangular and have sharp high-energy cutoffs (endpoints) which can be expressed as:

$$f(A,\theta) = \frac{T_{max}}{T_0} = \frac{\left[\frac{4\cos\theta}{A} + \left(1 - \frac{16}{A^2}\sin^2\theta\right)^{1/2}\right]^2}{(1 + 4/A)^2}$$

where

θ angle of scattering in the laboratory system
T_{max} maximum energy of the scattered α-particle
T_0 initial energy of the α-particle ($\sim$ 160° in the experiments)
A atomic mass number of the scatterer

The numerical values at 160° are not much different from those at 180° where the formula reduces to:

$$f(A, 180°) = \frac{T_{max}}{T_0} = \left(\frac{A - 4}{A + 4}\right)^2$$

For elements of low Z, the spectra show structure, but the high-energy cutoff is harder to establish. The separation of adjacent elements decreases as A increases; however, the sensitivity for elements increases with Z.

Alpha-particle-scattering spectra for materials of geochemical interest are given in figure 30. Figure 31 illustrates that above a Z of 11, the points cluster about a line of slope 3/2, which indicates a satisfactory agreement with the theoretical predictions of Rutherford scattering. For elements of atomic numbers below that of sodium, the regular be-

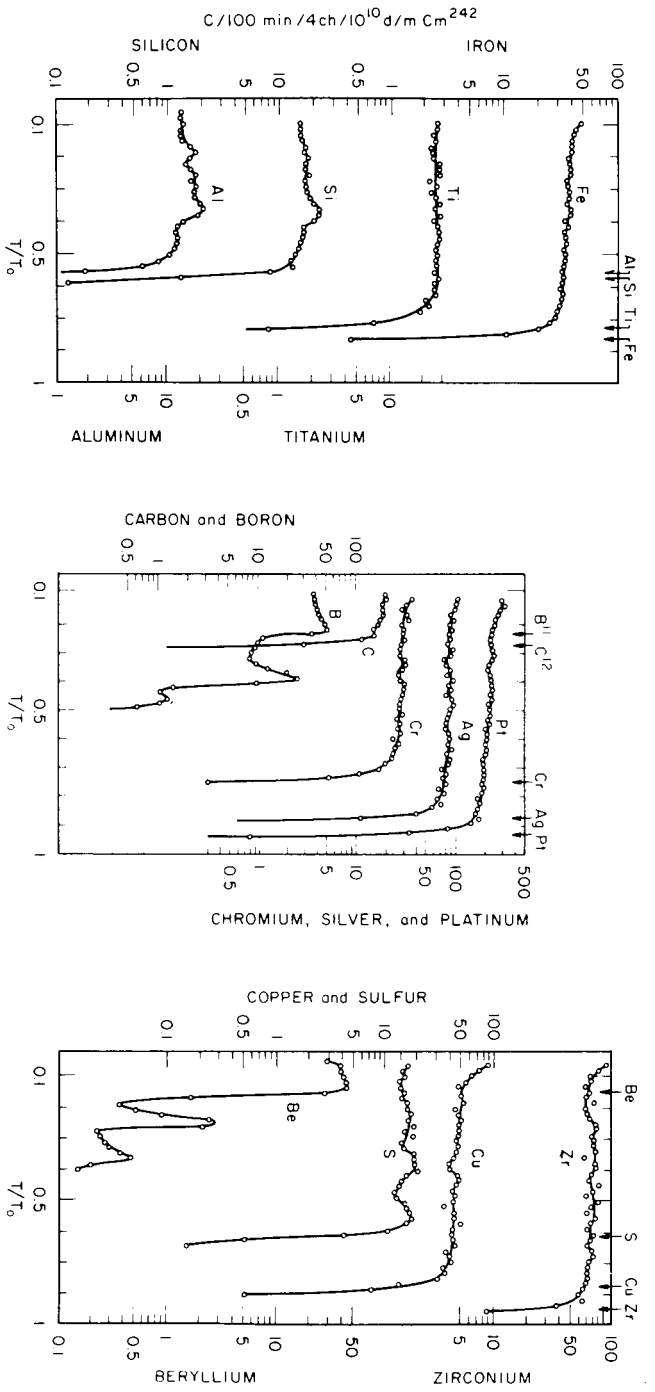

FIGURE 29.—Alpha-particle-scattering spectra from thick targets of some pure elements measured with the research apparatus. The ordinates are intensities of the scattered particles in units of counts/100 min/10^{10} d/m of Cm^{242} in the source/4 channels of the analyzer (approximately 0.02 in T/T_0). The arrows show, for each element, the predicted high-energy cutoff according to equation (1).

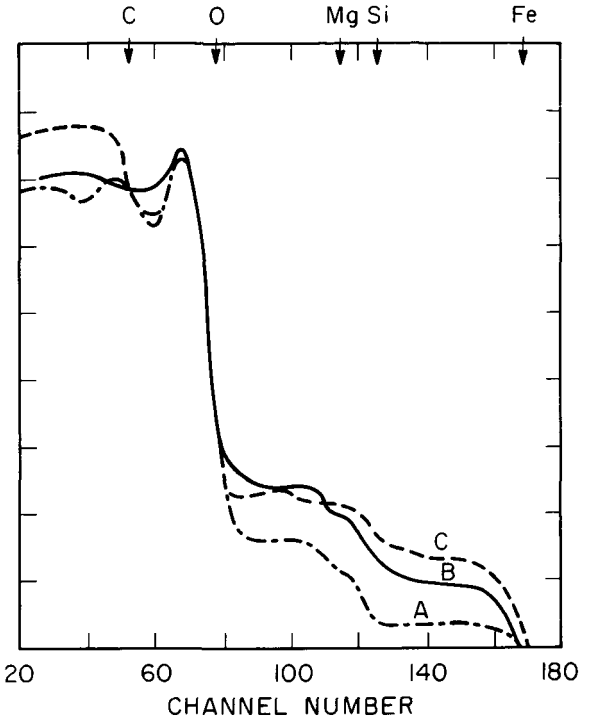

FIGURE 30.—Alpha-particle-scattering spectra from some materials of geochemical interest obtained with the research apparatus. The channel numbers are linearly related to the energy of the scattered α-particles. The ordinates are intensities on an arbitrary linear scale. Data are presented for (*A*) olivine, (*B*) bruderheim (a chondritic meteorite), and (*C*) mighei (a carbonaceous chondrite). The arrows indicate the positions of the theoretical high-energy endpoints according to equation (1) for some elements that are expected to be present.

havior disappears; the scattering intensity is much higher than predicted and varies irregularly.

Although the intensities of protons from (α, p) reactions are often much lower than those of the scattered α-particles, a detection system sensitive only to protons will enhance the sensitivity of the method for many elements. For example, the aluminum and sodium content of rocks is of geochemical interest, but the low abundances of these elements in the presence of large amounts of silicon and magnesium make the scattered α-particle spectrum an insensitive basis for their determination. Proton spectra from aluminum and sodium, however, give greater high-energy cutoffs than silicon and magnesium, and their characteristic curves provide further basis for differentiation.

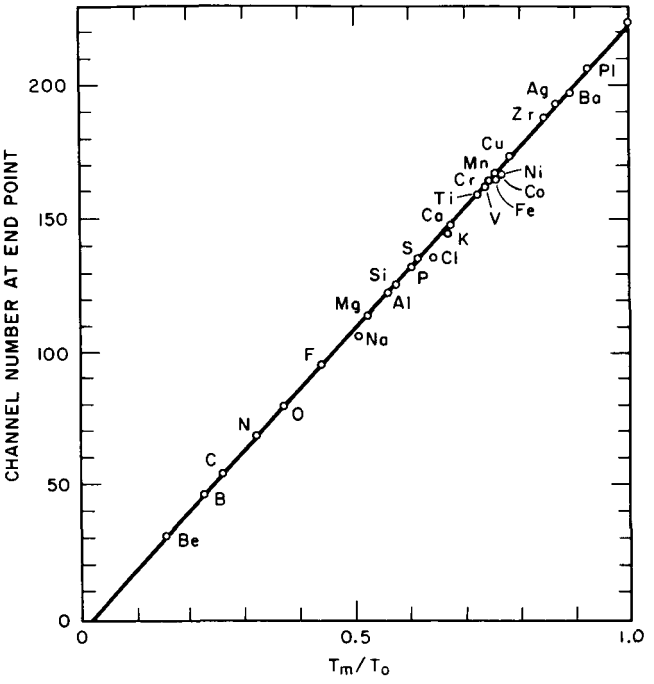

FIGURE 31.—Agreement of the observed and theoretical endpoints of various elements as obtained with the research apparatus. The straight line, drawn through $T_{max}/T_0=1$ at channel 224 (the channel of the peak energy of the incident α-particles), indicates how well the experimental endpoints agree with the predictions of equation (1). The negative intercept at $T_{max}/T_0=0$ is consistent with the positive energy threshold of the analyzer.

The α-particle-scattering spectrum for iron beyond the oxygen endpoint ($T/T_0 \leqslant 0.38$) indicates the same slope within statistical and experimental errors for metallic iron, Fe_2O_3 and Fe_3O_4. Similar comparison can be made for magnesium, aluminum, and silicon and their oxides; these spectra are illustrated in figure 32. A more severe test of the independence of the shape of the spectrum on chemical composition lies in the region of low energies. As an example, the oxygen contribution was obtained from magnesium oxide and two iron oxides by subtracting the metal contribution, assuming it was the same at low energies as beyond the oxygen endpoint. It would appear that, within statistical and instrumental drift errors, the shapes of the oxygen spectra computed from the metal-oxide spectra are the same; the procedure is illustrated in figure 33 for magnesium oxide.

The α-particle-scattering equipment described by Turkevich et al. is capable of measuring quantitatively the amount of elements present

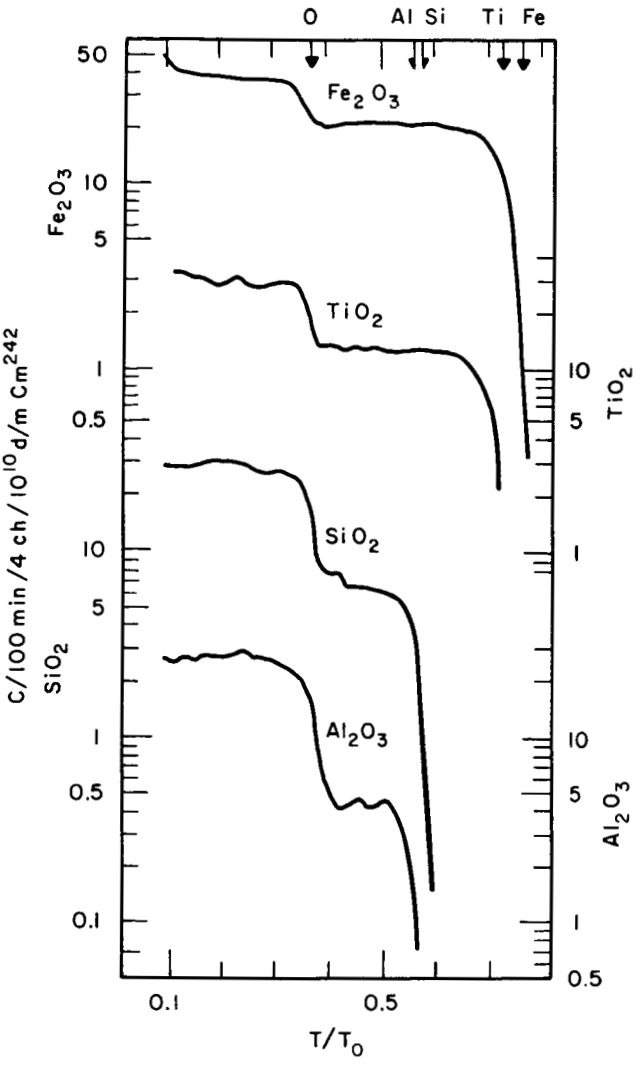

FIGURE 32.—Alpha-particle-scattering spectra for some oxides measured with the research apparatus. Data are presented for Al_2O_3, SiO_2, and Fe_2O_3. The positions of the expected high-energy endpoints according to equation (1) are indicated by arrows.

in surfaces in the atomic number range of Z=4 to 17; that is, beryllium to chlorine. The resolution is 2 Z from Z=18 (A) to 26 (Fe) and degrades progressively to Z=92 (U) where only groups of 10 Z can be resolved. The threshold sensitivity level is approximately 1 percent for most of the elements, except carbon, thorium, and uranium, where sensitivities are 0.1, 0.01, and 0.01 percent, respectively. The relative

accuracy of the analysis is approximately 1 percent of the total sample, but absolute errors of ±2 percent may result from matrix effects due to differences in densities or a variation in atomic number.

Since the analysis for elements with Z greater than 4 is automatically normalized to 100 percent (excluding Z=1 to 3), the hydrogen content

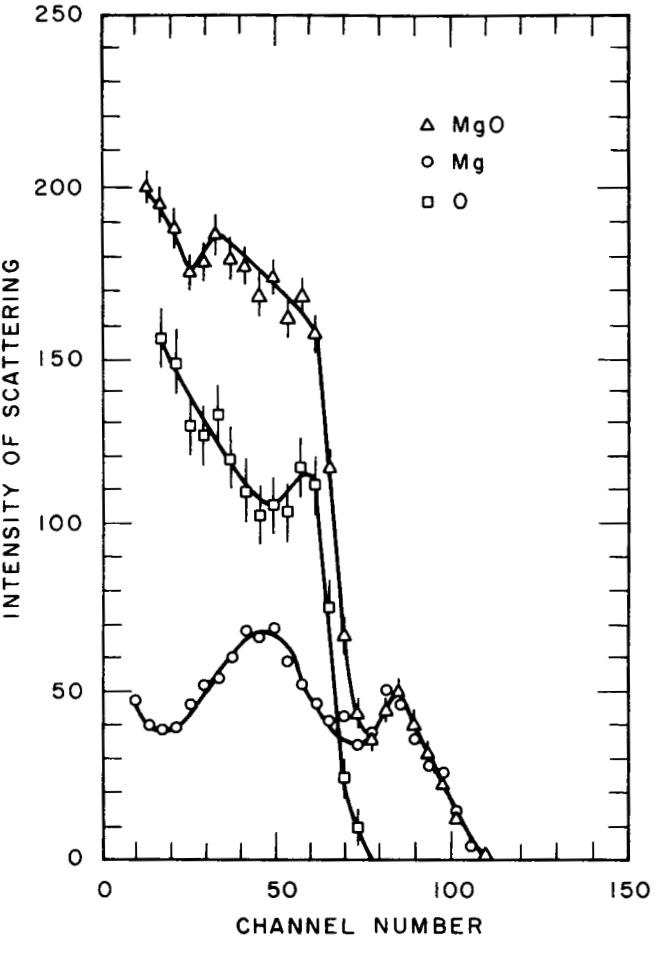

FIGURE 33.—Separation of the α-particle-scattering spectrum of MgO into Mg and O components. The vertical lines associated with each point represent statistical errors. The MgO spectrum is the observed curve, in units of counts per 4 channels per 100 minutes. The Mg spectrum is the observed curve multiplied by a normalization factor of 0.494±0.024 in order to fit it to the MgO spectrum above channel 72. The O spectrum was obtained by subtraction of the Mg spectrum from that of MgO. The slight peak in the O curve at around channel 60 may be due to instrument gain shifts between the time of measurement of the MgO and Mg samples. This is indicated by the slight peak shift of the Mg component at channel 85.

of minerals would not be determined on the lunar surface; thus, oxygen values would be in error if the surface rocks are hydrated. An illustration of the change in oxygen content of typical rocks with increasing water content is given in figure 34.

As indicated by Loomis (ref. 38), other limitations to the analysis of the lunar surface by α-particle scattering are the possible effects of prior meteoritic bombardment of the lunar surface and sputtering. Meteoritic impacts may have produced free iron which will create errors in metal-oxygen ratios of the order of ± 10 percent; however, measurements of magnetic susceptibility may aid in decreasing this error. Sputtering of the surface by solar particles may have created oxygen deficiencies which will also contribute to misleading metal-oxygen ratios. The most useful information about lunar-surface composition will be derived from the analyses of the elements listed in table IX with the probable ranges

TABLE IX.—*Probable Range of Elements To Be Sought on the Lunar Surface*

[Estimated from concentrations in meteorites and Earth rocks]

Element	Atomic number, (Z)	Probable range of concentration, atom-percent	Rock types and meteorites used for estimation
B	5	0–1	(max) Volcanic sublimate.
C	6	0–15	(max) Carbonaceous chondrite.
O	8	50–65	(min) Enstatite chondrite. (max) Siliceous igneous rock.
F	9	0–1	(max) Igneous rock or sublimate.
Na	11	0.5–7	(min) Chondrite. (max) Phonolite.
Mg	12	0.2–25	(min) Rhyolite. (max) Dunite.
Al	13	1–9	(min) Ultramafic. (max) Phonolite.
Si	14	15–30	(min) Dunite. (max) Quartz-rich rock.
S	16	0–5	(max) Carbonaceous chondrite or volcanic sublimate.
Cl	17	0–1	(max) Igneous rock or sublimate.
Ca(+K)	20(19)		
Ti	22	0.1–1	(max) Alkalic differentiates, ferrogabbros.
Fe(+Ni)	26(28)	0.5–15	(min) Magnesian or siliceous igneous rock. (max) High-iron chondrite.

TABLE X.—*Summary of Analyses by Various Workers For 8 Different Rocks of Basaltic Composition*[a]

[Composition in atom-percent, hydrogen-free. Actual hydrogen content in parentheses; note the variation in oxygen content with the amount of hydration]

Element	Rock							
	a	b	c	d	e	f	g	h
Si	18.1	18.5	17.5	18.5	18.4	17.6	18.0	18.2
Al	6.4	6.1	8.1	7.1	7.2	6.2	6.1	5.1
Ti	.4	.8	.4	.5	1.2	.3	.3	.1
Fe	3.6	3.4	2.9	3.4	2.9	2.7	3.9	5.4
Mg	3.9	3.8	4.2	3.2	2.2	4.5	3.7	5.5
Ca+K	4.7	4.9	4.2	3.9	2.2	3.9	4.8	4.2
Na	2.0	1.6	1.7	2.4	3.2	1.7	2.7	.6
O	61.9	60.9	60.8	61.6	62.7	63.1	60.5	60.8
H	(2.4)	(.3)	(1.0)	(3.0)	(6.9)	(10.5)	(1.4)	(1.0)

[a] a. Basalt flow
b. Basalt ash and pumice bed
c. Average chilled border gabbro
d. Amphibolite
e. Epidote-albite-chlorite schist
f. Glaucophane schist
g. Eclogite
h. Average Ca-rich achondrite

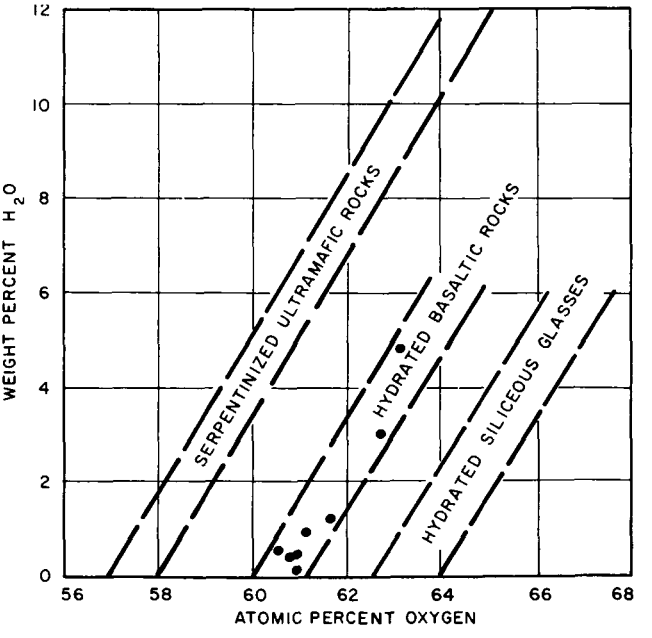

FIGURE 34.—Variation of oxygen content with increasing water content in hydrated rocks.

of their concentration. It is to be noted that α-particle scattering cannot differentiate nickel from iron nor potassium from calcium. Table X contains a summary of the compositions of the types of rocks which are considered to represent lunar material.

Martian Atmosphere Analysis

Marshall and Franzgrote (ref. 39) have proposed using α-particle scattering for the analysis of the atmosphere of Mars. The instrumentation was designed on the premise that N_2, A, and CO_2 would be the major constituents, since spectroscopic data have set upper limits of less than 1 percent for O_2, NO_2, CH_4, and NH_3. As described, it is proposed to expose an atmospheric sample to 6.1-MeV α-particles from Cm^{242}, and solid-state detectors are to be used to count the scattered particles. The energy spectra for back scattering from CO_2, N_2, and A at a pressure of 70 torr are given in figure 35.

Four coincidence circuits are to sort the discriminator output pulses for a given event into one of four channels, corresponding to the four energy windows, or determine that the event is not to be counted. Four

TABLE XI.—*Typical Discriminator Bias Levels and Output Pulse Widths for an α-Particle-Scattering Atmosphere Analyzer*

Discriminator	pulse width, μ sec	Bias, MeV	Function: definition of boundary
1	10	0.6	Lower boundary of CO_2 channel.
2	12	1.18	Upper boundary of CO_2 channel and lower boundary of redundant channel.
3	10	3.0	Lower boundary of A channel and upper boundary of redundant channel.
4	14	5.0	Upper boundary of A channel.
5	10	2.0	Lower boundary of N_2 channel.
6	12	4.0	Upper boundary of N_2 channel.

discriminators, connected to the α-particle detector-amplifiers, define the boundaries of three α-particle energy channels. Two discriminators, connected to the proton detector-amplifier, define the boundaries of the proton energy channel. Typical discriminator bias levels and output pulse widths are shown in table XI. The discriminator thresholds for existing models are stable to ± 0.2 percent over the temperature range from -50 to $+50°$ C.

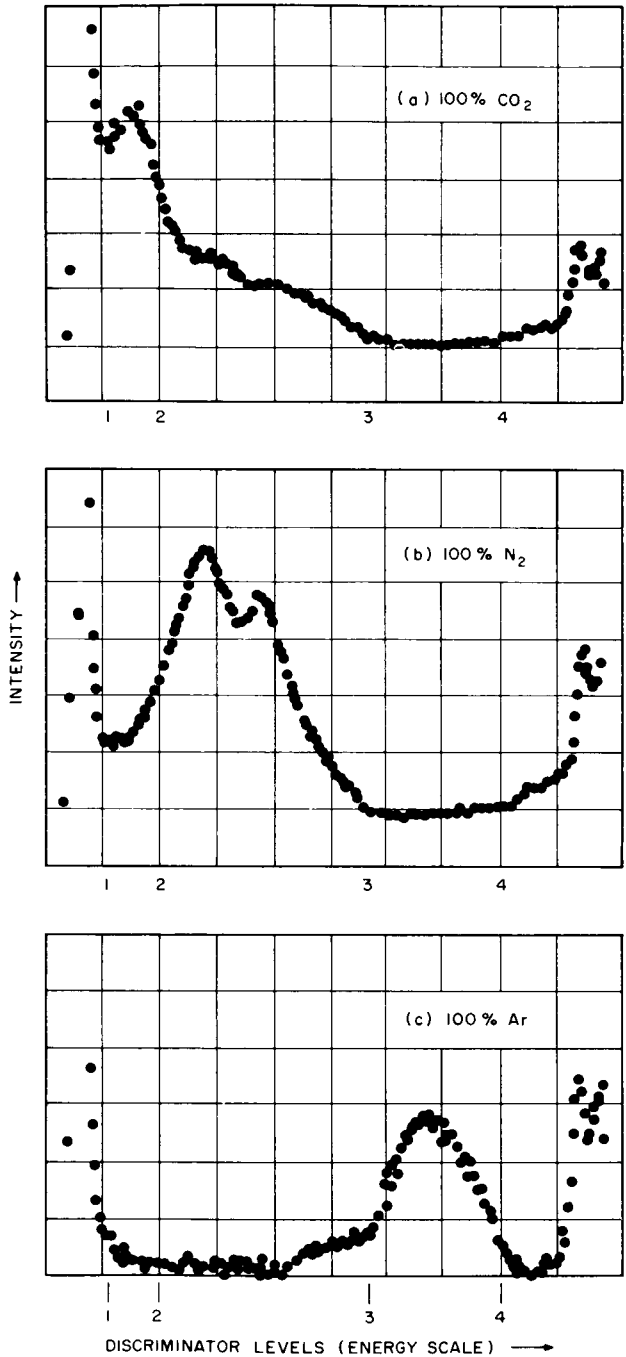

FIGURE 35.—Energy spectra for backscattering from CO_2, N_2, and A.

Neutron-Activation Analysis

Neutron-activation analysis involves the bombardment of a material with a beam of neutrons to convert the elements in the material to radioactive species. The radioactive species emit γ-rays which are sorted according to energy and counted by means of a multichannel differential analyzer, which permits identification and quantitative estimation of the elements present in the samples. Neutron sources are nuclear reactors, electrostatic particle accelerators, or radioactive isotopes.

The use of neutron-activation analysis has increased rapidly in the last decade, particularly for detection of trace elements in concentrations as low as 10^{-8} percent; this trace detection capability has been invaluable in forensic medicine and biomedical studies. Neutron beams for trace analyses are generally thermal neutrons (from reactors) with velocities of about 2200 meters per second. Analysis of the major constituents of minerals, however, requires fast neutron beams of the order of the speed of light (from accelerators).

Neutron activation has been investigated by NASA for lunar compositional analysis because of its adaptability to remote control and recording, minimum sample requirements, and the wide choice of available neutron sources and detectors.

NASA DEVELOPMENT CONTRIBUTIONS TO LUNAR SURFACE ANALYZERS

The neutron-activation analysis equipment developed for lunar surface analysis by Fite, Steel, and Wainerdi (ref. 40) of Texas A. & M. is based on (n, p) induced reactions with 14-MeV (fast) neutrons. As shown in figure 36, the source and detector used in experiments are placed at either end of a pivoting framework so that each may approach the surface alternately, thus reducing background. The detector is collimated so that the detected radiation comes from a specific volume of sample; combination of the defined volume measurements with the density obtained by backscattering provides the mass values needed for calculating the quantitative data summarized in table XII. Automation of activation analysis was also investigated by Fite et al. (ref. 41) and a computer-coupled scheme for lunar analysis is described by Menon (ref. 42).

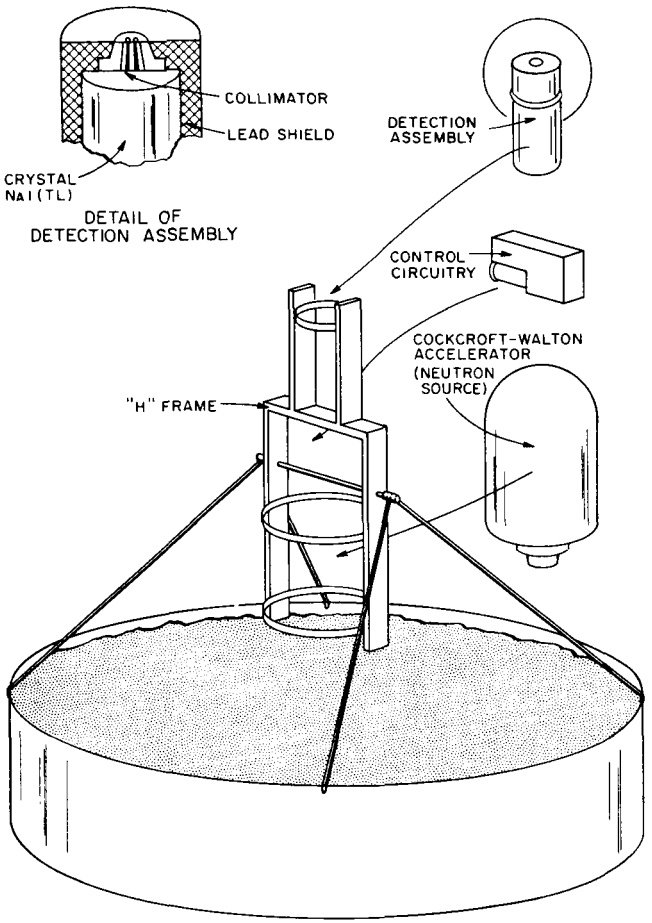

FIGURE 36.—Schematic diagram of neutron-activation analysis system.

Parameters affecting the performance of neutron-activation equipment for lunar analysis (ref. 43) have been evaluated by Metzger (ref. 44), for a 14-MeV source. The factors used and the results of calculations for sensitivities of elements to be determined on the lunar surface are given in table XIII.

Comparison of the minimum detectable limits (MDL), given in table XIII, with the composition of igneous rocks and meteorites shows that the compositional ranges of oxygen, sodium, aluminum, silicon, calcium, and iron in such minerals can be completely spanned by space-type, neutron-activation systems. The elements which would be detectable over most of their range of abundance are magnesium, titanium, and chromium. Sulfur and cobalt do not appear to be amenable to neutron-activation analysis.

TABLE XII.—*Precision of Oxygen Determination: Lunar Neutron-Activation Analysis System*

Run	Sample	Density	Flux	$A°$	$A°/g$	Oxygen added, percent	Oxygen found, percent	Error, percent
5	Al_2O_3	1.339	1.164	17 088	2712	47.06	45.68	−2.93
6	Al_2O_3	1.339	1.000	18 020	2860	47.06	48.18	+2.37
7	Fe_2O_3	.759	1.245	6 558	2876	30.06	30.95	+2.95
8	SiO_2	.937	1.007	13 457	2691	53.33	51.37	−3.67
9	MgO	.587	1.107	6 161	2644	39.69	37.56	−5.36
10								
11	Al_2O_3	1.339	1.143	17 656	2803	47.06	47.20	+.30
12	$Al_2O_3+SiO_2$	1.193	1.154	16 508	2808	49.30	49.54	+.48
13	$Al_2O_3+SiO_2$	1.193	1.064	16 906	2875	49.30	50.77	+2.91
14								
15	Fe_2O_3+MgO	1.077	1.009	10 173	2842	33.27	33.84	+1.70
16	$Al_2O_3+Fe_2O_3+MgO$	1.174	.927	12 218	2783	37.39	37.24	−.39
17	$Al_2O_3+Fe_2O_3+MgO+SiO_2$	1.296	1.000	16 169	2668	46.78	44.67	−4.50
18	$Al_2O_3+SiO_2$	1.193	.938	16 667	2835	49.30	50.01	+1.45
19	SiO_2	.937	1.066	13 822	2764	53.33	52.76	−1.06
20	$Al_2O_3+Fe_2O_3+MgO$	1.174	.905	12 390	2822	37.39	37.77	+1.01
21	Al_2O_3	1.339	.854	14 830	3131	47.06	52.74	+12.06
22	Fe_2O_3+MgO	1.077	.902	9 272	2590	33.27	30.84	−7.30

TABLE XIII.—*Factors Used in, and the Results of, the Computation of Sensitivities of Various Elements for Remote Compositional Analysis by Neutron Activation*

Target nuclide	Reaction	Product nuclide	$f_{\frac{1}{2}}$	f_i	f_d	$E\gamma$, MeV	f_w	A_d^z counts/min	ΣA_d^i counts/min	MDL, percent, (2σ)	WSI
O^{16}	n, p	N^{16}	7.4 sec	12 sec	12 sec	6.1	0.48	3.4×10^4	2.0×10^1	0.013	0.07
Na^{23}	n, α	F^{20}	10.7 sec	12 sec	12 sec	1.63	.07	1.90×10^4	3.5×10^2	.01	-------
Na^{23}	n, p	Ne^{23}	40 sec	120 sec	12+40 sec	.44	.07	7.9×10^3	7.9×10^3	.16	.11
Mg^{25}	n, p	Na^{25}	60 sec	120 sec	4 min	.98	.22	9.7×10^1	8.5×10^2	13	-------
Mg^{26}	n, α	Ne^{23}	40 sec	120 sec	12+40 sec	.44	.22	7.4×10^3	8.4×10^3	.54	.007
Al^{27}	n, p	Mg^{27}	9.5 min	20 min	4 min	.83	.12	6.1×10^4	6.7×10^3	.032	.003
Si^{28}	n, p	Al^{28}	2.3 min	120 sec	4 min	1.78	.35	1.06×10^5	1.00×10^3	.020	.01
P^{31}	n, p	Si^{31}	2.6 hr	200 min	80 min	1.27	.004	1.01×10^2	4.0×10^3	.50	.016
Cl^{37}	n, p	S^{37}	5.0 min	20 min	4 min	3.1	.001	1.82×10^0	3.0×10^1	.60	.40
K^{39}	$n, 2n$	K^{38}	7.7 min	20 min	4 min	2.1	.06	1.90×10^3	9.8×10^2	.19	.16
Ca^{44}	n, p	K^{44}	22 min	20 min	4+22 min	2.5	.12	1.42×10^1	1.50×10^2	.20	2
Ti^{48}	n, p	Sc^{48}	44 hr	200 min	24 hr	0.99–1.04	.025	9.1×10^2	1.91×10^2	.076	.016
V^{51}	n, p	Ti^{51}	5.8 min	20 min	4 min	.32	.001	2.5×10^2	8.3×10^3	.074	.014
Cr^{52}	n, p	V^{52}	3.8 min	120 sec	4 min	1.44	.004	2.1×10^2	4.3×10^2	.08	.06
Mn^{55}	$n, 2n$	Mn^{54}	280 days	200 min	24+120 hr	.84	.004	9.9×10^0	1.99×10^2	1.1	.077
Fe^{56}	n, p	Mn^{56}	2.6 hr	20 min	80 min	.84	.09	4.5×10^4	6.4×10^2	.10	.024
Co^{59}	$n, 2n$	Co^{58}	{ 9 hr 71 days }	200 min	80 min	.025	.006	1.82×10^4	$\sim 3.0 \times 10^4$	.01	.10
Ni^{60}	n, p	Co^{60}	10.5 min	20 min	4 min	.059	.009	5.3×10^4	$\sim 1.0 \times 10^4$	$\sim$ .04	.15

$f_{\frac{1}{2}}$ half-life of the product

f_i choice of a radiation time

f_d choice of decayed time

E_γ energy of the γ-ray used for identification

f_w wt-fraction in the 20-g sample to be determined

A_d^z counting rate in the photo peak at the detector

$\sum A_d^i$ interfering activity due to other reactions, plus the natural background

MDL minimum detectable limit for the 2σ (95 per cent) significance, calculated from

$$\text{MDL} = 2\sqrt{\sum_i A_d^i f_w} \Big/ A_d^z$$

WSI the (no interference) estimates of sensitivity, made by Well Surveys, Inc., adjusted to a flux of 10^9 neutrons/sec

NASA APPLICATIONS CONTRIBUTIONS TO GAMMA-RAY PULSE-HEIGHT SPECTRA ANALYSIS

A least-square fitting technique has been developed by Trombka (ref. 45) at JPL for complex γ-ray pulse-height spectra. A pulse-height spectrum is synthesized by using a series of normalized pulse-height distributions resulting from the monoenergetic components in the incident beam. The distributions are weighted so that their sum is a best fit, based on a least-square criterion, to the experimentally determined polyenergetic pulse-height distribution. Because pulse-height spectra are nonlinear in energy, analysis by a least-square technique is difficult. This difficulty is overcome, however, by using linear methods of solution but applying the constraint that only positive or zero values be allowed for the intensities or amplitudes of the various monoenergetic components. The analysis is only as good as the set of fitting spectra available, and spectra such as those due to bremsstrahlung should be included in the library of functions used for analysis.

CHAPTER 6

Mass Spectroscopy

Mass spectroscopy is concerned with the ionization and dissociation of atoms and molecules caused by electron impact. When a substance at low pressure ($<10^{-6}$ torr) is bombarded with low-energy electrons ($<$100-volt electrons), a beam of positive ions can be withdrawn from the impact area and sorted by magnetic fields according to their masses. The display of these masses forms the mass spectrum which can be recorded photographically (mass spectrograph) or detected electrically, amplified, and read from meters, strip charts, or oscilloscope presentation (mass spectrometer).

The discovery of positive ions by W. Wien in 1898 and the separation of the neon isotopes by J. J. Thompson in 1912 led to the development of the modern mass spectrograph. The first instrument, which produced lines on a photographic plate in positions according to the mass-to-charge ratio (m/e) of the ions, was developed by F. W. Aston at Cambridge University; at the same time (1919), A. J. Dempster at the University of Chicago developed the spectrometer that is most generally used today. In this spectrometer, a beam of ions of the same m/e and the same momentum needs only magnetic deflection for separation and focus onto an electrical detecting device. Other outstanding contributors to mass-spectroscopy instrumentation are K. T. Bainbridge, W. Bleakney, H. D. Smyth, and A. O. Nier. Impetus for the development and production of mass spectrometers was provided by the needs of the petroleum industry during World War II; thus, the application of mass spectroscopy to chemical analysis became practical about 1940.

Mass spectroscopy is used for the elucidation of molecular structure, the quantitative determination of the components of a mixture, qualitative identification of substances, isotope-ratio determination, detection of trace impurities, studies of chemical reaction kinetics, leak detection, detection of residual gases, and process control. A variety of instruments is available commercially for these applications.

Mass spectrometers for precision analytical work and for sophisticated structure elucidation or solids analysis may weigh from 1 to 4 tons. However, application of the same principles has made possible rocketborne instruments with less exacting requirements for mass range and resolution. Thus, the capability of the mass spectrometer to provide

a host of information about planetary surfaces and atmospheres has made it attractive for use in space exploration.

NASA DEVELOPMENT CONTRIBUTIONS

Mass Spectrometers for Aeronomy

A double-focusing mass spectrometer has been adapted by Spencer and Reber (ref. 46) at Goddard Space Flight Center for the quantitative measurement of atmospheric gases. The primary components of the system are a mass-spectrometer tube, an electrometer-amplifier system, an ionization-beam current regulator, and associated power supplies. The spectrometer tube is shown in cross section in figure 37; the path of the ions from their origin (at the small rectangle to the left of the repeller) can be traced through the slit into the electric sector and then into the magnetic sector where the ions are sorted according to mass and measured by various collectors corresponding to m/e values for helium (4), nitrogen (14 and 28), oxygen (16 and 32), and water (18).

The electrometer amplifier is attached directly to the collection flange; it has a minimum detection limit of 10^{-15} amperes (partial pressure

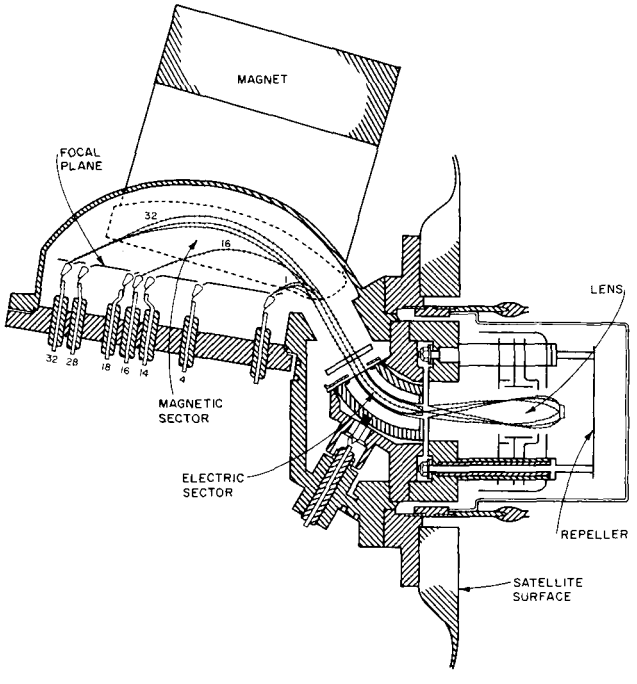

FIGURE 37.—Schematic line drawing of aeronomy mass-spectrometer tube showing major elements and representative ion paths.

of 10^{-11} torr) and can provide for either high- or low-sensitivity measurements at a collector by an appropriate choice of resistors. The spectrometer is designed for analysis at 700 to 1000 kilometers over Earth, weighs 12 pounds, and requires 20 watts of power.

The design of a rocketborne mass spectrometer for determining the altitude-density profile of helium in the atmosphere was described by Herzog (ref. 47) of Geophysics Corp. of America. Since accurate helium determinations cannot be made in air at ground level with a single-stage instrument because of excessive background scatter of N_2^+ and O_2^+ particles around the helium peak, this spectrometer uses two analyzer stages and is equipped with an electron multiplier. By suppressing the background completely and keeping electrical noise at an extremely low level, detection of helium partial pressures as low as 3×10^{-13} torr is anticipated. Laboratory results indicate that air at 10^{-6} torr produces a helium peak large enough to be measured accurately.

Mass Spectrometer for Solids

A mass spectrometer for the analysis of solids, using a sputter-ion source, has been designed and constructed by Herzog et al. (ref. 48) of Geophysics Corp. of America under sponsorship of NASA. Sputter-ion sources have been used for research studies for the past 20 years, but this is the first instrument designed for quantitative analysis of the surface composition of solid materials. This means of analysis will be particularly applicable to thin films and semiconductor materials, since the surface can be sputtered away in monolayers and, thus, variations in composition with depth can be determined. Although the analytical instrument weighs a ton and requires 400 watts of power, design considerations have indicated that the sputter-ion source can be combined with a suitably modified double-focusing analyzer to provide a flight model of reasonable performance for the analysis of lunar and planetary surfaces from a soft-landing probe.

The primary components of the analytical instrument are a noble-gas ion source, target chamber, mass analyzer, electronic ion detector, and vacuum system. In operation, a sample is introduced into the target chamber which is then evacuated to $<10^{-6}$ torr within 10 minutes. A low-voltage arc is initiated in the ion source which is maintained at about 10^{-2} torr from a noble-gas reservoir; a very dense plasma is created along the axis near the anode. An intense beam of ions is extracted through a pinhole in the anode and accelerated by a conically shaped electrode. The beam, of about 1 milliampere and small cross-sectional area, bombards the target sample at an oblique angle of incidence, causing a higher rate of sputtering than normal impact. The

secondary ions of surface material are focused electrostatically into the mass spectrometer for separation according to m/e in the magnetic sector and sorting according to energy in the electrostatic sector. The intensity of the ion current at a given m/e is measured electronically. Spectra may be obtained by either magnetic or voltage scanning and are recorded on a linear or logarithmic scale with an x–y recorder. For concentrations of less than parts per million, a digital memory oscilloscope is used.

Determination of the ion yields of pure metals was made by mounting three metal samples with a tantalum reference in the target chamber and then recording secondary ion emission from the samples and the reference successively. Comparison of the ion yields of a number of metals with tantalum and with bombardment by either helium or argon ions is given in table XIV.

TABLE XIV.—*Comparison of Ion Yields of Pure Metals With a Tantalum Standard*

Metal	8 kV Xe^+	8 kV A^+
Mg	20.9	107
Al	7.2	790
Fe	4.2	22.6
Co	1.5	3.2
Ni	1.68	1.8
Cu	.79	2.4
Zn	.95	3.2
Zr	.56	3.0
Nb	.09	3.7
Ag	.01	.94
Cd	.38	.11
In	1.67	5.0
Sn	.72	
Ta	1	1
Au	.006	.008
Pb	3.0	4.2

NASA APPLICATIONS CONTRIBUTIONS

Aeronomy

A Bennett-type radiofrequency mass spectrometer was used by Meadows-Reed and Smith (ref. 49) of Goddard Space Flight Center for determining the diffusive separation of nitrogen and argon in the upper atmosphere. The spectrometer was flown in an Aerobee 150A rocket from Wallops Island, Va. Results obtained with the spectrometer indicated that

the separation occurred beyond 110 kilometers in daylight; these were comparable with results obtained during previous night flights in the Arctic. The altitude profile of the argon-nitrogen ratio was also similar.

Analysis of the Lunar Surface and Atmosphere

Two studies have been conducted to evaluate the application of mass spectrometers to the analysis of the lunar surface and atmosphere. The mass spectrometers considered in detail by Brubaker (ref. 50) of Bell & Howell Research Center include only two nonmagnetic types which have been successful as laboratory instruments, a time-of-flight instrument and a quadrupole mass filter, with the latter being favored for overall performance capability. The state-of-the-art improvements recommended for space exploration include methods for sample vaporization and high-efficiency electron bombardment ion sources to be used in conjunction with the quadrupole mass filter and a similar quadratic ion detector. On the other hand, Kendall et al. (ref. 51) of Nuclide Corp. recommend a monopole mass filter with an electron bombardment ion source and electron multiplier detector. Both the quadrupole and monopole mass filters operate without a magnetic field; the quadrupole consists of four poles (electrodes) with given potentials applied to each pair, and the monopole consists of a single rod and a right-angle grounded electrode. Mass sweeping of both is accomplished by varying the radiofrequency or the amplitude of the radiofrequency sine wave and the superimposed direct-current voltage. The monopole apparently has the advantages of a small power requirement and multiple collection of ions.

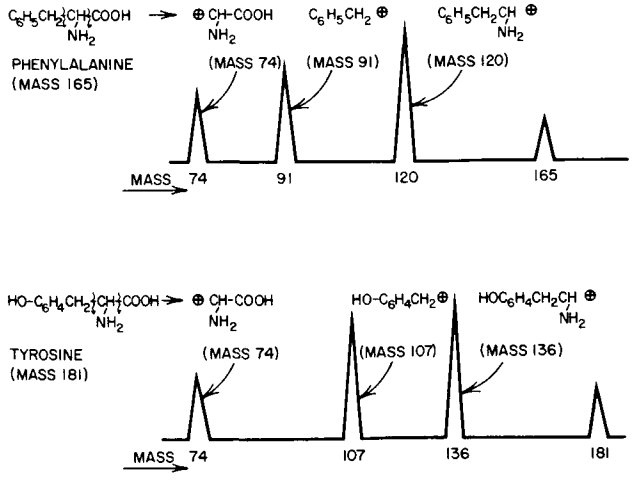

FIGURE 38.—The mass spectra of two aromatic amino acids.

Characterization of Amino Acids

The mass spectra of more than 25 amino acids, the principal components of proteins, have been examined by Biemann and McCloskey (ref. 52) at Massachusetts Institute of Technology. The mass spectra, obtained by use of a direct-introduction system, indicate fragment peaks typical of both carboxylic acids (M=45) and amines (CH_2NH_2) as well as the amino-acid grouping $CHNH_2COOH$. Examples of some characteristic peaks in the mass spectra of aromatic amino acids are given in figure 38. Other related biogenic materials which have been examined by Biemann (ref. 53) include small peptides, carbohydrates, nucleosides, purines, and pyrimidines.

CHAPTER 7

Gas Chromatography

Chromatography is an analytical technique for separating materials on suitable adsorbents by taking advantage of differences in adsorbability of various materials. The original development of this technique, in the early 20th century, is generally accorded to M. Tswett, a botanist, who separated plant pigments by adsorption of leaf-extract solutions on a solid adsorbent packed in a vertical column. Subsequently, partition chromatography (retardation of liquids by liquid-coated inert solids) was introduced in 1941, and the concept of gas chromatography was first reported in 1952. Since 1956, gas chromatography has been coupled with mass spectrometry to provide positive analysis of complex mixtures, particularly those extracted from natural products such as foods, oils, and waxes.

Gas chromatography is a general technique for separation of materials in the vapor state by sorption-desorption from solids; gas-liquid chromatography implies the separation of vaporized materials by liquid-coated inert adsorbents. Mixtures of gases or vaporized solid materials are introduced into a tube (column) packed with a suitable adsorbent system; a carrier gas (generally an inert gas such as helium) carries the sample vapor through the column. During their passage through the column, the various components of a mixture are retained and then desorbed according to their physical characteristics, and at some distance away from the point of introduction into the column the components have been separated. The desorbed, or eluted, materials may be trapped as they emerge from the column and may be thus collected as purified single materials or as materials which may need more refined separation. Alternatively, the emerging components may be detected by a variety of sensing systems, such as the change in thermal conductivity of the carrier gas or as an increase in the number of ions in a flame. By appropriate manipulation, the detecting systems may be used to measure quantitatively the various components in a mixture; the retention times of the various components may be associated with the nature of the materials and, thus, serve for qualitative identification. A block diagram for a typical gas-chromatography apparatus is shown in figure 39.

Gas chromatography is used for the detection of trace impurities (parts per billion) in pure gases and polluted atmospheres, identification

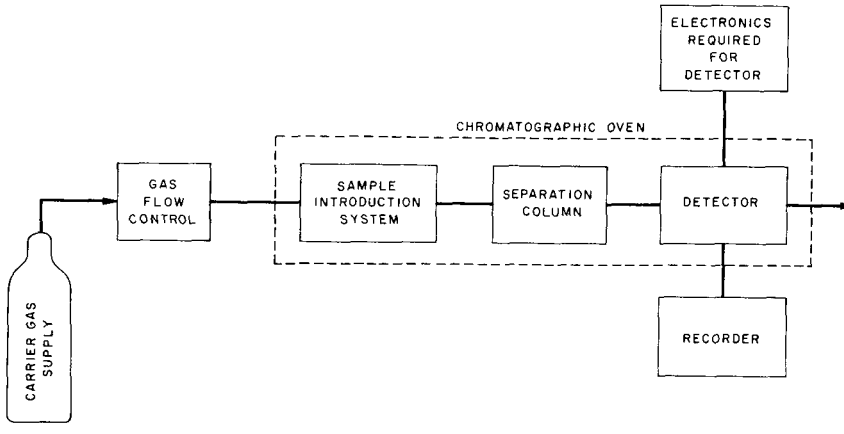

FIGURE 39.—Schematic diagram of a gas chromatograph.

of organic materials, separation of flavor components in foods and beverages as well as toxic materials in synthetic and natural drugs, and preparation of purified chemicals.

The gas chromatograph has found application in the analysts' laboratories, as well as in other systems, including automatic process-control systems, metabolic-analysis systems, and aircraft-cabin and human-incubator systems.

The general simplicity of the gas chromatograph and its proven adaptability to remote control and automation have made it attractive as an analytical tool in the space environment. It has been investigated by NASA for application to the detection of volatile constituents in the lunar surface, identification of compounds which may have biogenic origin, and analysis of planetary as well as space-cabin atmospheres.

NASA DEVELOPMENT CONTRIBUTIONS

Lunar Gas Chromatograph

The application of gas chromatography to the analysis of volatile constituents in the lunar surface (ref. 54) was studied at JPL and Aerojet-General Corp. On the premise that organic constituents remaining in the lunar surface (indicative of life processes existing in past millennia) would be of very low vapor pressure, it was determined that pyrolytic techniques would be necessary to prepare samples in suitable form for analysis by gas chromatography. By working with alanine (an amino acid) mixed in the ratio of 1:1000 with powdered dunite, gabbro, and granite, it was found that the products of pyrolysis varied with time, temperature, and the nature of the rock. As a result of this work,

conducted in vacuo as required to simulate lunar conditions, a prototype lunar gas chromatograph was proposed, including recommendations for sample size, oven temperature, column packing, glow-discharge detectors, and programing.

Subsequent developments in the concept for a lunar gas chromatograph, aided by S. R. Lipsky (Yale University) and J. E. Lovelock (Baylor University), led to the prototype assembly depicted in block form in figure 40 and illustrated photographically in figures 41 and 42.

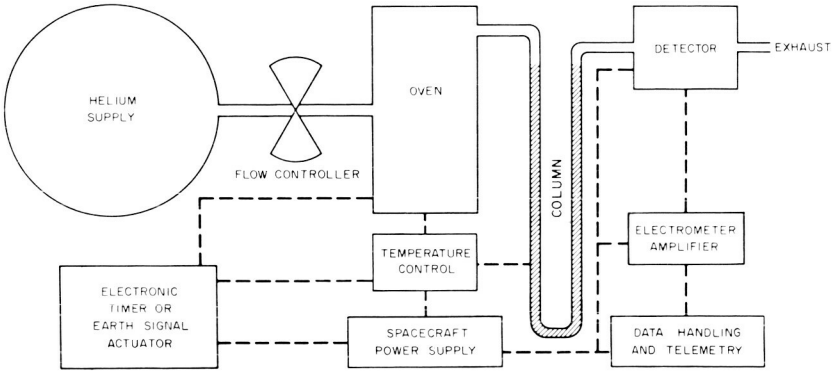

FIGURE 40.—Schematic drawing of the lunar gas chromatograph.

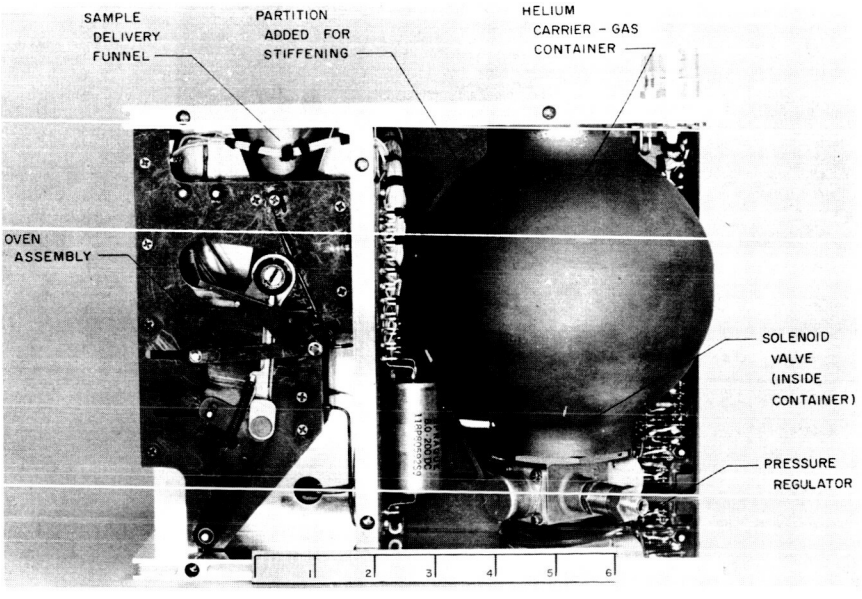

FIGURE 41.—View of lunar gas chromatograph showing oven assembly and helium container.

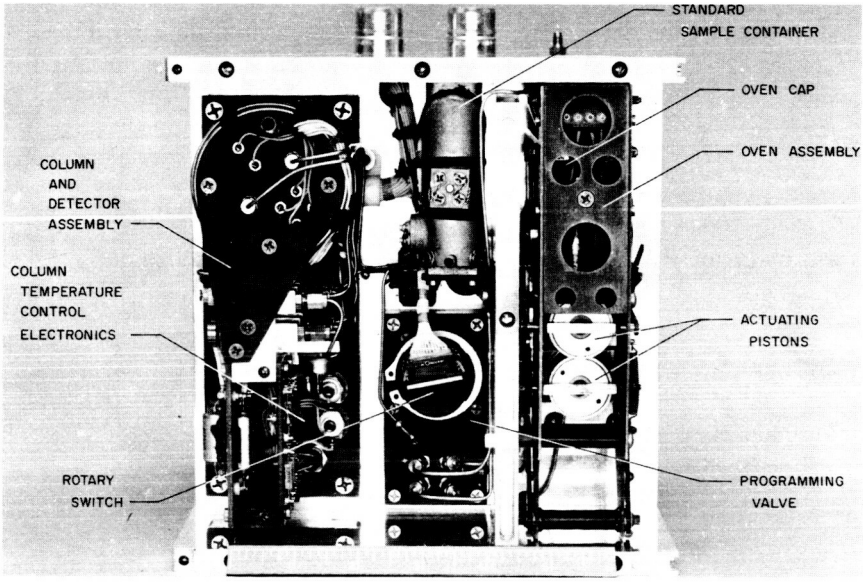

FIGURE 42.—View of lunar gas chromatograph showing programing valve and standard sample container.

The instrument, constructed by Beckman Instruments, Inc., weighs 14 pounds and has a volume displacement of 640 in.^{3}. The total operating energy required per 100-minute analysis is 24 watt-hours.

As conceived, samples are picked up by the spacecraft Surveyor and delivered to the gas chromatograph by way of the receiving funnel. The samples are dropped into the oven, where they are heated at one of three temperatures (150°, 325°, and 500° C) on command from Earth. The volatile materials are carried through the appropriate column by helium for determination of common gases, hydrocarbons, and other organic constituents. The glow-discharge detectors identify materials according to changes in the breakdown voltage of the helium carrier gas (fig. 43), and the information is telemetered to Earth.

Performance requirements for the lunar gas chromatograph are listed in table XV, and environmental requirements are listed in table XVI. A review by Wilhite (ref. 55) of JPL illustrates the many developments required to meet the performance and environmental specifications; these are described below.

When the sample is introduced into the oven, the opening must be sealed off so that all pyrolyzed materials pass only into the chromatograph. Since organic constituents are being sought, elastomers cannot be used, and the seal for the oven door must be made between metals which cannot cold-weld. A modified K-ring seal was found to be effective;

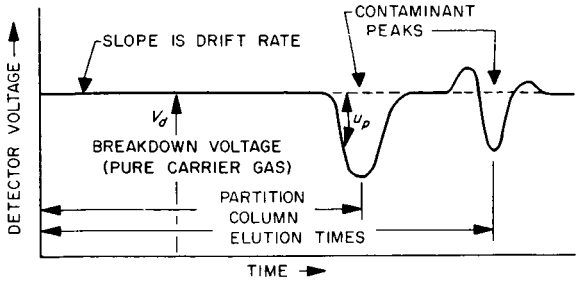

FIGURE 43.—Typical glow-discharge detector signal.

TABLE XV.—*Performance Requirements for the Lunar Gas Chromatograph*

Components to be resolved

Hydrogen	Propionaldehyde
Oxygen	Formic acid
Nitrogen	Acetic acid
Carbon monoxide	Butyric acid
Carbon dioxide	Benzene
Methane	Toluene
Ethane	Acetone
Propane	Acetonitrile
Butane	Acetylene
Methanol	Acrolein
Ethanol	Hydrogen cyanide
Propanol	Hydrogen sulfide
Formaldehyde	Ammonia
Acetaldehyde	Water

Performance requirements

Maximum retention time, min	10
Minimum detectable quantity in oven, mole	3×10^{-10}
Minimum dynamic range of detection	10 000 times minimum detectable quantity
Oven temperature control, °C	±10
Oven maximum heating time, min	4
Detector and signal processing:	
Output, V	0 to 5
Maximum noise level (peak to peak), mV	100
Minimum detectable signal twice the maximum noise level	
Accuracy, percent	±1
Oven seal maximum leakage (helium), cm^3/sec	$\pm10^{-6}$
Column temperature control, °C	±0.25
Valve maximum leakage (helium), cm^3/sec	10^{-4}
Retention time reproducibility, percent	1
Pressure regulation, percent	1
Calibration sample reproducibility, percent	4

TABLE XVI.—*Environmental Requirements for the Lunar Gas Chromatograph*

Item	Value
Sterilization:	
Heat	125° C (257° F) for 36 hr
Ethylene oxide	24 hr
Vibration	42 g peak-to-peak over frequency range of 20 to 1500 cps
Shock	35 g for 5 msec
Ambient survival temperature range	−185° to +125° C (−301° to +257° F)
Ambient operating temperature range	−50° to +125° C (−58° to +257° F)

the oven opening, made of Stellite, was ground optically flat, and the K-ring was gold plated heavily to prevent cold welding. A brush of glass fibers embedded in an epoxy resin was used to sweep the oven opening free of residual sample particles which might prevent a good seal.

One of the primary problems encountered in the use of the glow-discharge detectors was that of obtaining a zero baseline in the absence of a sample. It was found that a derivative readout of the detector (accomplished simply by coupling the detector to the electrometer amplifier through a capacitor) obviated the need for establishing a zero

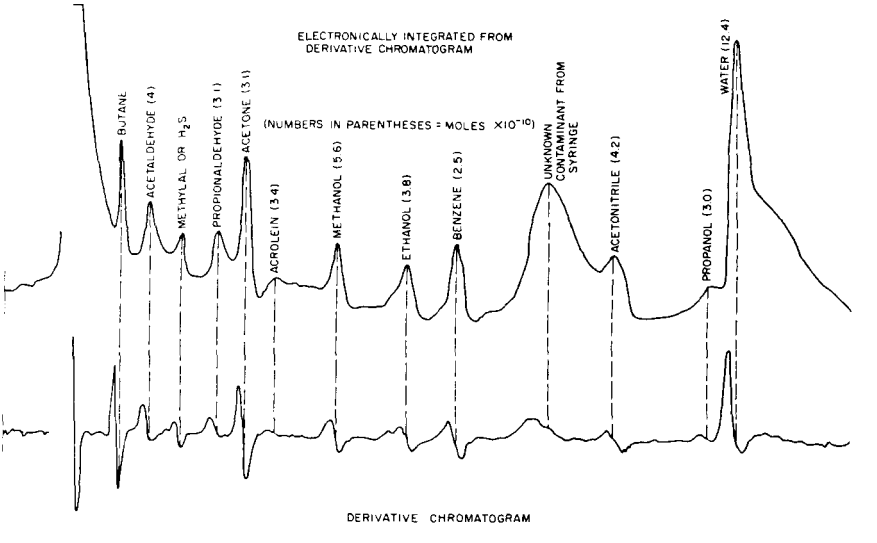

FIGURE 44.—Derivative readout chromatogram.

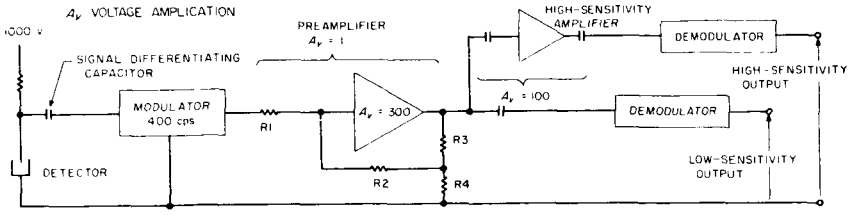

FIGURE 45.—Schematic drawing of electrometer amplifier.

baseline. This system has the added advantage of permitting accurate determination of the retention times of the various peaks (fig. 44).

Other features of the lunar gas chromatograph include the incorporation of a titanium sphere containing sufficient helium for 70 hours of operations, a standard-calibrant gas container for checking operation of the chromatograph, a programing valve to coordinate the programed pneumatic and electrical functions, and use of three chopper-stabilized electrometer amplifiers (fig. 45) in the detector-signal processing circuitry.

Planetary Gas Chromatographs

The development of a laboratory model of a planetary gas chromatograph at Melpar, Inc., for JPL is reported by Chaudet (ref. 56). Advanced state-of-the-art components and techniques were required to meet JPL specifications for resolution and quantitative measurement of the following gases:

hydrogen	krypton	ethane
oxygen	methane	carbon dioxide
argon	nitrogen	carbon monoxide
water vapor	ammonia	nitrous oxide

The chromatograph, designed with a complex arrangement of series-connected micro-cross-section detectors and separation columns, is shown schematically in figure 46. The novelty of the column system lies in the use of charcoal (col. 4B) to absorb oxygen irreversibly in order to effect oxygen-argon separation and the use of a short molecular sieve (col. 2C) to separate nitrous oxide and carbon dioxide. Utility of the other columns is summarized briefly:

Column 1 —Air, NH_3, H_2O
Column 2A—To delay passage of air to detector 2 until NH_3 is eluted from column 1
Column 2B—Kr, Xe, C_2H_6, CO_2
Column 3 —H_2-Ne, A-O_2, N_2, CH_4, CO, Xe
Column 4 —To delay elution into detector 4 to prevent interference with detector 3

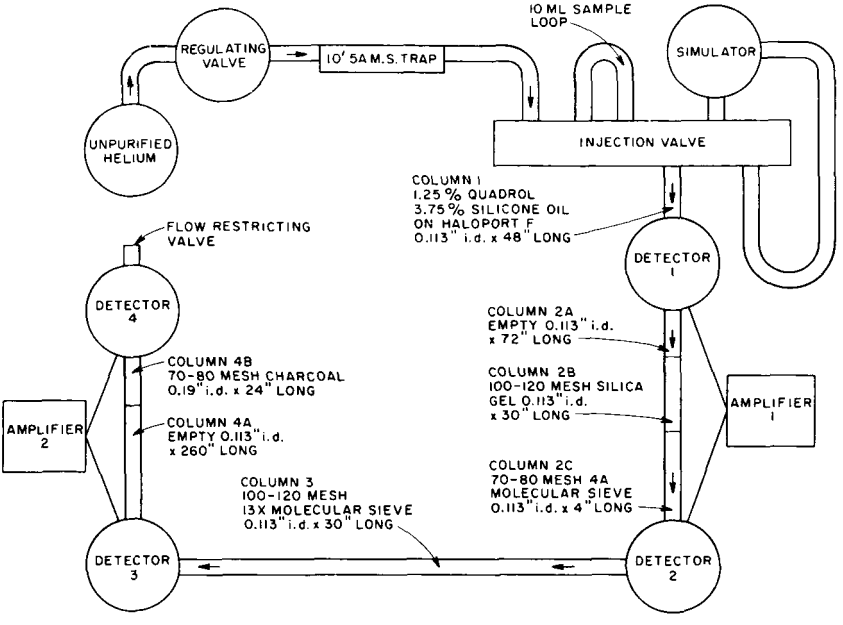

FIGURE 46.—Overall schematic of planetary gas chromatograph.

The detectors selected for this assembly use tritium foil as the ionization source; they have a moderate sensitivity and have a linear detection capability for gases ranging from parts per million to 100 percent.

A chemical-cartridge heating system was developed for the Melpar gas-chromatograph oven assembly (containing the injector valve, the columns, and the detectors). After considerable experimentation to control the thermite reaction for this operation, a $\frac{5}{8}$-inch cartridge was constructed which uses a $Zr\text{-}BaCrO_4$ primer on the bridge wire, an $Al\text{-}Fe_2O_3$ booster, and an Atlas Chemical Co. delay line charge. Sequential firing of 12 cartridges surrounding the oven permits elevation of oven temperature from 200° to 310° K, where it remains for about 1 hour without additional firing. The general configuration of the heater control cricuit is shown in figure 47. A salt heat sink ($Na_2HPO_4 \cdot 12H_2O$) is used to maintain oven temperature and prevent temperature overshoot. The oven proper is a 3-inch-diameter well, 3 inches deep, insulated by a laminate of aluminum foil and a low-density foam.

Figure 48 shows the response data for the oven in one test in which eight cartridges were fired over an interval of 20 minutes to raise the oven temperature to 310° K; the ambient temperature was maintained at 200° K. Eighty minutes were required for heat losses to reduce the oven temperature to 300° K; at the end of this time, another heater

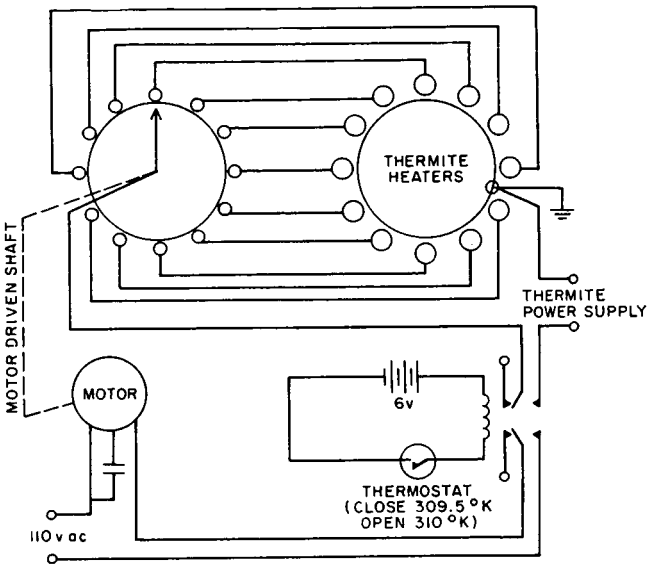

FIGURE 47.—Chemical heater control circuit.

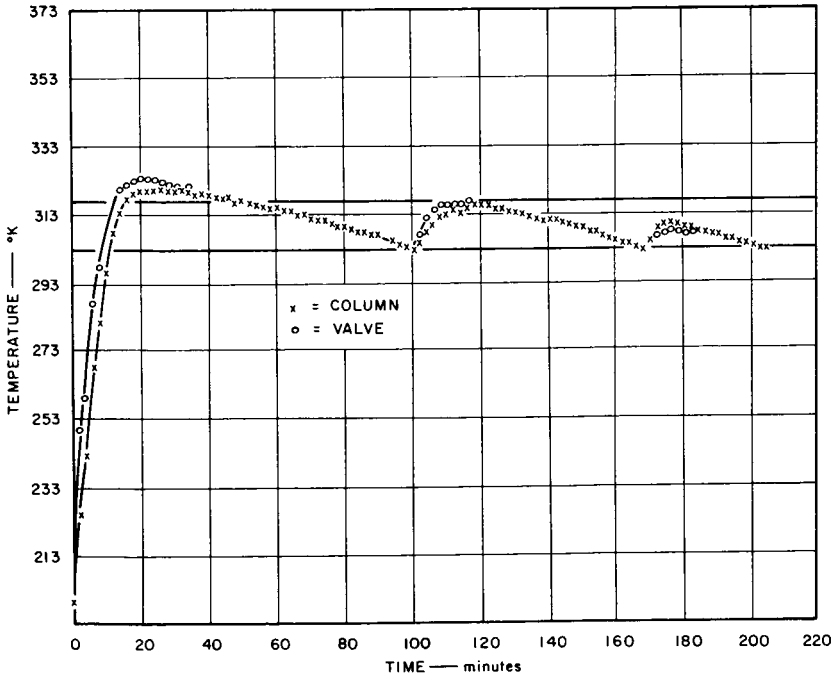

FIGURE 48.—Temperature characteristics of simulated oven heated with chemical heaters.

cartridge was fired and the temperature rose to 315° K. Sixty-eight minutes elapsed before the temperature again dropped to 300° K and an additional cartridge was fired.

The slider-injector valve developed for the chromatograph is actuated by squib firing and is shown in figure 49; the problems inherent with a nonretractable squib piston are circumvented by the use of toggle links and shear pins. The valve is sealtight and of low volume; internal construction is of stainless steel with Teflon gasketing.

Development of a working model of a planetary gas chromatograph for Mars was undertaken at JPL as proposed by Lipsky (Yale University) and JPL personnel (ref. 57). The chromatograph was to be capable of performing a complete gas analysis in a 60-second descent

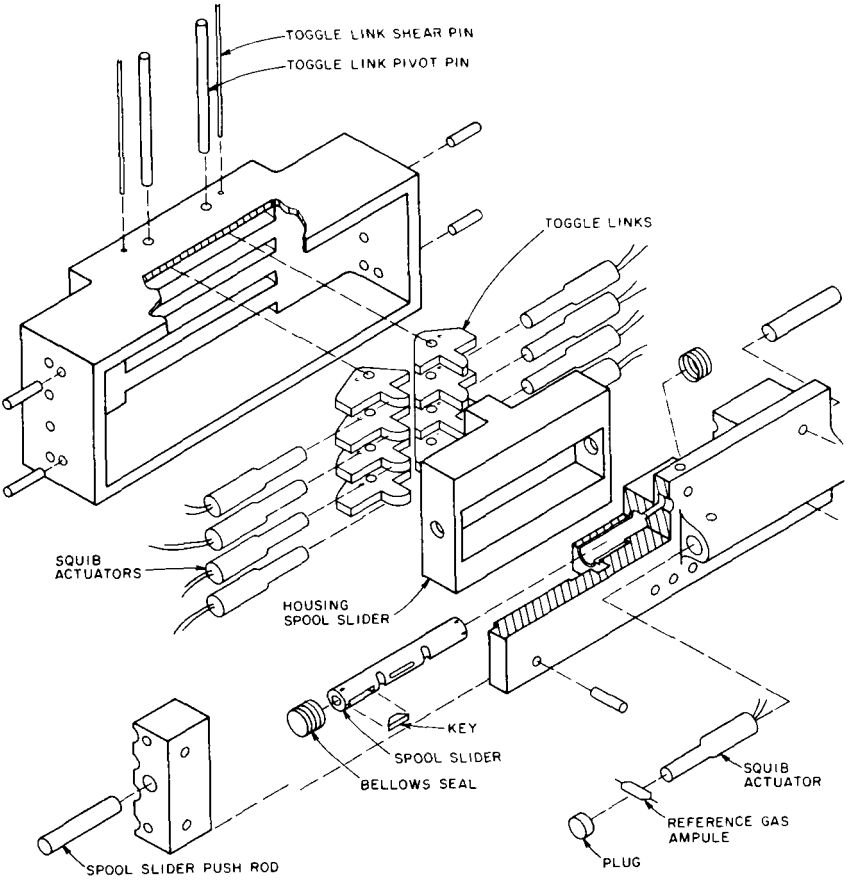

FIGURE 49.—Exploded view of slider-injector valve.

time of a capsule from a spacecraft to the Martian surface and of transmitting the information in 50 bits out of a total 150 bits allowed the capsule. Prior developments of electronic components for a planetary gas chromatograph were incorporated in this model (refs. 58–60), as well as a system for programing, signal processing, and data handling (ref. 61).

The electronics for quantitative measurements, described by Josias et al. (ref. 61), include an electrometer with a five-decade range for linear reproduction of all detector peaks (five-decade cross-section detector) and an electronic integrator with a minimum dynamic range of 6.5 decades to accommodate the lowest expected sampling pressure in an estimated pressure range of 30:1. The peak-height measurement system depicted in figure 50 includes a baseline-stabilized automatic range-switching electrometer, and figure 51 illustrates the use of the electrometer amplifier in an integrating system for the measurement of peak area rather than peak height. Many of the timing and transient elimination electronics necessary to the operation of the integration method are not shown in figure 51 (cf. fig. 50), nor are the logic elements that would be required to prevent readouts during scale-switching transients.

The characteristics of the dynamic-capacitor-type electrometer proposed for this system are summarized in table XVII.

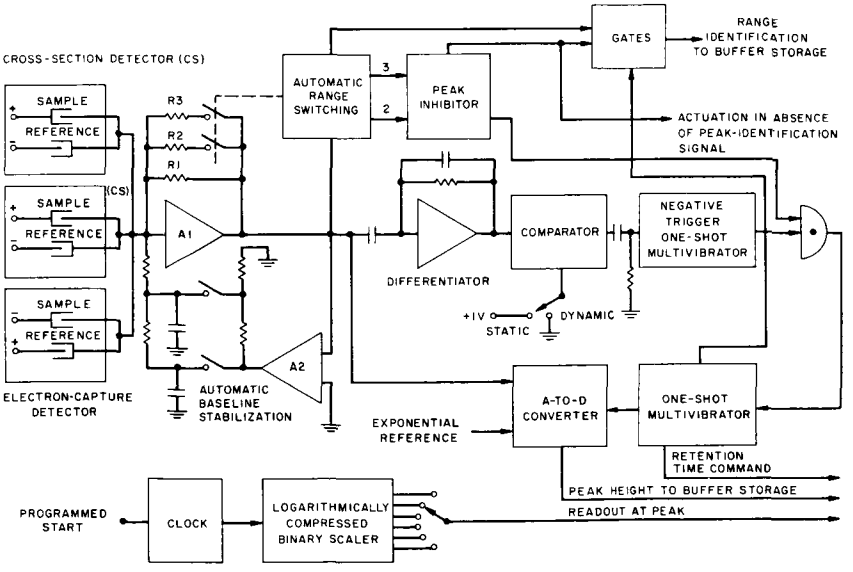

FIGURE 50.—Peak-height measurement system.

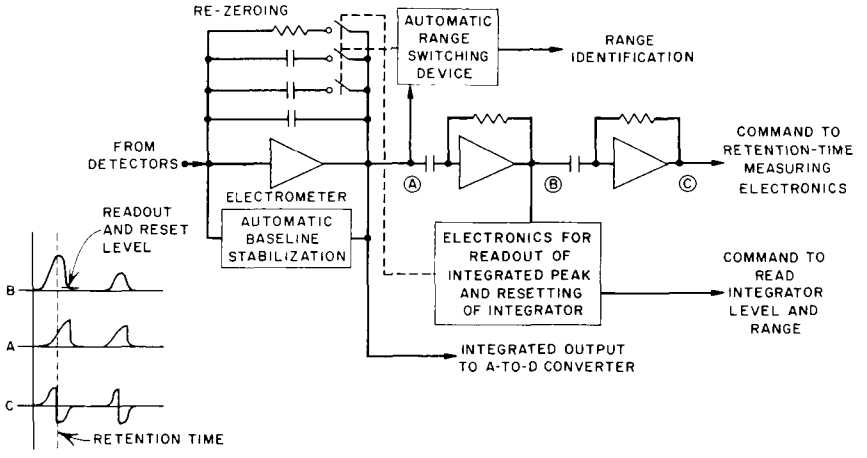

FIGURE 51.—Partial block diagram of peak-integrating electronics.

Automatic range switching (fig. 50) is accomplished by the incorporation of a scale-factor device, developed by J. H. Lawrence and modified by Marshall (ref. 58), with the three switching thresholds indicated in table XVIII.

A block diagram of the scale-switching electrometer system is shown in figure 52. The electrometer is all solid state with a vibrating-reed

TABLE XVII.—*Characteristics of Dynamic-Capacity-Type Electrometer*

Input leakage current, amp	10^{-15}
Voltage stability, μV/°C	70
Rise time (10 to 90 percent), msec	100
Rate limit, V/sec	100
Absolute dc accuracy (with perfect feedback elements), percent	0.1

TABLE XVIII.—*Switching Thresholds for Scale-Factor Device.*

Resistor	Electrometer output voltage	Corresponding input current, amp	Dropout voltage	Dropout current, amp
10^{11}	[a] 0.01 to 10	[a] 10^{-13} to 10^{-10}	[b]	[b]
10^{9}	0.1 to 10	10^{-10} to 10^{-8}	0.05	5×10^{-11}
10^{7}	0.1 to 10	10^{-8} to 10^{-6}	.05	5×10^{-9}

[a] Electrometer threshold.
[b] Not applicable.

capacitor-modulator. The tracking oscillator drives the reed at its resonant frequency and supplies a synchronized drive signal to the demodulator. The automatic scale-switching circuits (fig. 53) use a transistor chopper to convert the electrometer direct-current output into rectangular pulses that will pass alternating-current amplifiers. These pulses are used to trigger two discriminators which switch electrometer feedback resistors and change the sensitivity of the electrometer.

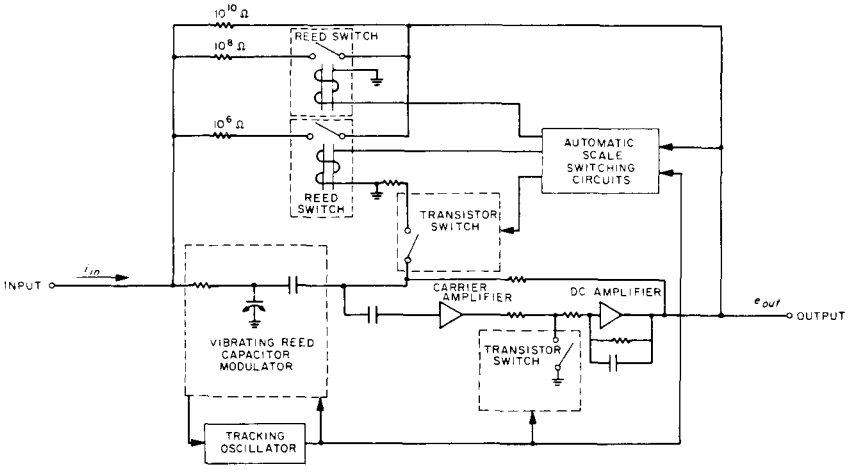

FIGURE 52.—Block diagram of automatic scale-switching electrometer.

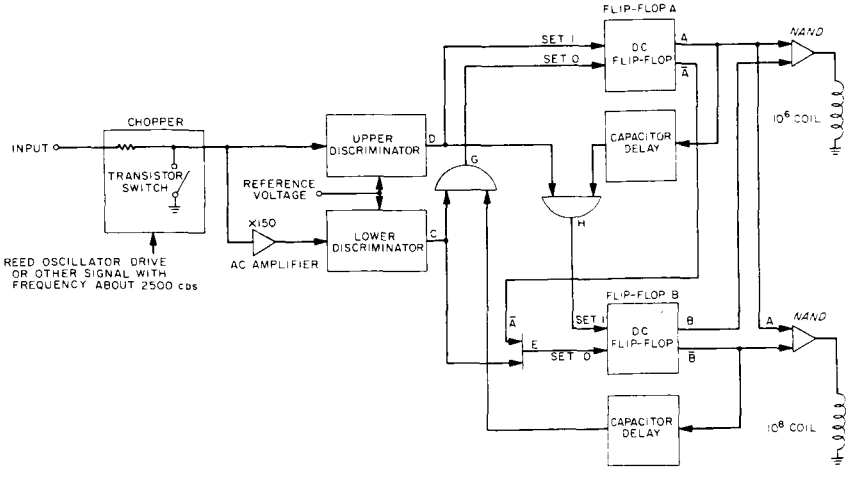

FIGURE 53.—Block diagram of automatic scale-switching circuits.

Baseline drift in the JPL planetary gas chromatograph is compensated by two techniques. The first, developed by Bowman et al. (ref. 59), maintains constant linear servo control of the electrometer against changes in the baseline, which is particularly effective with short-term drifts. The second, developed by Marshall (ref. 60), uses a system in which current from a capacitor storage cancels the detector quiescent current at the electrometer output.

A schematic diagram is given in figure 54 of the plan for the gas chromatograph sequencer-programer necessary for completely automatic operation by remote control.

Gas Chromatography—Mass Spectrometry

The advantages of coupling a mass spectrometer with a gas chromatograph for analysis of organic constituents which may be found on planetary surfaces has prompted an investigation of the feasibility of such a system at JPL, aided by S. R. Lipsky at the Yale University Medical School. As presented by Bentley et al. (ref. 62), identification of a mixture of two compounds with dissimilar mass spectra is readily made (fig. 55), but identification of a mixture of two compounds with similar spectra (fig. 56) is aided by knowledge of gas chromatographic retention times (fig. 57). Analysis of such mixtures is seldom a problem with laboratory mass spectrometers, but flyweight spectrometers have insufficient resolution and pattern stability.

The work thus far at JPL has been involved only with the development of a microminiaturized gas chromatograph which will be used at first with a miniaturized mass spectrometer such as the 60°-sector flyable

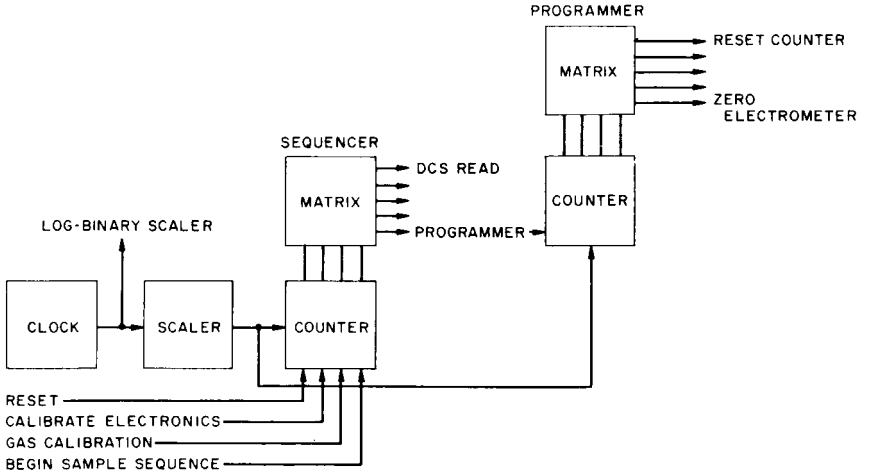

FIGURE 54.—Gas chromatograph sequencer and programer.

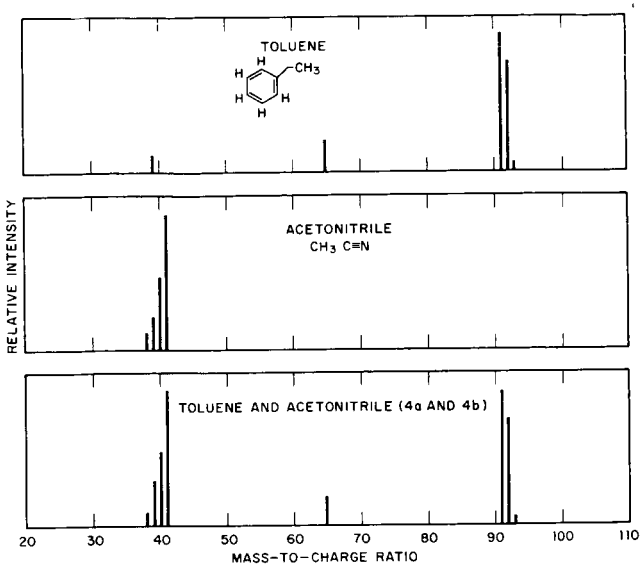

FIGURE 55.—Mass spectra of acetonitrile (4a) and toluene (4b) and mixture of toluene and acetonitrile from gas chromatographic peak (4a and 4b from fig. 57). The mixture mass spectrum can be readily analyzed in this case.

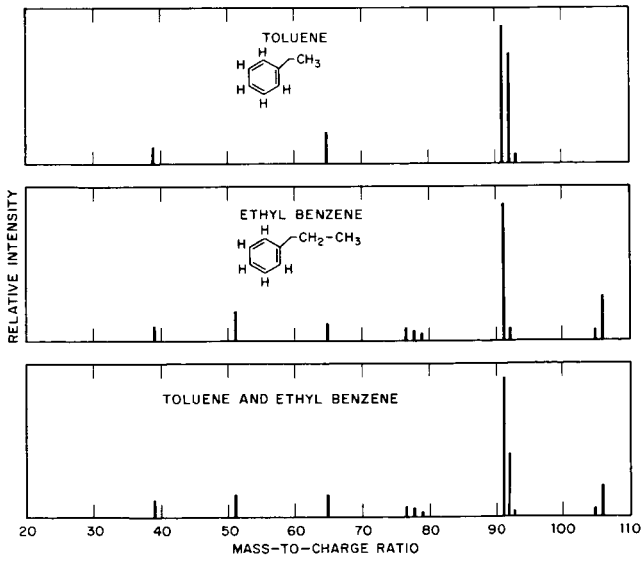

FIGURE 56.—Mass spectra of ethyl benzene, toluene, and a mixture of toluene and ethyl benzene. Note that the spectrum of toluene is "concealed" under the ethyl benzene spectrum in the mixture. The separation of ethyl benzene and toluene by gas chromatography is shown in figure 57.

(2.7 kg) mass spectrometer constructed for JPL by the University of Minnesota in 1961.

The micro gas chromatograph eventually will be a small unit of only 100 grams. Present efforts tend toward the development of suitable miniaturized chromatographic columns which will provide maximum separation of components for mass-spectrometry analysis with a minimum

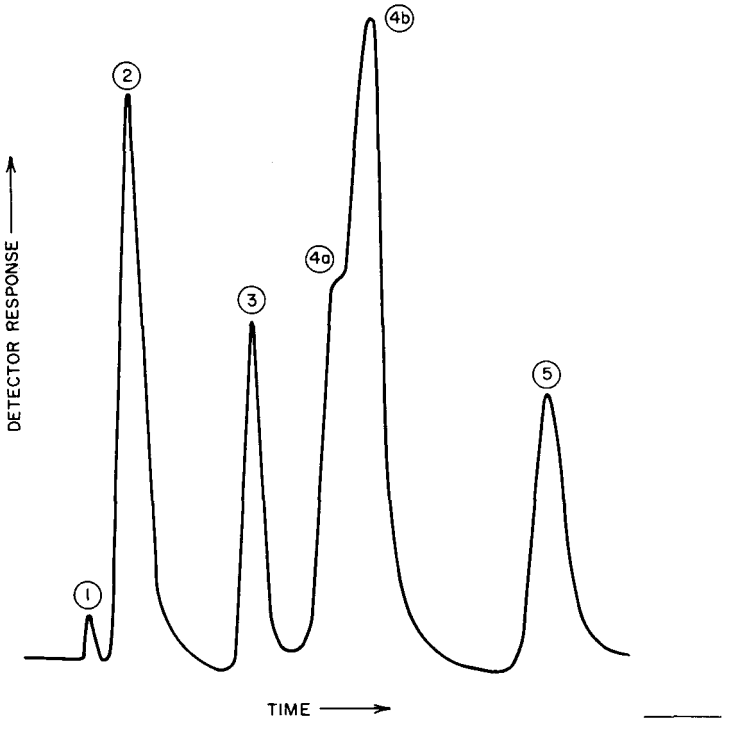

FIGURE 57.—Gas chromatogram showing good and poor separation: chosen column packing (Carbowax 20M on Chromasorb G) clearly separates peaks (1) (injection), (2) (carbon dioxide), (3) (benzene), and (5) (ethyl benzene), but fails to resolve completely (4) (4a acetonitrile and 4b toluene).

of carrier gas. Preliminary experiments have been based on the efficiency of separation of pyrolysis products of *N*-acetyl-L-phenylalanine, a peptide, since identification of similar components in pyrolyzed material from planetary surfaces may indicate the presence of past or present life; the eluted components are trapped and analyzed by standard mass-spectrometry techniques.

NASA APPLICATIONS CONTRIBUTIONS

Determination of Micro-Organisms

Gas chromatographic identification of the pyrolysis products of biological material has been suggested by Oyama (ref. 63) of Ames Research Center as a method for detecting life on Mars. A single strain of micro-organisms (unidentified), grown in trypticase soy broth under aerobic conditions at 30° C, was used to determine the optimum temperature for pyrolysis which would reveal the greatest amount of volatile components of thermal breakdown as separated by a gas chromatograph and detected by a hydrogen flame device. For this work, a 12-foot, ⅛-inch-diameter column packed with 15 percent SE–30 on 60/80 mesh Chromasorb W was maintained at 200° C. The stainless-

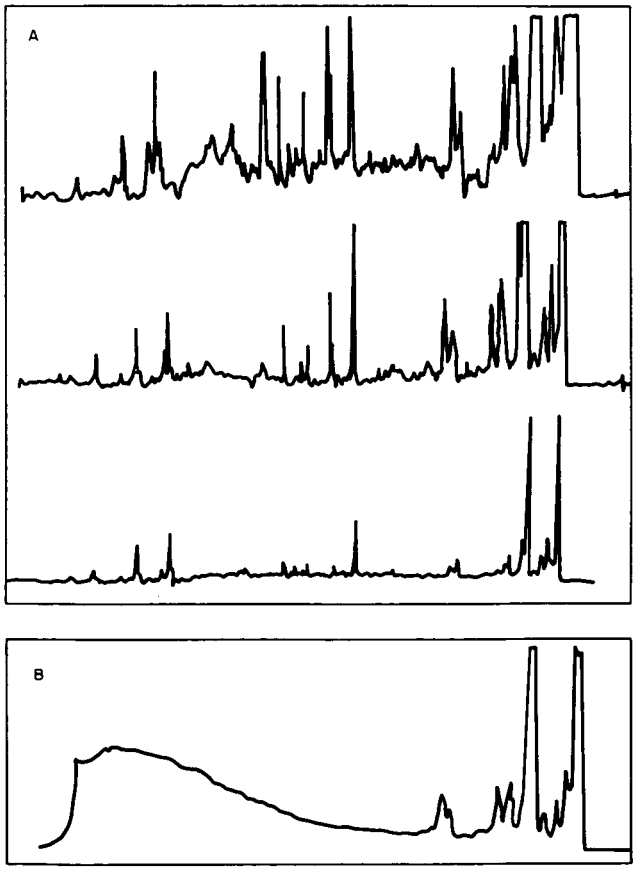

FIGURE 58.—Comparative chromatograms of: (*A*) three isolated soil micro-organisms; (*B*) crystalline bovine albumin.

steel-loop pyrolysis chamber was attached to a six-way linear valve paired with another linear valve (which provided for evacuation of the chamber, filling it with helium during pyrolysis and sweeping pyrolysis products into the gas chromatograph); valving and tubing were maintained at 125° C.

Using 10- to 200-μg samples, it was determined that no significant products were produced below 300° C; optimum temperature and residence time were 450° to 500° C for 2 minutes.

A capillary column, 0.01 inch in diameter and 300 feet long, coated with diethylene glycol succinate polyester was used for the analysis of pyrolytic products from micro-organisms isolated from soils. As shown by the chromatograms in figure 58, the characteristics of the pyrolysates of three isolated soil micro-organisms are similar to those of crystalline bovine albumin; apparently, similar patterns are obtained from proteins of either plant or animal origin.

Characterization of Alkanes

Gas chromatograms and mass spectra are being obtained by Meinschein (ref. 64) of the Esso Research & Engineering Co. for alkane hydrocarbons from living organisms, sediments, and abiotic products in order to provide a reference catalog for determining the origin of hydrocarbons that may be found extraterrestrially. More than 300 gas chromatograms and 100 mass spectra as well as various infrared and ultraviolet spectra have already been cataloged.

The most abundant naturally occurring hydrocarbons are C_1 to C_{40} *n*-paraffins; however, these are easily duplicated by abiotic reactions. On the other hand, many of the precisely structured isoprenoids which can be found in oils and oil shales in concentrations from 0.08 to 1 percent are considered to be of biological origin; 12 such terpanes already have been isolated, but only 2 of these are known to appear in biological lipids. The data accumulated thus far indicate that saturated hydrocarbons are the most widely distributed and best preserved products of former organisms on Earth; it remains to assess the factors controlling the composition of sedimentary hydrocarbons to gain insight into the origin of the alkanes in sediments.

CHAPTER 8

NASA Development Contributions to Specific Gas Analyzers

Most of the analytical instrumentation already described has been designed for the identification and determination of a broad range of gaseous, liquid, and solid materials. The basic principles of these versatile analytical instruments are also applicable to single-purpose instruments, such as an infrared monitor for carbon monoxide. In these instances, the instrument is designed to detect only one component, often in trace quantities. Instrumentation of this kind is invaluable for routine analyses in the laboratory (e.g., amino acid analyzer), for process control in industry (e.g., moisture meter), and for environmental monitoring (e.g., noxious gas analyzer).

Instrumentation for the detection of selected substances, particularly gases, is of considerable importance to NASA because a life-supporting atmosphere must be insured and controlled in manned spacecraft, a safe atmosphere must be maintained in the vicinity of propellants, and rapid, sensitive tests are required in studies of combustion as well as studies of metabolism.

OXYGEN ANALYZERS

An analyzer designed for use at pressures of 10^{-5} to 10^{-8} torr is based on the chemisorption of oxygen by a heated tungsten filament contained in a simple triode. The analyzer, developed by Collins and Hoenig (ref. 65) at the University of Arizona, is shown in schematic form in figure 59. The filament is outgassed at 2300° K for 5 seconds and then cooled to 1400° K, at which temperature oxygen is chemisorbed on the filament while carbon dioxide and nitrogen are not. The chemisorption causes a change in work function, detected as a decrease in filament emission current with time; the time required for the current to decrease is a function of the partial pressure of oxygen. Figure 60 illustrates this relationship at several pressures of pure oxygen. The small effect of nitrogen on a single pressure of oxygen is shown in figure 61; it has been found that at a filament temperature of 1400° K, carbon dioxide concentrations at ratios up to 20:1 have no effect.

The principles of gas-phase polarography have been applied to the development of a miniature prototype oxygen detector by Halpert et al.

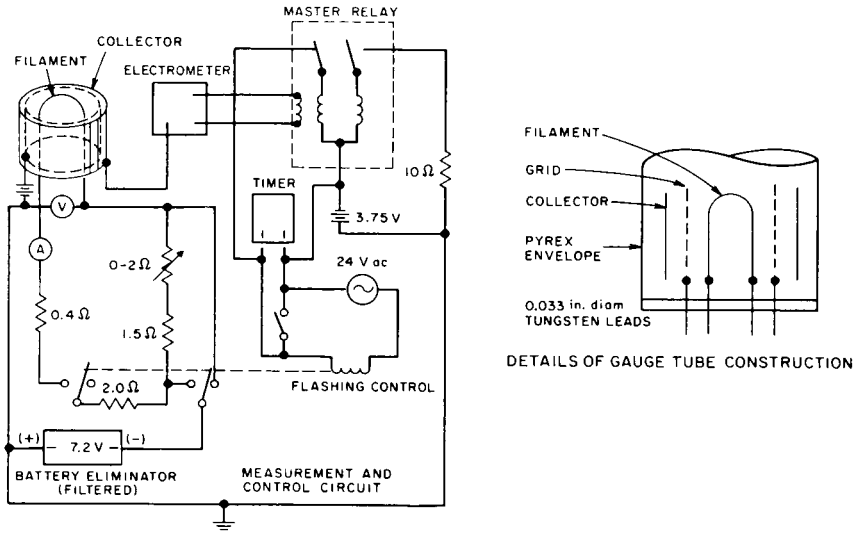

FIGURE 59.—Chemisorption oxygen detector.

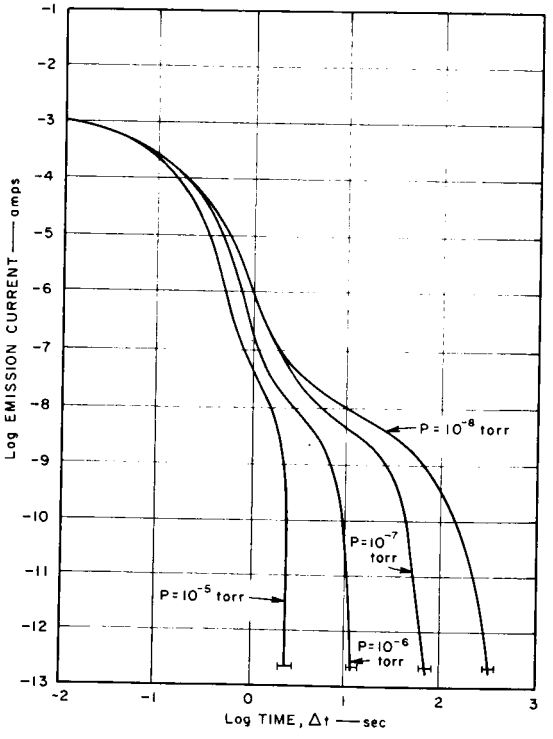

FIGURE 60.—Experimental performance curves for the chemisorption of oxygen on tungsten.

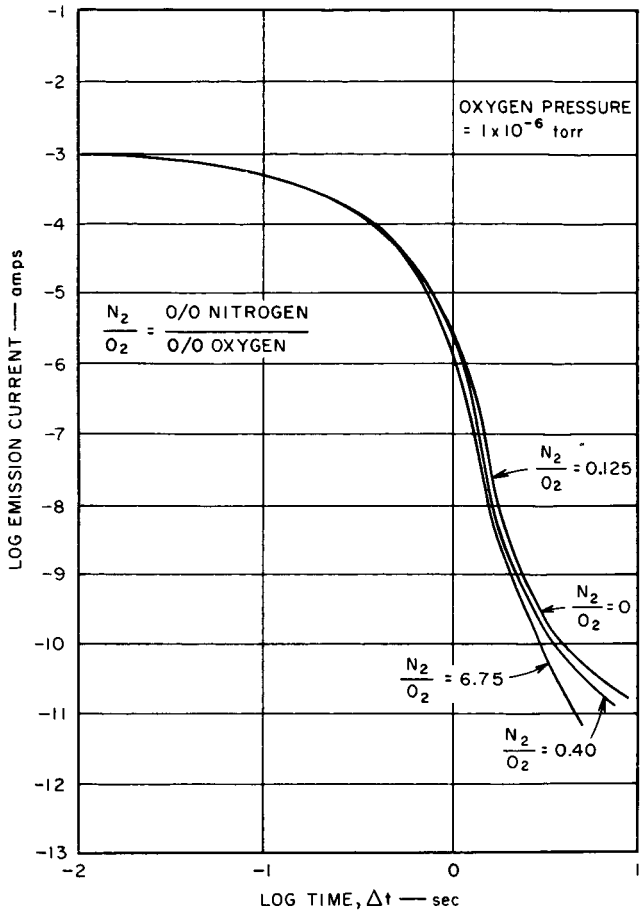

FIGURE 61.—Experimental performance curves for the chemisorption of oxygen on tungsten; the effects of nitrogen on the detection of oxygen.

(ref. 66) at Melpar, Inc., for JPL. The detector is capable of operating over a temperature range of —25° to +80° C and a pressure range of 760 to 10 torr; detection range is 10 parts per million to 100 percent of oxygen. The temperature dependence of the detector is shown in table XIX.

In the detector shown schematically in figures 62 and 63, the gas under test diffuses through a Teflon membrane and into an electrolyte solution in which a platinum microelectrode and a concentric silver-silver chloride reference cell are immersed. To permit sterilization prior to spacecraft use, the device is designed almost entirely of stainless steel and Teflon; arrangement is made for retaining the electrolyte in a closed container

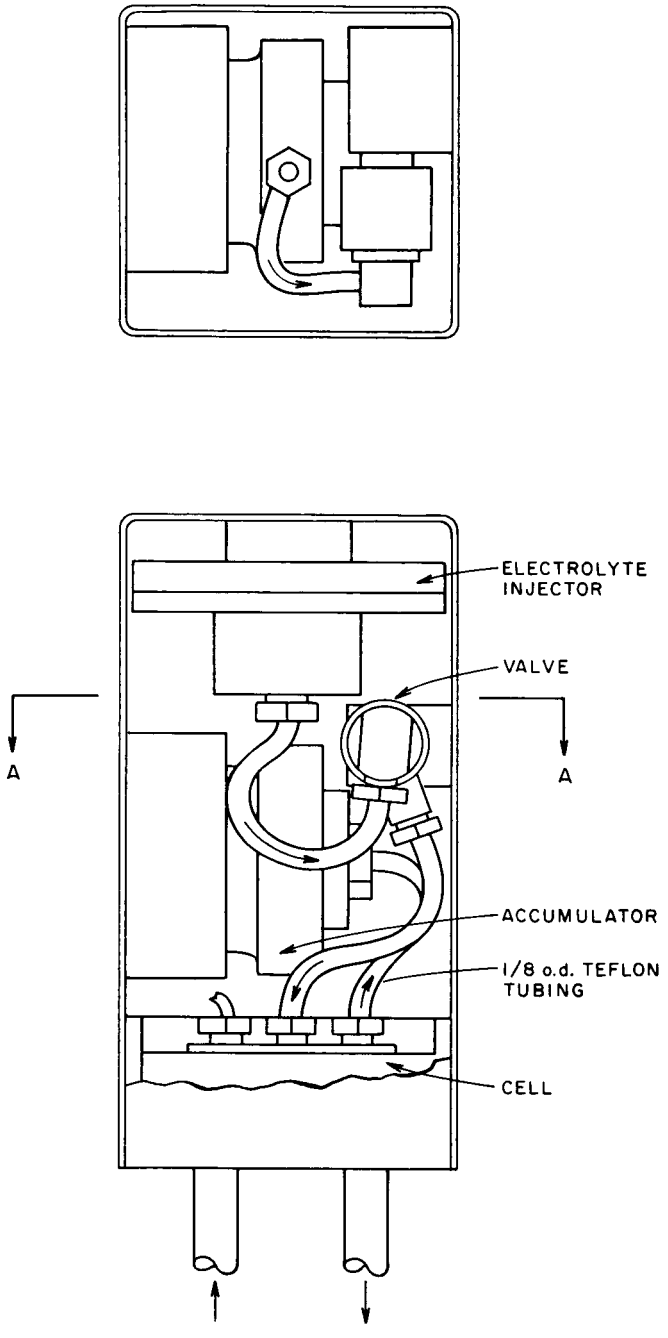

FIGURE 62.—Polarographic oxygen detector.

TABLE XIX.—*Temperature Dependence of the Prototype Polarographic Oxygen Detector*

Oxygen, percent	*Temperature coefficient, μA/°C*
21	0.9
10	.5
1	.1

during sterilization and then injecting it into the cell. The electrolyte found suitable for operation even at low temperatures is a water-methanol-potassium chloride solution (71–24–5 weight-percent) with a phosphate buffer.

The estimation of the oxygen present in an atmosphere is made from the output voltage of a hydrogen-oxygen fuel cell (ref. 67). If a constant stream of hydrogen is supplied to one electrode of the fuel cell, the output will be dependent on the supply of oxygen to the other. Tests were performed with an experimental cell, using platinum-black disks as electrodes and a sulfuric acid electrolyte contained in a thin-glass

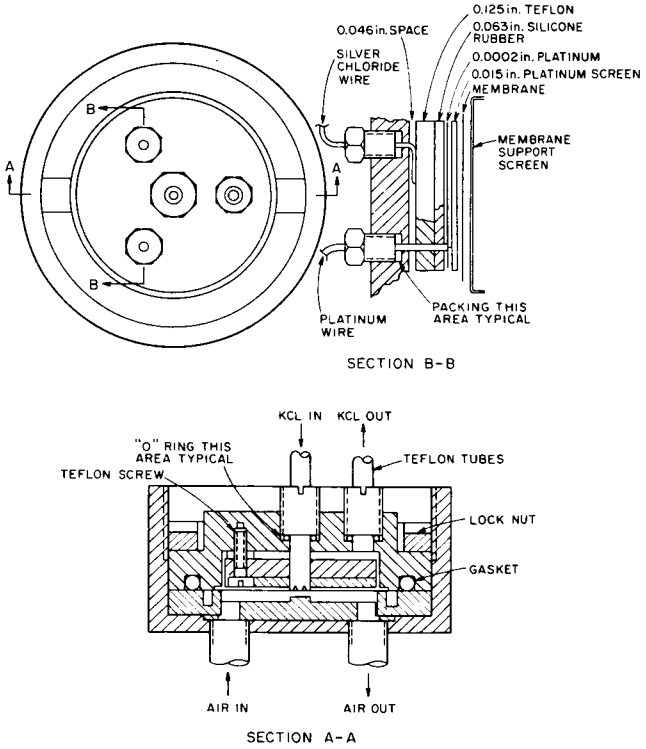

FIGURE 63.—Cell schematic of polarographic oxygen detector.

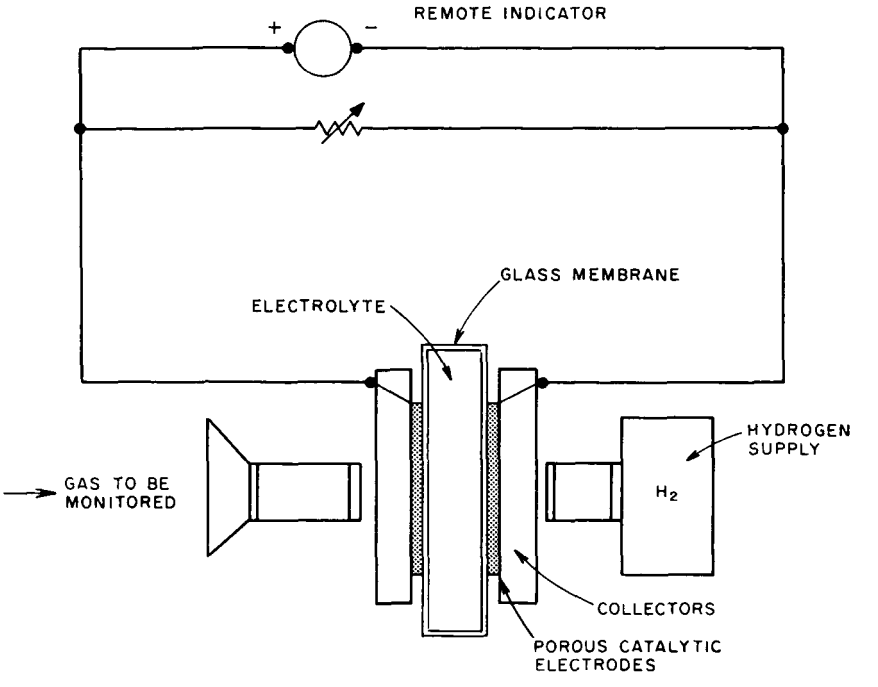

FIGURE 64.—Schematic of fuel-cell oxygen detector.

cylinder. The device, shown schematically in figure 64, is most sensitive to oxygen at partial pressures of 0 to 10 torr, but is nonlinear in response, and therefore calibrations must be made for each unit.

HYDROGEN ANALYZERS

A chemisorption hydrogen analyzer has been developed by Eisenstadt and Hoenig (ref. 68) at the University of Arizona for the detection of hydrogen at pressure ranges of 10^{-5} to 10^{-8} torr. The detector, shown in figure 65, uses a palladium filament operating at 1000° to 1100° C; the change in filament current emission as a function of temperature is shown in figure 66. The detector is ineffective in the presence of oxygen and is slightly affected by the presence of nitrogen (fig. 67).

A miniature hydrogen detector for use in unpressurized sections of rocket booster and sustainer stages is described by Michaels (ref. 69) of the Bendix Research Laboratories. The sensing element of the detector is a thin palladium film deposited on a glass substrate; mechanical and electrical designs were formulated so that a recorded change in resistance would be only a function of the hydrogen partial pressure at the surface of the element. The device operates over a temperature range of —20°

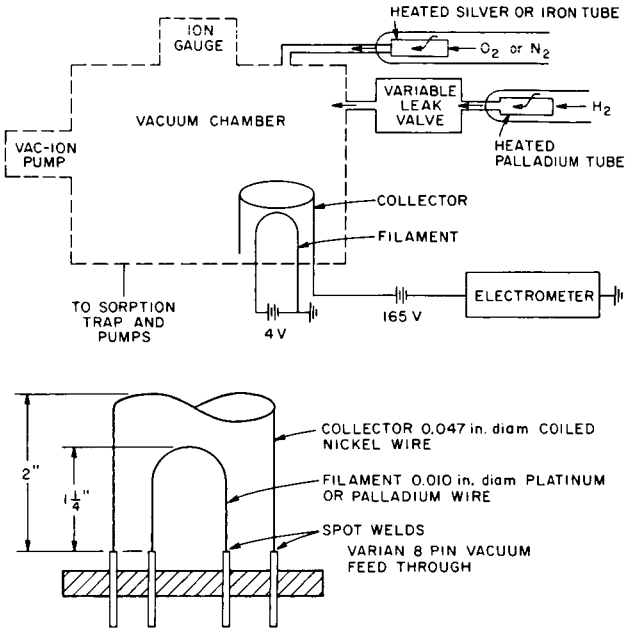

FIGURE 65.—Schematic of chemisorption hydrogen detector.

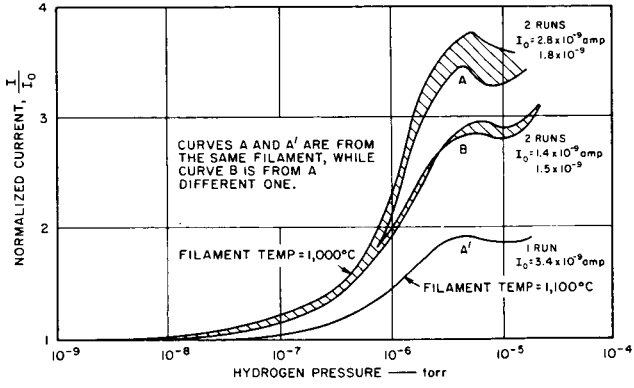

FIGURE 66.—Emission current versus hydrogen pressure.

to +75° C and a pressure range of 760 to 10^{-3} torr; the presence of oxygen may decrease sensitivity for hydrogen from 1 part per million (in nonoxidizing gases) to 1000 parts per million.

CARBON DIOXIDE ANALYZERS

An infrared system developed by the Perkin-Elmer Corp. for the detection of carbon dioxide in spacecraft cabins is described by Bush

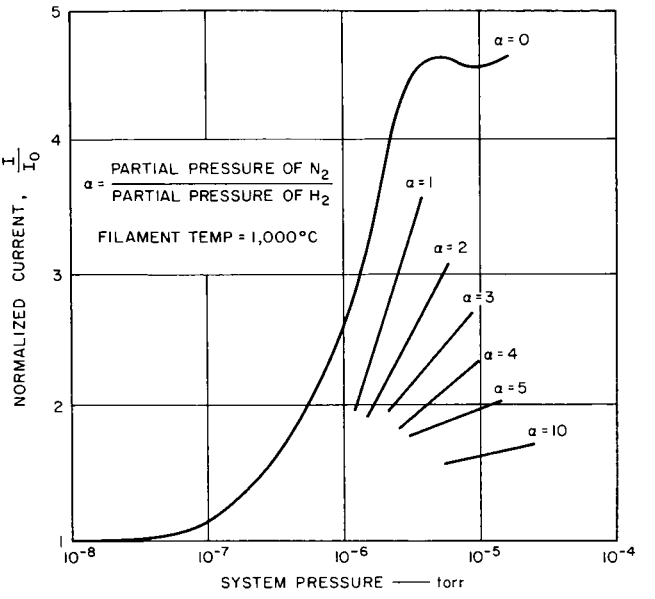

FIGURE 67.—Effect of nitrogen on hydrogen-detector operation.

(ref. 70). The system, shown in figure 68, employs a miniature infrared source, a tuning-fork filter chopper, and an indium antimonide detector which produces a square-wave voltage signal proportional to transmitted infrared energy. The filters, with bandpasses of 4.1 μ and 4.3 μ, are

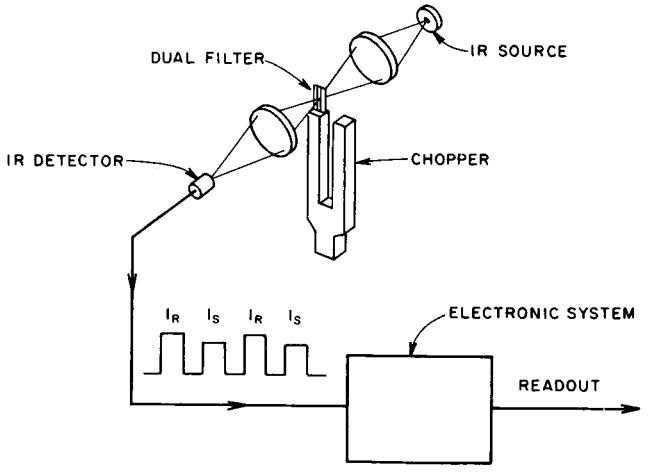

FIGURE 68.—Infrared carbon dioxide sensor.

alternately exposed to the infrared beam by the vibration of the tuning fork; light transmitted through the 4.1-μ filter provides a zero reference for the light transmitted at 4.3 μ which is strongly absorbing for CO_2. The voltage difference of the cycles is proportional to the CO_2 concentration.

A pneumatic, single-beam infrared CO_2 analyzer developed by Beckman Instruments for Ames Research Center is described by Pintar (ref. 71). The CO_2 sensor is a pneumatic detector (fig. 69), which consists of sample and reference detectors optically in tandem and charged with carbon dioxide and carbonyl sulfide, respectively. The CO_2 cell absorbs virtually all incoming infrared energy in the CO_2 absorption band, and the COS cell absorbs infrared energy at the outer fringes of the CO_2 band. A block diagram of the total system is given in figure 70.

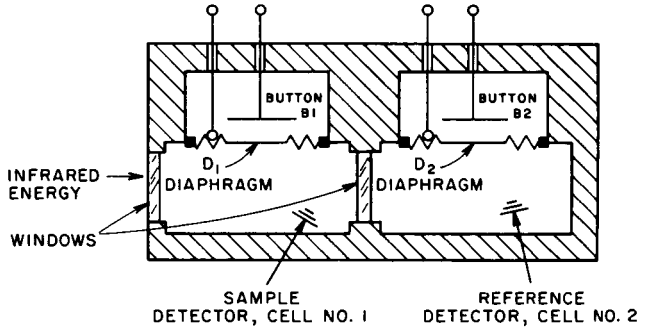

FIGURE 69.—Functional diagram of single-beam pneumatic detector.

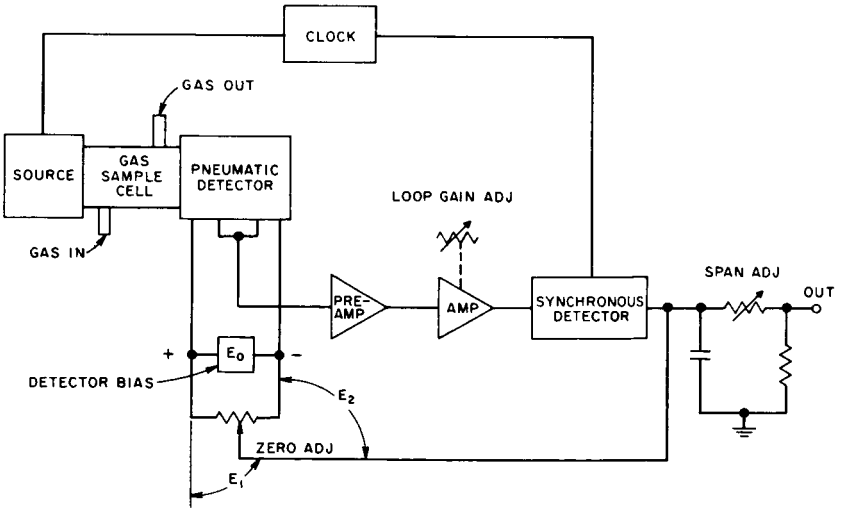

FIGURE 70.—Block diagram of single-beam pneumatic detector.

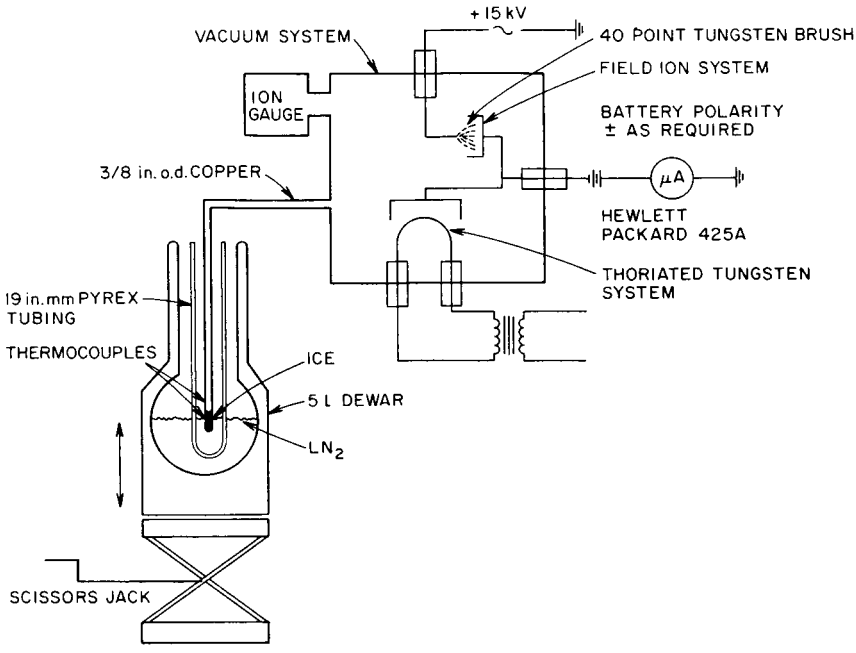

FIGURE 71.—Water-vapor detection and calibration system.

When a gas containing CO_2 is introduced into a modulated infrared beam focused on the detector cells, the loss of infrared energy in cell No. 1 is greater than in cell No. 2; the relative change is indicative of CO_2 concentration and is detected by measuring the volume change in each cell by means of a capacitance-diaphragm system (D1–B1 and D2–B2 in fig. 69). Since the input energy is time varying, an alternating-current signal is produced in each detector cell; by biasing the diaphragm capacitors in opposition, the alternating-current signals are made to cancel out when there is no CO_2 in the reference beam. When CO_2 is present, the signal is reduced in the first cell, causing an unbalance in the second cell; this creates a signal which is amplified and synchronously rectified to indicate CO_2 concentration.

WATER VAPOR ANALYZERS

Electrochemical moisture meters already in wide use for industrial process control are based on the reaction of phosphorus pentoxide with water to form phosphoric acid and its subsequent destruction by electrolysis (regeneration of P_2O_5). The current required to destroy the acid is a function of the amount of moisture which has been trapped. A miniaturized version of this monitor for detection of water vapor in

the Martian atmosphere has been developed for JPL by MacCready (ref. 72) at Meteorology Research, Inc. The breadboard model consists of a moisture sensor, flowmeter, pumping system, readout system, and power supply; it weighs 11 ounces, has a volume of 450 cubic centimeters, and requires 500 milliwatts of power. The range of detection has been demonstrated at three to several hundred parts per million in pressure ranges down to 300 millimeters, with possible adaptation to 100 millimeters.

The feasibility of using field ionization for the specific detection of water vapor at partial pressures of 10^{-6} to 10^{-3} torr in planetary atmospheres was investigated by Hoenig et al. (ref. 73) at the University of Arizona.

When atoms or molecules contact a high electrostatic field (10^7 volts) they are ionized, giving rise to small currents. This high field can be produced by applying a potential of, say, 10^4 volts to a point source of the order of 10^{-5} cm. Field ionization has been used for studies in microscopy (Müller), and at least one commercial version is available for use in mass spectroscopy.

It was found that moisture will be drawn to the tip of the point source(s) maintained at 5 kV and then ionized by a 15-kV pulse. The laboratory system used for the experimental work is illustrated in figure 71; the results obtained by using single or 40-point tungsten tips are shown in figure 72. The equipment shown in figure 71 was also used

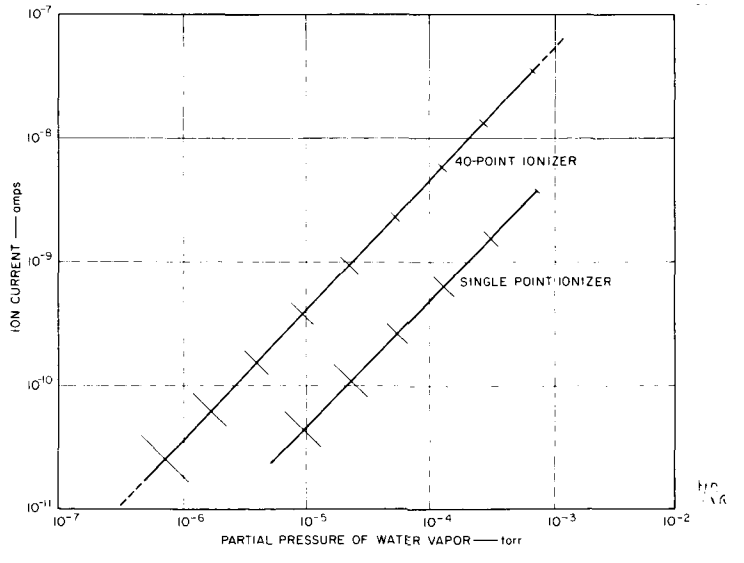

FIGURE 72.—Ion currents versus water-vapor pressure with field ionization system.

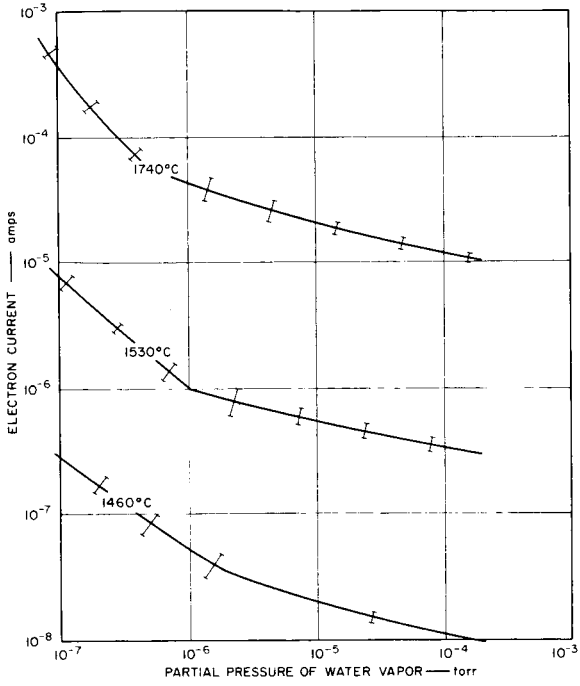

FIGURE 73.—Chemisorption water-vapor detector results.

to study the application of a thoriated tungsten filament for the detection of water vapor at low pressures, since contact with water or oxygen increases the work function of this filament material. As illustrated by the results which are plotted in figure 73, the slope of the emission current changes with partial pressure of water vapor, since the rate of removal of surface thorium by reaction with water vapor changes. The water vapor calibration system used by Hoenig and coworkers is also illustrated in figure 71. The pressure of water vapor in the vacuum system is computed from the temperature-vapor pressure curves for ice; temperature is measured with copper-constantan thermocouples and is controlled by the position of the ice relative to the liquid nitrogen. For calibration of the ion gage, the ice is maintained at liquid-nitrogen temperature (78° K) while the system is pumped down to 10^{-9} torr; then the ice is raised to a warmer temperature, and the reading of the ion gage is compared with the known pressure for ice at its measured temperature.

CHAPTER 9

NASA Development Contributions to Vacuum Equipment

Vacuum systems are an integral part of many analytical instruments (e.g., mass spectrometers, electron microscopes) and an important accessory for many others (e.g., thermogravimetric balances, ultraviolet and infrared spectrometers), as well as indispensable items for many analytical techniques and procedures (e.g., purification, mixing, transfer of gases, vacuum distillation, and chemical reactions in controlled atmospheres). The expanding scope of analytical chemistry includes design and calibration of vacuum systems and components, design and operation of apparatus for use in vacuum systems, and the evaluation of materials in a vacuum environment.

The interest of NASA in the applications of vacuum systems is quite clear since men, materials, and instruments must all survive the vacuum of space.

VACUUM-GAGE CONTROL

A simple, compact, and efficient ionization-gage control unit was designed by Benton (ref. 74) at Goddard Space Flight Center and subsequently flown aboard Aerobee-Hi rockets. A transistorized feedback amplifier was used to maintain a constant emission current over variations in pressure and supply voltage. Ion current was measured in a single range from 10^{-8} to 10^{-4} amperes; a Zener diode was used as a logarithmic element in the collector circuit. The circuitry was one of the forerunners of modern, solid-state ionization-gage controls.

VACUUM-GAGE CALIBRATION

A method for calibrating vacuum gages at pressures as low as 10^{-13} torr was developed and tested by Feakes et al. (ref. 75) at National Research Corp. The method is an extension of the dynamic pressure ratio technique for calibration of gages at pressures greater than 10^{-9} torr reported by Roehrig and Simons (Trans. 8th Natl. Vac. Symp., 1961, p. 511); it involves bleeding helium gas from a known pressure source through a known conductance into a high-vacuum chamber. Helium pressure at the inlet to the capillary conductance is measured by a Nottingham-type gage as shown in figure 74. Gages to be tested are

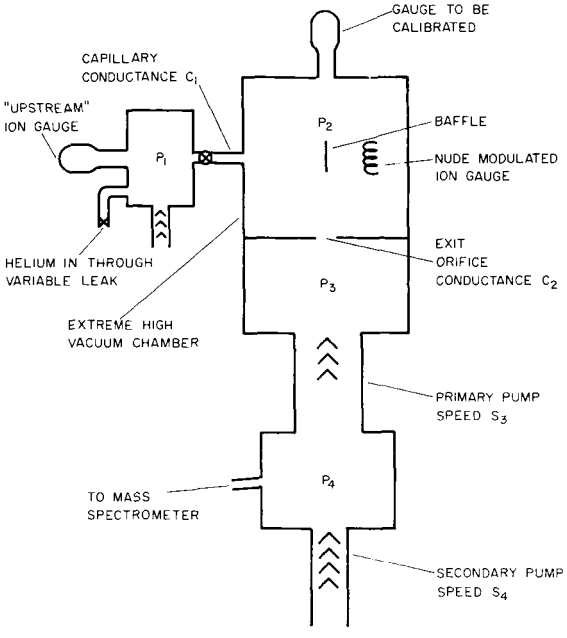

FIGURE 74.—Schematic of National Research Corp. XHV calibration system.

located in the tunnel section of the extreme high vacuum system (XHV)[1] and are tubulated to the XHV chamber, shown in figure 75. The flow of helium from the test chamber is restricted by an orifice of known conductance. With this system, gages can be calibrated independently, without reference to other gages, by using the simple equation

$$P_2 \simeq C_1 P_1 / C_2$$

where

P_2 pressure in test chamber, torr
C_1 conductance of capillary, l/sec
P_1 "upstream" pressure, torr
C_2 conductance of exit orifice, l/sec

The calibrations were cross-checked first by measuring the ratio P_1/P_2, using a nude Nottingham-type gage mounted in the test chamber; the P_1/P_2 ratio remained constant (± 7 percent) for values of P_2 from 5×10^{-9} to 3×10^{-11} torr. Final check was for the ratio of helium pressure P_1 to mass spectrometric measurement of helium partial pressure P_4; the ratio P_1/P_4 remained constant for values of P_1 from 1×10^{-9} torr to 3.6×10^{-6} torr.

[1] A trademark of National Research Corp.

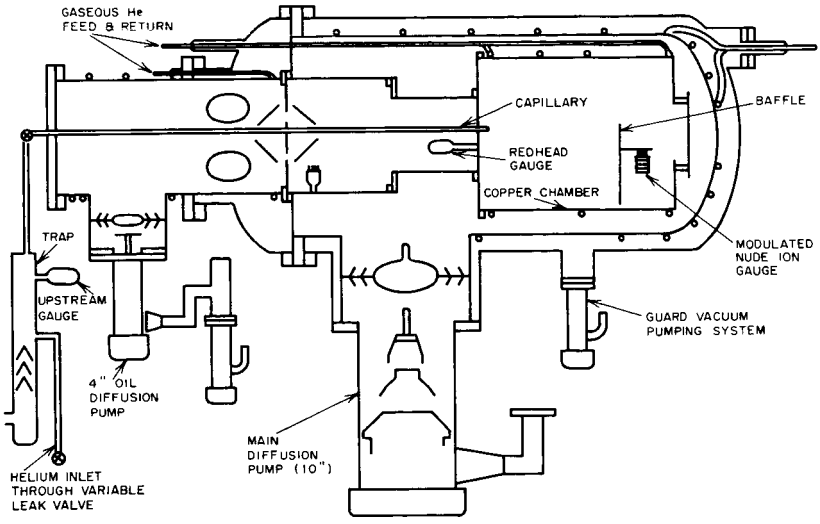

FIGURE 75.—National Research Corp. XHV system.

High-vacuum gages calibrated by Feakes and coworkers included a normal magnetron gage, an inverted magnetron gage, a nude modulated ion gage, and a modulated suppressor grid gage. The performance of these gages is indicated in figure 76.

McLEOD GAGE EXTENSION

The McLeod gage, a highly refined mercury manometer, is used as a standard for calibration of other pressure gages; its accuracy is generally considered to be about 1 to 2 percent for pressures greater than 1×10^{-4} torr. A multiple-compression technique was developed by Kreisman (ref. 76) at the Geophysics Corp. of America for extending the range of a McLeod gage to 10^{-6} torr with greater accuracy and precision than is available with single measurements. For multiple compression measurements, the gage is equipped with a valve which will permit storage of successive additions of gas in the closed end of the capillary. The gas to be measured is compressed into the capillary, and the small valve is closed below the mercury level; then the mercury is lowered, leaving a short column above the valve, and a second sample is let into the compression bulb; the second sample is compressed by raising the mercury, and the valve is opened so that the two samples are combined in the closed end of the capillary; the cycle is repeated several more times (reminiscent of a Toepler pump). Measurements can be made after each compression. This system effectively increases the range of pressures measurable by a McLeod gage and tends to eliminate the

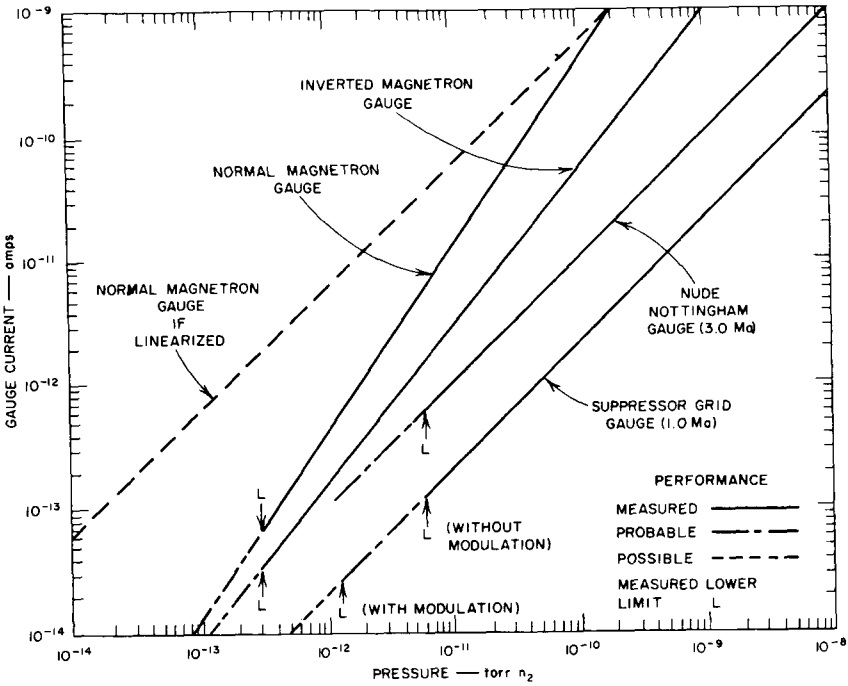

FIGURE 76.—Comparison of gages at extreme low pressures.

effect of random variations of capillary depressions and reading errors. A summary of the results obtained with this technique is given in table XX.

The valve found most suitable for use with the multiple-compression technique is a magnetic sphere which can be manipulated by means of a small permanent magnet or an electromagnet as shown in figure 77; the sphere has a diameter just a little larger than the capillary (about 3/32 inch) and may be made of chrome alloy, 440 stainless steel, pure nickel, Kovar, or iron. No modification to the McLeod gage is required unless the sphere cannot be seated properly.

DIFFUSION-PUMP BAFFLE

To prevent the backstreaming of diffusion pump oil into vacuum systems, the use of a heated grid to decompose the oil vapor into low-molecular-weight compounds that can be pumped away is suggested (ref. 77). The grid, which would replace a cryogenic baffle, is made by threading a nichrome wire through two high-temperature insulating rings and positioning the rings so that the installed wires are perpendicular to each other. It operates at 900° C and requires a current of 10 amperes at 200 volts.

TABLE XX.—*Comparison of Pressure Readings and Their Deviations for Multiple-Compression McLeod-Gage Measurement*

[Each value is an average of 5 readings]

(1) Number of compressions	(2) Ionization gage system pressure reading, mm Hg	(3) Combined sample average mercury column length, mm [a]	(4) Combined standard sample deviation of mercury column length, mm	(5) Combined sample average pressure, mm Hg	(6) Fractional standard deviation of combined sample pressure percent	(7) Differences of combined sample average pressures, mm Hg	(8) Average pressure of a single sample, mm Hg [a]	(9) Fractional standard deviation of average sample pressure, percent
1	9.10×10^{-6}	8.94	0.134	3.185×10^{-6}	2.99	8.18×10^{-6}	8.18×10^{-6}	2.99
2	9.10×10^{-6}	13.28	.144	1.806×10^{-5}	2.17	9.88×10^{-6}	9.03×10^{-6}	2.17
3	9.00×10^{-6}	16.06	.167	2.641×10^{-5}	2.08	8.35×10^{-6}	8.80×10^{-6}	2.08
4	8.95×10^{-6}	18.61	.108	3.546×10^{-5}	1.16	9.06×10^{-6}	8.87×10^{-6}	1.16
5	8.90×10^{-6}	20.79	.065	4.426×10^{-5}	.63	8.79×10^{-6}	8.85×10^{-6}	.63

[a] These values are based on the assumption that the individual contributions of each sample or compression are equal. According to col. (7), these contributions are quite equal.

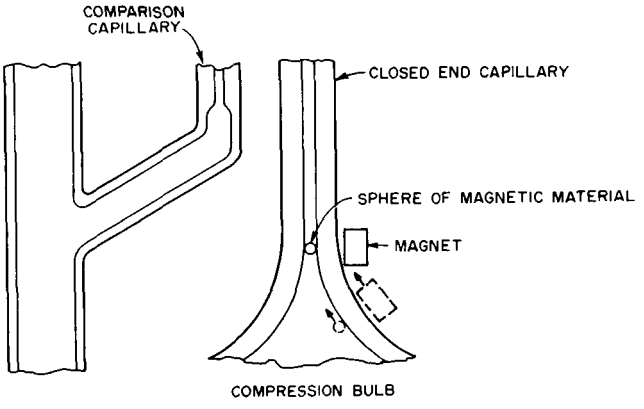

FIGURE 77.—Magnetic-sphere valve arrangement for storing gas in a McLeod gage capillary.

The diffusion pump used with the heated-baffle vacuum system must be several times larger than those ordinarily employed because of the increased gas load (from decomposition of oil); furthermore, the baffle must be designed to insure that oil molecules backstreaming from the pump come into contact with the heated coils.

PERMEABILITY CELLS

The selection of appropriate materials for use as sealants or diaphragms in vacuum systems requires a knowledge of the permeability of the materials to gases in order to minimize gas leaks from the atmosphere into the vacuum system; alternatively, permeability data are used for the selection of materials to contain pressurized gases for spacecraft use without undue leakage into the vacuum of space. In general, a permeability apparatus consists of a fixture to hold a sample film which is attached on one side to a source of gas of known pressure and on the other side to a device which will measure the increase in pressure of a previously evacuated volume as the gas permeates the sample. Basically, a permeability cell consists of two metal flanges between which a sample film is placed; the film is supported by sintered or screen metal, and the unit is sealed with O-rings.

An improved permeability cell to be used with a mass-spectrometry technique was designed by Muraca et al. (ref. 78) at Stanford Research Institute. By using a mass spectrometer as the pressure-measuring device, the identity of the gas being measured is firmly established, minute quantities of gases can be detected, and the flow rate of each gas in a mixture can be determined simultaneously. Figure 78 shows

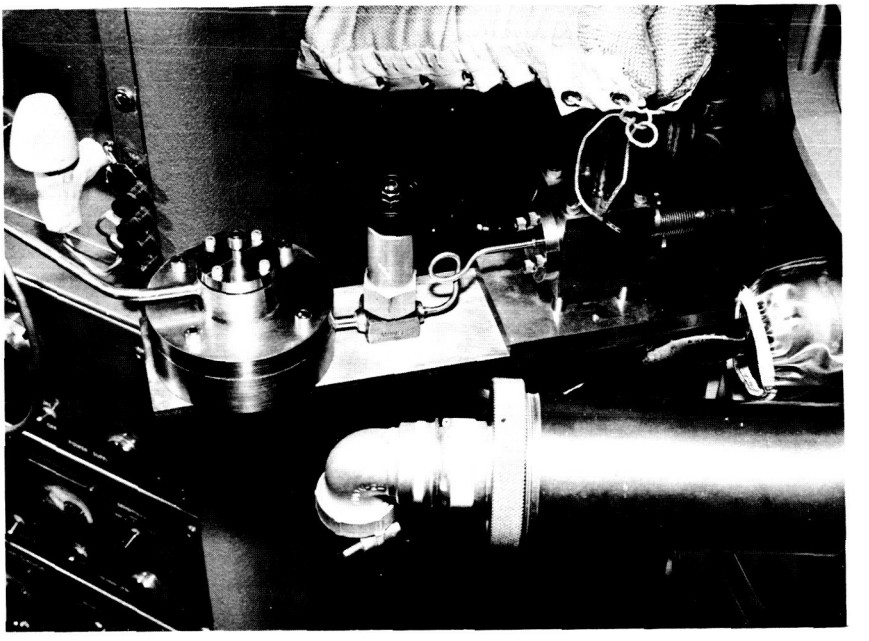

FIGURE 78.—Permeability cell in place on a modified CEC model 21–103C mass spectrometer.

the cell in place on a modified CEC Model 21–103C mass spectrometer. The sample is outgassed on both sides prior to a determination by use of the inlet system and the exhaust system of the spectrometer. The Hoke valve permits accumulation of very slowly permeating gases into a known volume for periodic measurement.

The cell is so constructed that a thin-film polymeric sample of the order of 1-mil thickness or a film up to 50-mil thickness can be used; provision is made for compressing a film in place so that observations can be made as to whether gas diffusion rates through a polymer under compression differ from those for a polymer in a relaxed state. As shown in the schematic drawing in figure 79, the cell also can accommodate thin plates or other incompressible materials.

Permeable membranes have been used for the calibration of a residual gas analyzer. By using a simple permeability cell in conjunction with a CEC Model 21–620 mass spectrometer, Caruso (ref. 79) at Marshall Space Flight Center measured the permeability rates of a number of polymers to atmospheric gases in order to select a material which would provide a leak standard for a residual gas analyzer (CEC Diatron). A 1/32-inch-thick Teflon diaphragm was finally selected, since the permeation of gases through this material was large enough to be measured

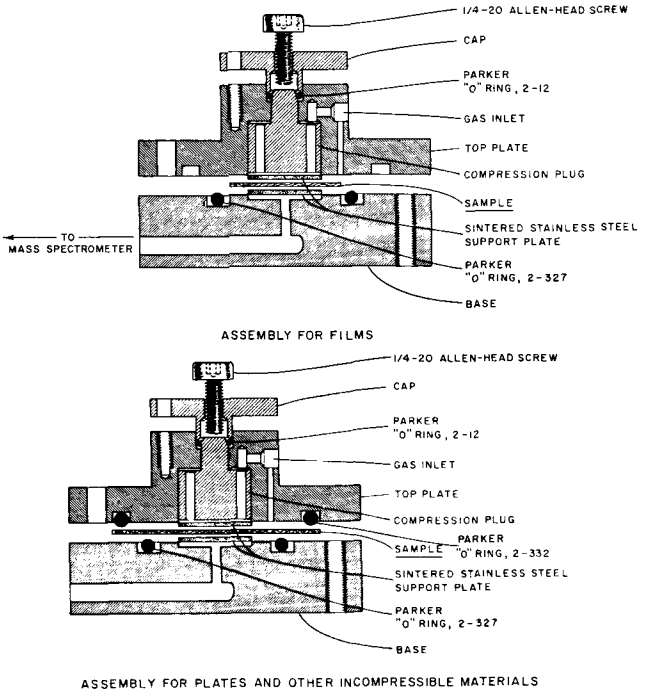

FIGURE 79.—Schematic drawing of permeability cell for a mass spectrometer.

by the Diatron but not so large as to increase appreciably the pressure of the vacuum system being checked. When the Diatron was set in place on the vacuum system, gases were allowed to permeate through the Teflon standard into the vacuum system, and the Diatron was calibrated for its sensitivity to a continuous flow rate for each gas.

POLYMER SCREENING APPARATUS

Vacuum systems and space systems are easily contaminated by certain substances which outgas from polymeric materials. In view of the "polymer explosion" of recent years, there is need for rapid, multiple screening of materials. The two properties which provide the most immediate information are the loss in weight under thermal-vacuum conditions and the quantity of volatile condensable material (VCM) which is released. A micro-VCM apparatus has been designed by Muraca et al. (ref. 80) at Stanford Research Institute to provide the above information for JPL. The apparatus is a multiple unit which will provide within 24 hours values for the maximum VCM which will be released and the weight loss which will be incurred by polymeric materials exposed to an environment of 125° C and 10^{-6} torr.

The apparatus is attached via a 6-inch elbow to a high-speed vacuum system; as shown in figure 80, the elbow is fitted with vacuum gages and utility plugs which carry the lines for power, water cooling, and thermocouples. The apparatus consists of 2 units, each of which is set up for 12 samples. The front or back of each unit is shown in figure 80; samples are contained in solid copper blocks in individual bored-out compartments, which are covered by the copper disks shown in the front of the photograph. The heating element for the block is Xactglo wire

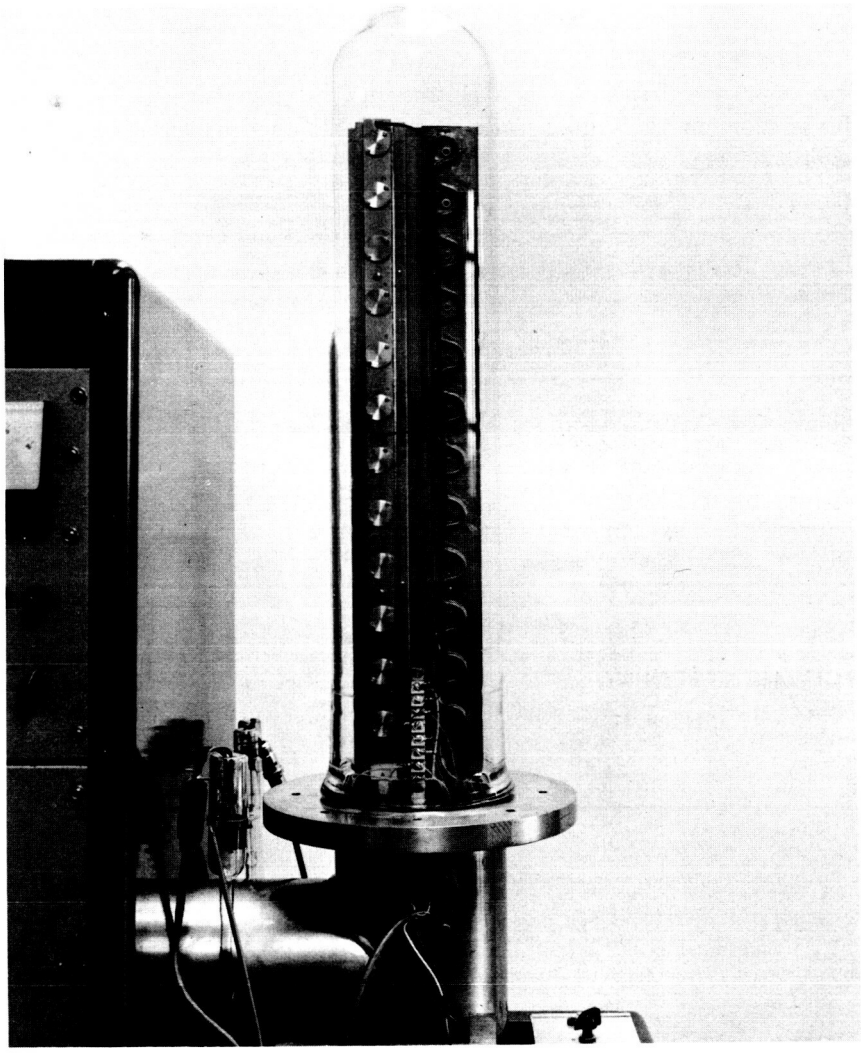

FIGURE 80.—Micro-VCM apparatus mounted on 6-inch vacuum console.

which has been soldered in place at sufficient intervals to maintain uniformly a block temperature of 125° C. Also shown in the photograph is the copper plate which holds the VCM collector plates, maintained at 25° C by the cooling lines shown soldered in place; the screw heads appearing between the cooling lines hold the collector plates in place; the plates cannot be seen in the photograph.

The path from the sample compartments to the collector plates is defined by a hole of large size in comparison with the compartment size; cross-contamination between compartments is eliminated by insertion of an egg-crate-like baffle. Sample sizes are of the order of 100 milligrams, and both samples and VCM collector plates are weighed on a microbalance. Some typical results, showing a range of good to poor performance, are given in table XXI; the various polymers listed are used for elastomers, conformal coatings, structural applications, and circuit boards.

TABLE XXI.—*Micro-VCM Determinations* [a]

[24 hr at 125° C and 10^{-6} torr; VCM collector plates at 25° C]

Material	Mfr [b]	Total wt loss, percent	VCM, wt-percent	Noncondensable wt loss, percent	Notes [c]
Enjay butyl EX-1090	ECC	0.80	0.24	0.56	1, 3
Enjay butyl EX-1091	ECC	.70	.20	.50	1, 3
Enjay butyl EX-1092	ECC	.86	.10	.76	1, 3
SE-555 (gray)	GE	.53	.30	.23	1, 2
Hycar-520-67-108-1	BFG	1.90	.17	1.73	1, 2
JPL-1001	AA	.20	.10	.10	1, 4
JPL-1002	AA	.19	.03	.16	1, 4
Lexan 100-111	GE	.06	.02	.04	1, 2
Lexan 101-111	GE	.08	.01	.07	1, 2
Lexan 101-112	GE	.09	.04	.05	1, 2
Lexan 103-112	GE	.08	.00	.08	1, 2
Micarta H-2497	WE	.18	.00	.18	1, 2
Micarta 65M25	WE	.43	.00	.43	1, 2
Nordel A5411A-115	DuP	1.80	1.29	.51	1, 5

[a] Values are average of 2 determinations: for duplicate samples, VCM and wt loss may vary ±0.06 percent abs.

[b] Abbreviations used in the table are as follows: ECC, Enjay Chemical Co.; BFG, B. F. Goodrich Co.; AA, Ablestik Adhesive Co.; GE, General Electric Co.; WE, Westinghouse Electric Co.; DuP, E. I. du Pont de Nemours Co., Inc.

[c] 1. Conditioned in 50 percent humidity for 24 hours before initial weighing, and stored in desiccator for 30 minutes before final weighing
2. Sample used as received
3. Postcured 4 hours at 150° C
4. Cured 4 hours at 75° C
5. Postcured 18 hours at 175° C

CHAPTER 10

NASA Development Contributions to Life-Detection Techniques

One of the oldest biological techniques for seeking direct evidence of life such as micro-organisms is the exposure or inoculation of a sterile nutrient and subsequent examination of the nutrient under the microscope for unicellular or multicellular activity; activity in this sense does not mean simply movement, but the continuous growth characteristic of the lower forms of life. Extension of this examination has been provided by the biochemist in his studies of metabolism; for example, the relationship of oxygen consumed to carbon dioxide formed in the case of human life and a reversal of the process in the case of most plant life. In turn, it has become the task of the analytical chemist to isolate and identify the structures which give continuity to life and those which destroy it, and to develop procedures which provide a quantitative measure for inorganic and organic components in living systems.

The analytical chemist may employ any or all of the instrumentation previously described in this survey in the quest for life itself or for substances which imply the presence of life. For example, amino acids may be analyzed by gas chromatography; the presence of ketones, esters, amines, etc., can be determined by ultraviolet and infrared spectroscopy as well as by classical chemical procedures; the role of metallic elements may be traced by flame photometry, nuclear activation, and radioactive tracer techniques; and the structure of enzymes, vitamins, etc., may be determined by mass spectrometry.

The search for life or life-indicating substances by NASA is prompted not only by scientific intent to determine the extent to which life has been established on the planets in our universe but also to obtain insight into the formation of planets and the generation of atmospheres so as to lead to the unraveling of the mystery of our universe.

The application of instrumental techniques to the characterization of organic compounds that may be indicative of life has been discussed in the chapters on ultraviolet spectroscopy, mass spectrometry, and gas chromatography.

For actual space exploration, modern analytical techniques for life detection require miniaturization and remote operation; they also often

require concentration on one specific functional determination which will yield maximum information.

GULLIVER

The development of Gulliver, a radioisotope biochemical technique for detection of life on Mars, was initiated at Resources Research, Inc., by Levin et al. (refs. 81 and 82) and continued at Hazleton Laboratories, Inc., by the same investigator (ref. 83). The technique involves the measurement of the radioactive carbon dioxide which will be released by the metabolism of an isotope-labeled nutrient by extraterrestrial micro-organisms; the prototype models of the device, developed by the American Machine & Foundry Co. (refs. 81 and 83), provide for the collection of extraterrestrial soil, release of the nutrient to the sample, and the measurement of resulting labeled carbon dioxide by Geiger counters.

Two types of nutrient media have been developed, both containing labeled compounds. The first is a complex medium incorporating vital inorganic salts, organic extracts, and compounds; it is designed to

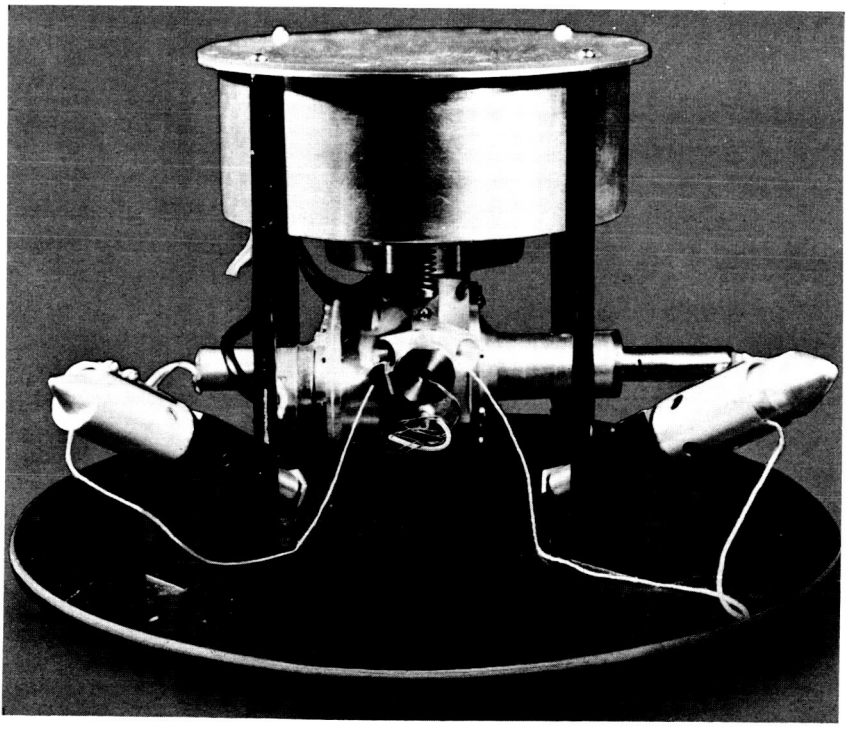

FIGURE 81.—Gulliver III.

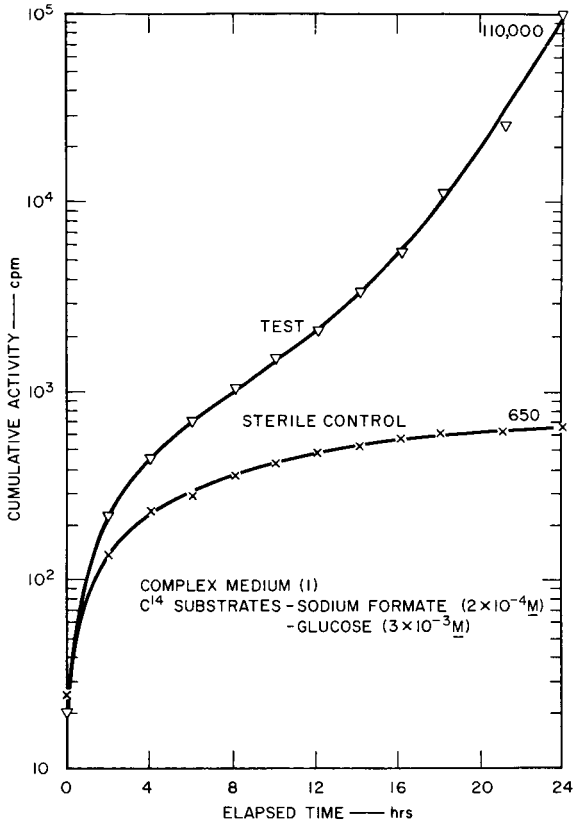

FIGURE 82.—Field test of Gulliver, November 27, 1962.

support a wide variety of micro-organism species. Aerobes, anaerobes, facultative anaerobes, thermophiles, mesophiles, psychrophiles, heterotrophs, autotrophs (including phototrophs and chemotrophs), sporeformers and nonsporeformers have been successfully detected with this medium. Since certain species of micro-organisms are inhibited by various organic compounds present in complex media, a simple medium was also developed, which, except for the labeled compounds, contains no organic constituents.

The selection of radioactive compounds for incorporation into the medium was based upon their rapid metabolic conversion into radioactive carbon dioxide by both aerobic metabolism (Krebs cycle) and anaerobic metabolism (Emden-Meyerhof route). The most suitable radioactive substrates have been a combination of carbon 14-sodium formate and uniformly labeled carbon 14-glucose. Other C^{14}-labeled compounds such as amino acids, microbial extracts, and similar com-

pounds have been evaluated. Racemic mixtures of the labeled and non-labeled optically active compounds will be incorporated into the media wherever possible, since optically active specificity, different from that of terrestrial micro-organisms, may be exhibited by life on Mars.

The instrument is shown in figure 81. Two of these instruments, one test and one control, will be incorporated into a capsule designed to land on Mars; the radioactive media are contained in sealed ampoules to permit heat sterilization of the instruments. Upon landing, squibs fire projectiles which deploy 25-foot lengths of silicone grease-impregnated retrieval line over the surface of the planet. A motor then reels the line, together with the adhering particulate matter, into the incubation chamber. After the line has been retrieved, the incubation chamber is sealed and the ampoule broken, releasing the radioactive medium onto the line. A thermostatically controlled heater prevents freezing of the

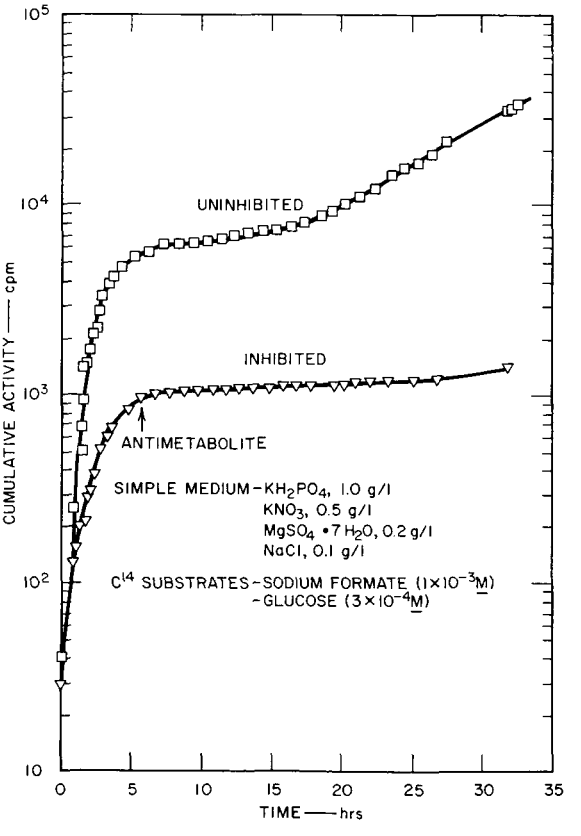

FIGURE 83.—Field test of Gulliver, February 7, 1963.

media. If organisms are present on the soil particles and are able to metabolize any of the labeled substrates, radioactive gas will be produced.

A thin-window Geiger tube is mounted above the incubation chamber. Metal and solid-foam baffles prevent the Geiger tube from "seeing" the radioactive media; however, gas produced by metabolism is free to travel through the baffles. The window of the Geiger tube is coated with barium hydroxide which traps and absorbs carbon dioxide. As $C^{14}O_2$ collects on the coated window, it is detected by a rise in measured radioactivity. The active Geiger tube is surrounded by a ring of Geiger tubes connected in anticoincidence circuitry to differentiate metabolic activity from a high background resulting from cosmic rays or other radioactive sources.

Simultaneous with the inoculation of the test instrument, the control instrument is inoculated and then injected with a broad-spectrum anti-

TABLE XXII.—*Composition of Basal Media*

Medium and composition	Concentration (g/l)
M9 (C^{14} substrates):	
K_2HPO_4	1.0
KNO_3	.5
$MgSO_4 \cdot 7H_2O$	.2
NaCl	.1
Soil extract, ml	100.0
M8 (C^{14} substrates):	
K_2HPO_4	1.0
KNO_3	.5
$MgSO_4 \cdot 7H_2O$	.2
NaCl	.1
M5 (C^{14} substrates):	
K_2HPO_4	1.0
KNO_3	.5
$MgSO_4 \cdot 7H_2O$	.2
NaCl	.1
$FeCl_3$	.01
Na_2SO_3	.2
Malt extract	3.0
Beef extract	3.0
Yeast extract	13.0
Ascorbic acid	.2
L-cystine	.7
Bacto casamino acid	4.0
Proteose peptone No. 3	20.0
Soil extract, ml	250.0

metabolite. The production of a typical biological growth curve from the test instrument and a negative or substantially reduced response from the control instrument would constitute evidence of the presence of microbial life on Mars.

Gulliver has been tested in the laboratory and in the field a number of times. Figure 82 presents field test data obtained from two of the instruments, one serving as a test, the other as a sterile, uninoculated control. Self-degradation of the radioactive compounds in the medium resulted in a 650-counts-per-minute evolution of $C^{14}O_2$ by the sterile control in 24 hours; the flight instrument is designed to provide non-radioactive carrier CO_2 to flush out radioactive CO_2 accumulated during an 8-month flight to Mars.

The results of a field test in which an antimetabolite was injected into the control instrument are shown in figure 83. The timing of the

TABLE XXIII.—*Organisms Evolving* $C^{14}O_2$ *When Tested in M5 Medium*

Organism	CPM	Organism	CPM
Response within 3.5 hours			
Arthrobacter simplex	1 629	*Mycobacterium phlei*	1 913
Azotobacter agilis	28 956	*Pseudomonas delphinii*	971
Azotobacter indicus	1 868	*Pseudomonas fluorescens*	6 701
Bacillus subtilis spores	11 784	*Pseudomonas maculicola*	16 266
Bacterium bibulum	7 221	*Rhodopseudomonas capsulata*	365
Chlorella spores	323	*Rhodospirillum rubrum*	420
Clostridium pasteurianum	1 698	*Saccharomyces cerevisiae*	3 093
Clostridium roseum	5 367	*Staphylococcus epidermidis*	3 219
Clostridium sporogenes	664	*Streptomyces fradiae*	443
Escherichia coli	65 389	*Xanthomonas beticola*	58 189
Micrococcus cinnabareus	840	*Xanthomonas campestris*	537
Response within 6 hours			
Photobacterium phosphoreum	2 423	*Thiobacillus thiooxidans*	102
Thiobacillus novellus	141		
Response between 6 and 24 hours			
Rhizobium leguminosarium	1 123		

NOTE.—Radioactive substrates: glucose - C^{14} (uniformly labeled) and sodium formate - C^{14}.

antimetabolite injection was unfortunate in that injection coincided with the initial plateau demonstrated by the uninhibited culture. Nevertheless, the difference in response between the inhibited and uninhibited culture is quite apparent.

Laboratory tests were conducted both with known micro-organisms and with soils collected from the eastern section of the United States and desert areas. The most satisfactory basal media for these experiments are listed in table XXII; the responses of 26 micro-organisms to medium M5 are summarized in table XXIII. All of about 80 soil samples tested yielded a positive response to the radioactive inoculation, and some typical results are given in table XXIV.

TABLE XXIV.—*Evolution of* $C^{14}O_2$ *From Various Soils Incubated in Planchets*[a]

Test sample	Quantity used, mg	Time elapsed after inoculation, min	Radioactivity less sterile control, CPM
Desert soils:			
No. 1	25	45	4 083
No. 75	25	45	1 478
No. 1	50	45	3 450
No. 1	50	180	9 100
No. 74	50	45	336
No. 74	50	180	1 140
No. 75	50	45	4 760
No. 75	50	180	11 800
No. 1	100	210	5 725
No. 74	100	210	2 799
No. 75	100	210	5 099
Garden soils:			
A	100	45	6 747
B	100	45	7 132
C	100	45	1 040
Field soils:	10	30	3 802
	25	45	4 000
		180	8 750
	50	45	5 000
		180	8 150
	100	45	5 550
	100	180	10 300

[a] Data are taken from many experiments carried out under various conditions and in different media.

MARBAC

"Marbac" is the name given by the Marquardt Corp. to the life-detecting system which was developed by Ellis (ref. 84). The system is based on the measurement of the changes in oxidation-reduction potentials which are caused by the metabolic processes of microbial life. As shown in figure 84, Marbac consists of multiple cells which permit the use of nutrients of several different compositions in test cells and control cells; by the difference in redox potentials generated by the metabolic reaction in solutions of differing compositions, the identification of various kinds of micro-organisms may be established.

Platinum and saturated calomel electrodes were used for measuring the redox potentials; the calomel electrodes were connected to a Luggin capillary salt bridge (0.9 weight-percent NaCl). The platinum-wire electrodes were coated with a chemically resistant paint and only the tips were exposed. The electrode system is sterilizable by autoclaving. As shown in figure 85, the reproducibility of potential readings is well within 20 millivolts. It was also found that the system could be miniaturized so that essentially the same changes in potential could be obtained for 0.4 milliliter of nutrient and desert-soil micro-organisms as for 31 milliliters of nutrient with the same micro-organisms (690 mV).

The effects on the redox potentials of growth media and growth factors with time were studied by using *Escherichia coli,* an organism commonly used for metabolic studies; potential changes as high as 600 millivolts within 3½ hours were observed. Many other organisms and many compositions of nutrient were studied as well as parameters of time and temperature; the rates of potential changes varied with differing combinations, but in all cases the presence of bacteria produced a change in potential.

MULTIVATOR

Multivator is an instrumental concept devised by Lederberg and Leventhal (ref. 85) at the Stanford University School of Medicine for conducting a series of biochemical experiments on Mars. Detection techniques under study include nephelometry, fluorometry, and colorimetry. The general design of Multivator is shown in figure 86. Each of the 15 modules contains a reaction chamber, solvent-storage chamber, tapered-pin valve, explosive-charge bellows, and filtered light source. The solvent chamber is sealed prior to operation by a thin diaphragm placed in front of the pointed valve tip.

In operation, dust containing microbes is filtered to eliminate large particles and blown through the inlet tube into the reaction chambers where it is collected on sticky walls; the dust-free "air" is then exhausted through a port. Inlet and outlet ports are closed, and the solvent is

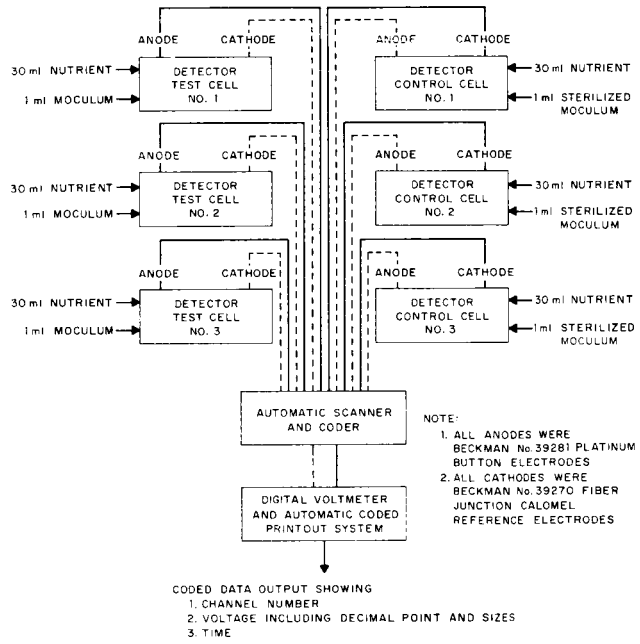

FIGURE 84.—Typical laboratory system for Marbac.

INOCULUM: 1 gram SOIL IN 10 ml STERILE, DEIONIZED WATER, SHAKEN 10 min
INOCULUM SIZE: 1 ml ABOVE SUSPENSION (AFTER SETTING) IN 30 ml OF MEDIA* (APPROXIMATELY)

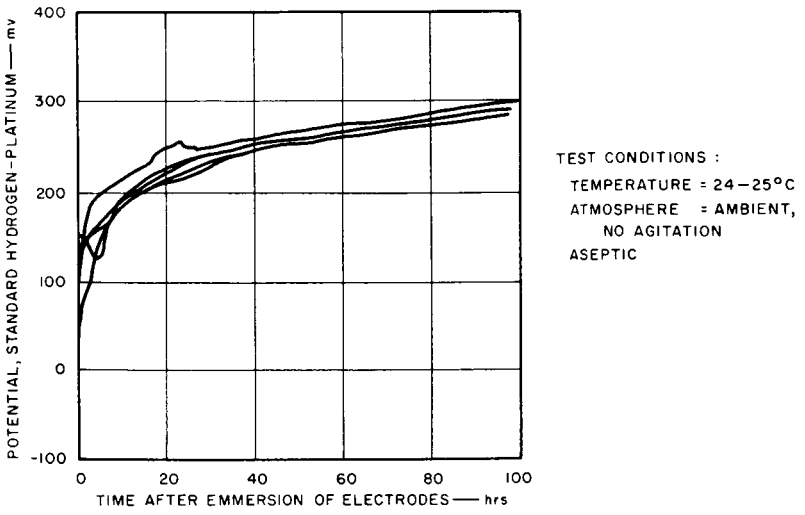

FIGURE 85.—Reproducibility of Marbac electrode potentials.

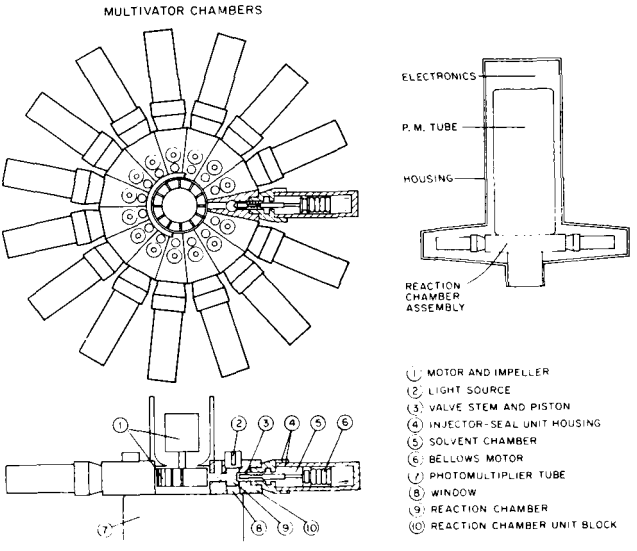

FIGURE 86.—Schematic of Multivator assembly.

injected into the reaction chambers which contain a substrate of dry reagents. After a predetermined time for hydrolytic reaction, fluorescent excitation lamps are turned on sequentially, and the fluorescent level in each chamber is detected by a phototube.

Particular attention has been paid to the assay for phosphatase activity since it occurs widely in terrestrial organisms, catalyzes a wide range of reactions with moderate specificity, is involved with the role of phosphorus in metabolism and energy transfer, and can be detected with high sensitivity. The assay of soil enzymes by fluorimetry is reported by Hochstein (ref. 86). The assay for phosphatase is based on the hydrolysis of 1-naphthyl phosphate in the presence of an enzyme to 1-naphthol and inorganic phosphate. The mixture is irradiated with light at 336 mμ and the fluorescence due to formation of 1-naphthol is measured at 460 mμ. The results of the assays of samples collected throughout the United States indicate that two types of phosphatase activity exist; that is, one with maximum activity in acidic solution, and the other with maximum activity in alkaline solution; soil pH could not be used to differentiate the activities. A "blank" fluorescence arising from active substances in soil complicated the analysis; there was no correlation of this with the amount of phosphatase.

The assay for soil aminopeptidases uses L-leucyl-2-naphthylamide as the substrate. The hydrolysis yields 2-naphthylamine which fluoresces at 423 mμ. Not all of the soils tested indicated peptidase activity; for

those that did, there was no correlation with phosphatase activity. Although the peptidase assay is not as sensitive as the phosphatase, it is considered a good candidate for an ancillary life-detection method.

In addition to the hydrolytic techniques described above for the Multivator, Lederberg and Leventhal (ref. 85) are investigating the use of semipermeable membranes to achieve separation of the smaller enzymatic breakdown products from a substrate. Another use for the semipermeable membrane might be the separation of labeled carbon dioxide from a radioactive substrate.

WOLF TRAP

The Wolf Trap, named for its designer, Wolf Vishniac (refs. 87 and 88), is based on the detection of two effects that micro-organisms have on a nutrient solution: change in pH, or acidity, of the solution; and change in light transmission, or turbidity, of the solution. Change in pH is detected by pH electrodes; change in turbidity is detected by a light-scattering technique. The rate of change of pH and turbidity provide information for the interpretation of acquired data.

The device, shown in figure 87, is designed to pick up dust samples and force them through a venturi into the nutrient chamber by use of a

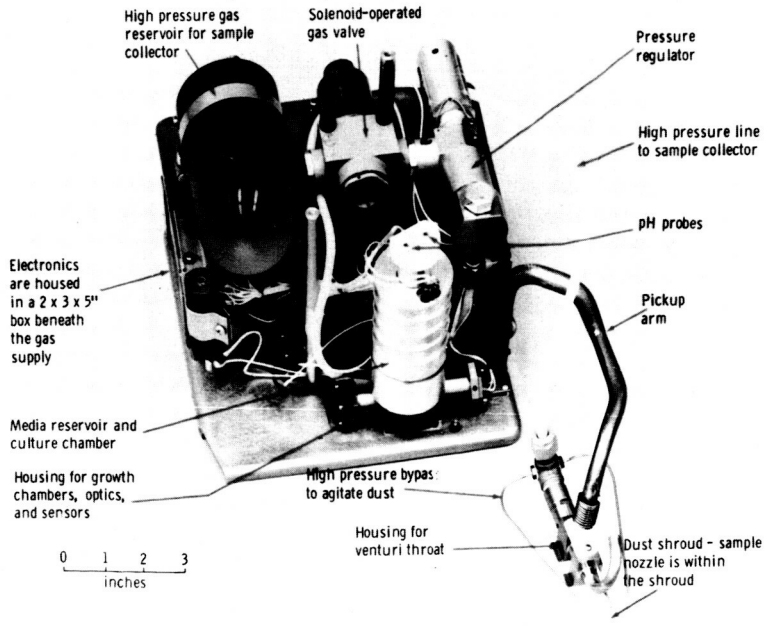

FIGURE 87.—Engineering breadboard model of Wolf Trap.

compressed gas. The instrument can detect a turbidity corresponding to 10^7 micro-organisms per milliliter and a change of 0.5 unit of pH.

Since Mars is not expected to have much oxygen in its atmosphere, growth media were developed for satisfactory metabolism of the major categories of anaerobic micro-organisms: (*a*) photosynthetic bacteria, (*b*) sulfate-reducing bacteria, (*c*) nitrate-reducing bacteria, (*d*) methane-forming bacteria, and (*e*) putrefactive bacteria, such as *Clostridium*. The media were either 0.2 percent yeast extract or 0.2 percent yeast extract, plus 0.3 percent glucose; they were adjusted to pH 7.0, and the culture tube and connecting parts were sterilized by heat before use.

By impacting test models on the laboratory floor to seek available bacteria, it was found that about 5 hours of time were required before changes in either pH or turbidity were noted for either medium; the medium supplemented with glucose evoked an earlier response than that of the yeast extract alone.

OPTICAL ROTATION

Since the ability to rotate the plane of polarized light is a property of many of the chemical compounds found in living systems, the design of instrumentation and techniques for the detection of optically active substances in extraterrestrial soils has been under development at Melpar, Inc. (ref. 89). Preliminary investigations with a Rouy-type polarimeter system (ratio of the difference to the sum) indicated that the problems of matching Glan prisms could not be overcome and the data could not be quantitative. A more suitable technique, a modification of a simple-ratio system (ratio of the difference to a constant), was developed and proven with a Cary Model 15 spectrophotometer and provided the basis for the design of a polarimeter to be used for the detection of extraterrestrial life. A schematic drawing of the optical system design for the flight prototype is given in figure 88.

A sample is placed between two polarizing filters, and plane-polarized light passes through the sample into the second filter which is rotated so that no light can penetrate. If the sample can rotate polarized light, some light will pass through the second, or analyzer, filter. The angle to which the analyzer must be rotated to restore the initial condition of the light leak is a measure of net optical rotation.

Evaluation of the optical activity of soil extracts and horse serum in solutions of varying pH led to the choice of 0.15 *N* NaOH as being the most suitable extraction system to be used with the flight-prototype polarimeter. A soil sample is delivered to the sample collection chamber in dry powder form; the inlet and outlet ports of the chamber are closed and the alkaline solution is injected and circulated (by means of a pneumatically driven double-end reciprocating pump) until the solution

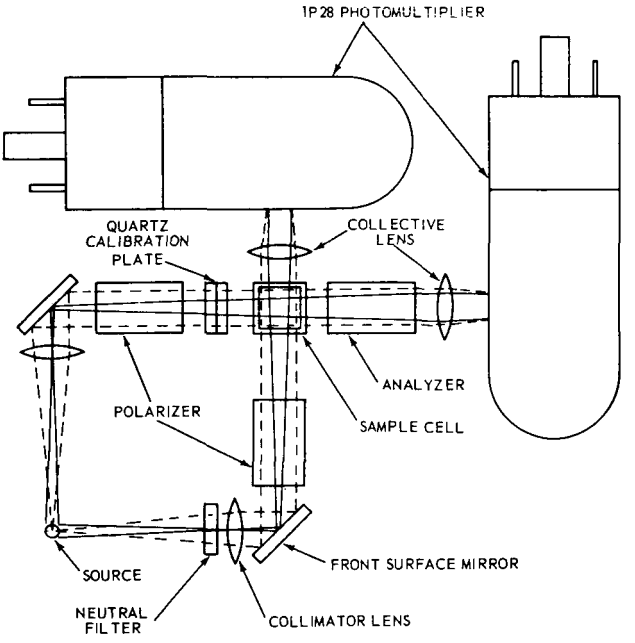

FIGURE 88.—Schematic of optical rotation device.

light transmission is reduced to some predetermined level. Then the pump is stopped and the analysis made. Detection of optical activity in 0.08 milligram/milliliter of dissolved soil components has been demonstrated (the optically active components have not been identified).

CATALASE ACTIVITY

A method of detecting micro-organisms by their catalase activity was investigated by Weetall, Weliky, and Vango (ref. 90) at JPL. Catalase is an enzyme which catalyzes the decomposition of hydrogen peroxide to water and oxygen:

$$2H_2O_2 \rightarrow 2H_2O + O_2$$

It is found universally in plants, higher animals, and in most algae and fungi. To determine the concentrations of intracellular catalase which one might find in various desert soils, the quantity of enzyme found in an average bacterium is estimated as follows, based on values found in the literature for pure cultures. If 10^{-9} to 10^{-10} moles of heme are found in 1 milligram of organisms and up to 10 percent can be catalase, then 1 milligram of organisms contains 10^{-10} to 10^{-11} moles of catalase.

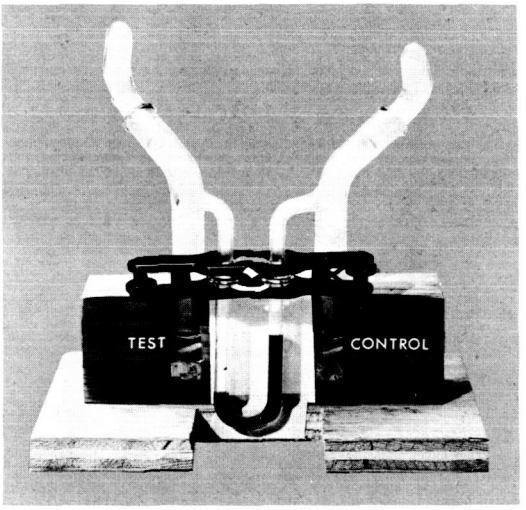

FIGURE 89.—Detection of micro-organisms in soil by their catalase activity.

The first experiments were carried out in the simple apparatus shown in figure 89. Soil samples of equal weight were placed in the bottom of each test tube. Buffer was added to the control side, and the enzyme muramidase was added in an equal volume of buffer to the sample side. The enzyme muramidase hydrolyzes muramic acid, a constituent of the cell walls of many bacteria and algae. After a 20-minute time interval for reaction of the muramidase, the upper reagent vessels were turned to allow hydrogen peroxide solution to pour into the test tubes. If catalase was released from the bacteria by the muramidase, excess oxygen from the hydrogen peroxide decomposition increased the pressure on that side, causing the liquid in the U-tube to move. Several desert soils showed a reasonable correlation between catalase activity and bacterial content as measured by plate count; a garden soil had catalase activity many orders of magnitude greater.

An apparatus with more sensitive differential manometers was fabricated so that smaller pressures could be read accurately; this permitted detection of 10^{-16} moles active enzyme, producing 9 μl of oxygen in 40 minutes. Based on the amount of catalase expected per micro-organism, the method can detect 10^3 to 10^4 micro-organisms in a relatively short time. The rate of oxygen production by various concentrations of enzymes is illustrated in figure 90.

CURRENT WORK AT AMES RESEARCH CENTER

Life-detection techniques currently under investigation at Ames Research Center have been described by Oyama (ref. 91); the information provided by Oyama is based on preliminary unpublished data.

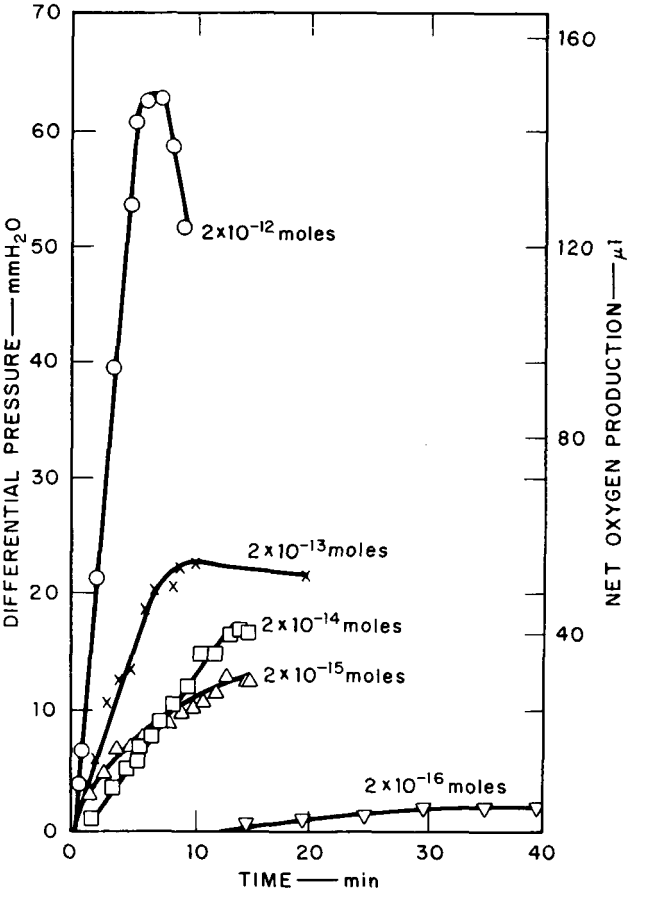

FIGURE 90.—Oxygen production by various concentrations of enzymes.

The development of the techniques is proceeding along two primary methods of approach. One is to measure some parameter vital to the composition, physical structure, or organization of the life process; the other is to detect the process of physiological functions of living substances. Many techniques are under study for the determination of proteins, nucleic acids, and polysaccharides which are distributed in all known living forms. For example, it is not known whether the amino acids which may be present on Mars would have levorotatory or dextrorotatory configurations, compared with terrestrial amino acids which have levorotatory configurations in all structurally and functionally important proteins. Although polarimetry cannot distinguish the stereoisomeric form of a particular molecule in a mixture of optically active substances, D and L amino acids have been separated by a gas-

chromatography technique which uses the physical differences inherent in diastereoisomers. Thus, the asymmetric secondary butyl ester derivatives of amino acids are separable if the amino group is protected as the trifluoroacetyl derivative. Specially developed columns with optically active stationary phases have been used to separate the secondary butyl derivative as the free amine.

For organic compound analysis on Mars, it is necessary to determine the amount of organic material that may occur in the inorganic matrix. One method under study at Ames uses molecular-sieve separation of macromolecules from soils. Another is involved with pyrolysis in an inert atmosphere and the analysis of pyrolyzates with a hydrogen flame detector. Pyrolysis of microbial samples results in a number of compounds which can be separated by an appropriate gas-chromatography system. The chromatogram of a single type of organism is highly reproducible when the optimum pyrolysis conditions are used. Chromatograms of a number of organisms show both similar and dissimilar retention peaks. The dissimilarities are most noticeable between widely separated taxonomic groups. In fact, pyrolysis gas chromatography is being developed as a valuable technique for chemotaxonomic classification.

To overcome the difficulties of using soil-extract nutrient with life-detection systems, several techniques were developed according to Oyama:

> These are (1) the technique of measuring optical changes surrounding soil particulates on semisolid media, (2) a dilution technique whereby the soil particulates are diluted or washed out at a rate less than that of the rate of growth, and (3) the technique of physically separating the soil sample from the growth medium proper by a porous plate. In the latter technique, which appears to be the preferred one, the soil is held on a porous stage and separated in and above the fluid medium.

As the fluid wets the porous plate by capillary action, the surface of the soil contiguous with the porous plate is wetted. Growth proceeds through the porous plate without migration of the particulate matter in the soil. Thus, growth is obtained in the body of the medium without the "noise" which is normally part of the soil matrix.

The porous-plate method for measuring growth is adaptable to a number of techniques to measure other biological phenomena. Among these are changes in gas composition that generally accompany microbial activity. In addition, other chemical and physical changes are measurable with the use of porous-plate methods. Refractive index, viscosity, optical spectra, and optical activity are changes currently being investigated as potential ancillary monitors.

Two identifying characteristics are found in the metabolic processes of all living systems. First, measurable thermal output is produced by the metabolic process of the living system. The profile of this caloric

output is distinguishable from ordinary heat generation as a result of chemical reaction. Heat-output measurement by microcalorimetry may be a desirable technique to monitor the metabolic activity of living systems. Even the sparsest desert-soil samples produce a measurable heat output in the presence of a nutrient medium. The second indication of metabolism is the presence of a porphyrin structure in all living systems. The porphyrin structure is the base substance of structures such as chlorophylls, cytochromes, and hemes. Currently, Ames Research Center is also concerned with the measurement of physical and chemical characteristics of porphyrins that can be isolated from organisms compatible with the Martian environment.

Summary

This survey combines within a single volume a review of NASA contributions to the design, development, and application of instrumentation for analytical chemistry. It also demonstrates the ingenuity of NASA analytical chemists in their effort to detect and to comprehend the nature of substances existing on distant planets without leaving their laboratories.

Some of the NASA developments discussed in this survey have now been incorporated in commercially available instruments; other developments reported by industrial concerns under contract to NASA will no doubt find use in commercial instrumentation. On the other hand, a number of designs and techniques noted in this survey are concepts which will require further development before they can be incorporated in devices suitable for a highly competitive market. Almost all of the applications of analytical instrumentation included in this survey are definite advances in the technology of analytical chemistry and will no doubt prove useful to other chemists.

NASA work on ultraviolet spectroscopy has been spearheaded by the necessity of detecting ultraviolet radiation in space and because it provided a definitive analysis of stellar and planetary atmospheres. The need for selective and more sensitive methods for detecting ultraviolet radiation has resulted in improved fabrication techniques for photomultiplier tubes and a novel ceramic photoionization-chamber detector which is now available commercially; although intended for rocket astronomy, the chamber may also find use as a reference standard for laboratory instruments. A vacuum ultraviolet polarizer and analyzer has been used experimentally by NASA for the study of crystal structures, but it seems to be adaptable to the examination of solid-state materials and in techniques for the optical pumping of lasers. The special accessories and fixtures for ultraviolet instrumentation developed by NASA merit consideration by organizations using such instruments and should be candidates for development by manufacturers. The ultraviolet air-density meter may be particularly useful for flight testing of aircraft and for use on meteorological sounding rockets. The availability of an ultraviolet recording microspectrophotometer should be welcomed by medical researchers and by analytical chemists who must work with small samples.

The applications of ultraviolet and J-band absorption techniques to the detection of protein constituents in waters and soils (indicative of living organisms) will be of inestimable value to medical research and for the protection of public health, particularly when it is necessary to detect traces of materials which may promote or destroy life.

The detection of infrared radiation is as important to the meteorologist as infrared absorption is to the analytical chemist. NASA work in the detection of infrared energy has led to the development of a dielectric bolometer, instrumentation for determining the heat balance of Earth and other planets, a telescope for measuring infrared radiation from distant planets, and a submillimeter interference spectrometer; all of these may have direct application to the acquisition of meteorological data from Earth, aircraft, and spacecraft which lead to better weather forecasts and thus better management of the flow of national products. The accuracy of such devices may be calibrated by a monochromator developed under NASA sponsorship. Although some forms of infrared microscopes are commercially available, patent application has been made for a fast-scan system which can substantially increase the utility of this form of microscopy.

The application of infrared absorption techniques to the identification of rocks and rock surfaces performed under NASA sponsorship has reached the stage where it can be recommended as a laboratory technique. Moreover, since the vagaries of mineral composition have defied specific classification, infrared data for laboratory specimens may well be the forerunners of a more positive categorization of minerals and their constituents.

The restrictions of power and volume requirements for space exploration have necessitated the miniaturization of X-ray spectrometers; these instruments are an important class of analytical tool because they provide diagnostic information on the structure of crystals. Portable X-ray spectrometers have been developed for the national space program, but they are destined to be used on Earth by geological and geochemical expeditions to locate minerals of industrial importance. NASA studies of the application of X-ray techniques to the determination of the silicate content of rock glasses form an important contribution to the basic technology of mineralogy and analytical chemistry.

The nondestructive analysis of particulate matter and solid surfaces by α-particle scattering has not been used widely, chiefly because of the unwieldy equipment required. Miniaturization of the equipment and ready availability now make it possible to suggest its employment as a process monitor for the ceramics and glass industries, as well as an exploratory tool for fundamental studies in surface chemistry.

Neutron-activation analysis facilities are usually complex and expensive. Results of work in NASA programs suggest that a miniaturized neutron-activation instrument will serve a useful purpose in such things as water-pollution control and drug and food control where samples can be generous and allowable limits for elemental contaminants are in the parts-per-billion range.

Miniaturized mass spectrometers have already found their way into the commercial market as residual gas analyzers, and a laboratory model of the sputter-ion source mass spectrometer for solids as developed for NASA is now available from the Geophysics Corp. of America. The instrument permits analysis of solids, such as semiconductors, thin films, and alloys, and has a sensitivity for elements in concentrations of parts per million or less.

The application of gas chromatography to space exploration has required modifications to improve the construction and operation of automated models, to increase the reliability of electronic circuitry, and to provide efficient separation of compounds in complex mixtures. Manufacturers of gas chromatographs should be particularly interested in NASA developments because they suggest valuable routes for producing more reliable automated equipment for use on Earth.

The application of pyrolytic gas-chromatography techniques by NASA analytical chemists to the detection of micro-organisms has generated information which supplements available data obtained with abiogenic materials. These techniques will be of particular interest to laboratories engaged in health and sanitation services and may prove more rapid than classical procedures of inoculation and incubation for identification or classification of the lower forms of life.

The compilation of gas chromatographic and mass spectral data for terpanes is a definite contribution to the working tools of the analytical chemist.

The specific gas analyzers which are discussed in this survey employ basic physicochemical principles and are designed to measure trace quantities of gases at atmospheric or reduced pressures. Since many manufacturing concerns are involved as NASA contractors, it is certain that significant developments will be incorporated into commercial products.

The transistorized ionization-gage control unit was one of the forerunners of similar modern solid-state devices. The technique for calibration of gages at pressures as low as 10^{-13} torr should be of interest to both manufacturers and vacuum-system engineers. The method reported for increasing the range and precision of the classical McLeod gage may induce manufacturers to offer the magnetic-sphere valve as an accessory.

The techniques described in the survey for calibrating a residual gas analyzer or a leak tester by the permeation of gas through a polymeric diaphragm should be of interest to physical chemists as well as to manufacturers of mass spectrometers. In view of the increasing availability of simple, low-cost mass spectrometers, the permeability cell for mass spectrometers may find use in those organizations which are interested in permeability studies, such as pressure-vessel manufacturers, gasket, seal, and diaphragm manufacturers, propellant manufacturers, and the Technical Association of the Pulp and Paper Industry. The polymer-screening apparatus, which provides for the rapid determination of weight loss and volatile condensable material (VCM), should be of interest to the polymer industry, particularly as a quality-control measure.

Life-detection techniques involve the use of many standard analytical procedures which have been or will be miniaturized and automated. At first, laboratory instrumentation is used for exploratory work; additional work involves the evaluation of miniaturized laboratory models. For example, tracing radioactive carbon 14 is not new to scientists studying metabolic processes; however, the configuration for Gulliver has required the development of automated sampling, handling, and recording techniques, as well as a universal medium; the electrometric system Marbac has required similar development. The design of the Multivator is based on the miniaturization and automation of spectrophotometric procedures; an important outcome of this laboratory work was the observation of the lack of correlation between phosphatase and aminopeptidase enzymes in soils. The Wolf Trap provides a miniaturized and automated version of pH and turbidimetric measurements. The work with polarimetry has been concerned with the development of a suitable extraction and handling system for soil organisms which might be present on planetary surfaces, instrument development has not been completed. The evaluation of a technique for determining organisms by their catalase activity may provide a new technique for bacteriological surveys.

Current work in life detection at Ames Research Center is concerned with gas-chromatography techniques, porous-plate techniques, calorimetry, and the detection of porphyrin structures, which insures continuing contributions to analytical chemistry.

In general, the life-detection techniques are not new; however, the various approaches, development of media, and exploratory results will be of great interest to bacteriologists, virologists, and biochemists, as well as laboratories concerned with health and sanitation.

References

1. DUNKELMAN, L.: Ultraviolet Photodetectors. J. Quant. Spectr. Radiative Transfer, vol. 2, 533, 1962.
2. SOMMER, A. H.: Spectrally Selective (Solar Blind) UV Photomultipliers With Fluoride Windows. Rev. Sci. Instr., vol. 32, 356, 1961.
3. STOBER, A. K.; SCOLNIK, R.; and HENNES, J. P.: A Vacuum Ultraviolet Photoionization Detector. Appl. Optics, vol. 2, 735, 1963.
4. CHIN, E.: Goddard Space Flight Center, Private Communiction, Dec. 17, 1965.
5. WALKER, W. C.: Pile-of-Plates Polarizer for the Vacuum Ultraviolet. NASA TMX-55022, 1964.
6. AXELROD, N. N.: A Spectrophotometric Attachment for the Vacuum Ultraviolet. J. Opt. Soc. Am., vol. 51, 899, 1961.
7. FASTIE, W. G.: Instrumentation for Far Ultraviolet Rocket Spectrophotometry. NASA TN D-2250, 1964.
8. VAN ORNUM, D. G.: Investigative Study Along With Design and Development of an Ultraviolet Air Density Meter. Plasmadyne Corp., Final Rept., NASA Contracts NAS5-427 and NAS5-2184, 1963.
9. WOLKEN, J. J.: Microspectrophotometric Instrumentation for the Study of Pigments and Organic Molecules Within Living Cells. Univ. of Pittsburgh School of Med., Semiannual Status Rept., NASA CR-55521, 1963.
10. NELSON, S.: Research on the Detection of Extraterrestrial Life by Ultraviolet Spectrophotometry. Melpar, Inc., Final Rept., NASA CR-55655, 1964.
11. KAY, R. E.: Experimental Studies for the Detection of Protein in Trace Amounts. Ford Motor Co., Final Tech. Rept., NASA CR-50385, 1963.
12. JELLY, J. E.: Molecular Nematic and Crystal States of 1:1 diethyl ψ-cyanine chloride. Nature, vol. 139, 631, 1937.
13. HANEL, R. A.: The Dielectric Bolometer, A New Type of Thermal Radiation Detector. NASA TN D-500, 1960.
14. HANEL, R. A.: A Low-Resolution Unchopped Radiometer for Satellites. NASA TN D-415, 1961.
15. KAPLAN, L. D.: Interference of Atmospheric Structure From Remote Radiation Measurements. J. Opt. Soc. Am., vol. 49, 1004, 1959.
16. DREYFUS, M. G.; AND HILLEARY, D. T.: Satellite Infrared Spectrometer. Aerospace Eng., Feb. 1962, p. 42.
17. JARRELL, R. F.: Stigmatic Plane Grating Spectrograph With Order Sorter. J. Opt. Soc. Am., vol. 45, 259, 1955.
18. FASTIE, W. G.: A Small Plane Grating Monochromator. J. Opt. Soc. Am., vol. 42, 641, 1952.
19. WESTPHAL, J. A.; MURRAY, B. C.; AND MARTZ, D. E. An 8–14 Micron Infrared Astronomical Photometer. Appl. Optics, vol. 2, 749, 1963.
20. HENDERSON, B. D.; AND ZERUCHA, J.: Infrared Spectrometer Calibration Monochromator Study. Beckman Instruments, Inc., Final Rept., NASA CR-61, 1964.
21. RIVERS, W. K.: A Submillimeter Interference Spectrometer. Georgia Inst. of Tech., NASA CR-56839, 1964.

22. Fast Scan Infrared Detection and Measuring Instrument. Raytheon Co., NASA CR-56839, 1965.
23. LYON, R. J. P.: Evaluation of Infrared Spectrophotometry for Compositional Analysis of Lunar and Planetary Soils. NASA TN D-1871, 1963. (See also: Lyon, R. J. P., Econ. Geol., vol. 60, 715, 1965.)
24. LYON, R. J. P.: Minerals in the Infrared. Stanford Res. Inst., 1962.
25. Lunar X-Ray Diffractometer. Philips Electronic Instruments, NASA CR-57976, 1964.
26. METZGER, A.: An X-Ray Spectrograph for Lunar Surface Analysis. NASA CR-609340, 1964.
27. METZGER, A.: A Nondispersive X-Ray Spectrometer for Extraterrestrial Geochemical Analysis. JPL, Space Programs Summary 37-31, vol. IV, Feb. 28, 1965, p. 273.
28. WYCKOFF, R.; AND DAVIDSON, F: Windowless Tubes for X-Ray Spectroscopy. Rev. Sci. Instr., vol. 34, 572, 1963.
29. Jet Propulsion Laboratory, Space Programs Summary 37-20, vol. VI, Apr. 30, 1963, p. 96. (See also JPL TR 32-515, July 1963.)
30. NASH, D. B.: Results of X-Ray Diffraction Analysis of Proton-Irradiated Rock Powders. JPL, Space Programs Summary 37-30, vol. IV, Dec. 31, 1964, p. 178.
31. SNYDER, C. W.; ET AL.: A Magnetic Analyzer for Charged-Particles from Nuclear Reactions. Rev. Sci. Instr., vol. 21, 852, 1950.
32. RUBIN S.; PASSELL, T. O.; AND BAILEY, C. E.: Chemical Analysis of Surfaces by Nuclear Methods. Anal. Chem., vol. 29, 736, 1957.
33. SEMMLER, R. A.; ET AL.: Application of Alpha-Particle Scattering to Chemical Analysis. Univ. of Chicago, AEC No. C00-712-89, Oct. 1964.
34. DEISLER, P. F., JR.; MCHENRY, K. W., JR.; AND WILHELM, R.: Rapid Gas Analyzer Using Ionization by Alpha Particles. Anal. Chem., vol. 27, 1366, 1955.
35. GRAVEN, W. M.: Ionization by Alpha-Particles for Detection of the Gaseous Components in the Effluent From a Flow Reactor. Anal. Chem., vol. 31, 1197, 1959.
36. TURKEVICH, A.: Chemical Analysis of Surfaces by Use of Large-Angle Scattering of Heavy Charged Particles. Science, vol. 134, 672, 1961.
37. PATTERSON, H. H.; ET AL.: Chemical Analysis of Surfaces Using Alpha Particles. J. Geophys. Res., vol. 70, 1311, 1965.
38. LOOMIS, A. A.: Interpretation of Lunar Alpha-Scattering Data. J. Geophys. Res., vol. 70, 3841-3849, 1965.
39. MARSHALL, J. H.; AND FRANZGROTE, E. J.: Analysis of Martian Atmosphere by Alpha-Particle Bombardment. JPL, Space Program Summary 37-26, vol. IV, Apr. 30, 1964, p. 148.
40. FITE, L. E.; STEELE, E. L.; AND WAINERDI, R. E.: Texas A. & M., NASA Ann. Rept., 1963.
41. FITE, L. E.; ET AL.: Investigations in Automated Activation Analysis. Texas A. & M., TEEES-2671-2, TEEES-E-63-64, Nov. 1962.
42. MENON, M. P.: An Investigation of Computer-Coupled Automatic Remote Activation Analysis for Lunar Surface Analysis. NASA CR-63059, 1965.
43. Instrumentation of Lunar Compositional Analysis Study Program. Well Surveys, Inc., Final Rept. to JPL, Dec. 15, 1960.
44. METZGER, A. E.: Some Calculations Bearing on the Use of Neutron Activation for Remote Compositional Analysis. JPL, TR-32-286, Aug. 5, 1962.
45. TROMBKA, J. I.: Least-Square Analysis of Gamma-Ray Pulse Height Spectra. JPL, TR 32-373, Dec. 15, 1962.
46. SPENCER, N. W.; AND REBER, C. A.: A Mass Spectrometer for an Aeronomy Satellite. W. Priester, ed., Space Research III: Proc. of the Third International Space Science Symposium, Interscience Publishers, 1962, p. 1151.

47. HERZOG, R. F.: Planetary Aeronomy III: Determination of Atmospheric Parameters by the Use of Rocket-Borne Mass Spectrometers. Geophysics Corp. of America, NASA CR-12-9, 1963.

48. HERZOG, R. F. K.; ET AL.: Solids Mass Spectrometer. GCA Corp., Final Rept., NASA Contract NASw-839, Feb. 1965.

49. MEADOWS-REED, E.; AND SMITH, C. R.: Mass Spectrometric Investigations of the Atmosphere Between 100 and 227 Kilometers Above Wallops Island, Virginia. J. Geophys. Res., vol. 69, 3199, 1963.

50. BRUBAKER, W. M.: Study Directed Toward Selection of Apparatus for Analysis of Lunar Crust and Atmosphere. Bell & Howell Res. Center, Summary Rept., NASA CR-56540, 1963.

51. KENDALL, B. R. F.; ET AL.: Analysis of the Lunar Surface and Atmosphere by Mass Spectrometry. Nuclide Corp., Summary Rept., NASA CR-56552, 1964.

52. BIEMANN, K.; AND MCCLOSKEY, J. A.: Mass Spectra of Organic Molecules II: Amino Acids. J. Am. Chem. Soc., vol. 84, 3192, 1962.

53. BIEMANN, K.: The Detection and Identification of Organic Matter by Mass Spectrometry. MIT, 2nd and 3rd Semiannual Rept., NASA CR-50678, 1963.

54 OYAMA, V. I.; VANGO, S. P.; AND WILSON, E. M.: Applications of Gas Chromatography to the Analyses of Organics, Water, and Adsorbed Gases in the Lunar Crust. JPL, TR 32-107, Apr. 1961.

55. WILHITE, W. F.: The Development of the Surveyor Gas Chromatograph. JPL, TR 32-425, May 1963.

56. CHAUDET, J. H.: Gas Chromatographic Instrumentation for Gas Analysis of Martian Atmosphere. Melpar, Inc., Final Rept. (II), NASA CR-59773, 1962.

57. LIPSKY, S. R. (Yale University); BENTLEY, K.; BOWMAN, L.; JOSIAS, C.; MERTZ, H.; AND WILHITE, F.: Mariner B 1966 Mission: Analysis of the Atmosphere of Mars by Gas Chromatography Instrumentation. Proposal to JPL by S. R. Lipsky, Nov. 15, 1963.

58. MARSHALL, J. H.: An Automatic Scale Factor Device for Use With Spacecraft Electrometers. JPL, Space Programs Summary 37-23, vol. IV, Oct. 31, 1963, p. 245.

59. BOWMAN, L.; ET AL.: Gas Chromatograph Instrument Development. JPL, Space Programs Summary 37-20, vol. IV, Apr. 30, 1963, p. 169.

60 MARSHALL, J. H.: A Capacitor Storage Scheme for Gas Chromatograph Detector Quiescent Current Compensation. JPL, Space Programs Summary 37-24, vol. VI, Dec. 31, 1963, p. 213.

61. JOSIAS, C.; BOWMAN, L.; AND MERTZ, H.: A Gas Chromatograph for the Analysis of the Martian Atmosphere. JPL, Space Programs Summary 37-27, vol. IV, June 30, 1964, p. 85.

62. BENTLEY, K. E.; ET AL.: Detection of Life-Related Compounds on Planetary Surfaces by Gas Chromatography-Mass Spectrometry Techniques. JPL, TR 32-713, Aug. 30, 1965.

63. OYAMA, V. I.: Use of Gas Chromatography for Detection of Life on Mars. Nature, vol. 200, 1058, 1963.

64. MEINSCHEIN, W. G.: Development of Hydrocarbon Analysis as a Means of Detecting Life in Space. Esso Research Engineering Co., Ann. Rept., NASA CR-53096, 1964.

65. COLLINS, D. J.; AND HOENIG, S. A.: Chemisorption Detector for Oxygen. Rev. Sci. Instr., vol. 35, 15, 1964.

66. HALPERT, G.; ET AL.: Analysis for Oxygen by Gas-Phase Polarography at Low Temperatures and Low Pressures: A Prototype Assembly. Rev. Sci. Instr., vol. 35, 950, 1964.

67. NASA Tech Brief No. 65–10066, Fuel Cell Serves as Oxygen Level Detector, 1965.
68. EISENSTADT, M. M.; AND HOENIG, S. A.: Chemisorption Detector for Hydrogen. Rev. Sci. Instr., vol. 36, 66, 1965.
69. MICHAELS, P. A.: Design, Development, and Prototype Fabrication of an Area Hydrogen Detector. Bendix Res. Lab., Summary Rept., NASA CR–59975, 1964.
70. BUSH, W. H.: Carbon Dioxide Measuring Systems for Manned Spacecrafts. J. Aerospace Med., Oct. 1964, p. 951.
71. PINTAR, R. R.: Ruggedized Infrared Carbon Dioxide Analyzer. Beckman Instruments, Inc., Final Rept., NASA CR–53359, 1963.
72. MACCREADY, P. B., JR.: Moisture Analyzer for Martian Atmosphere. Meteorology Res., Inc., Final Rept., NASA CR–56454, 1962.
73. HOENIG, S. A.; ET AL.: Detection Techniques for Tenuous Atmospheres. Univ. of Ariz., Third Six-Month Rept., NASA CR–60278, 1964.
74. BENTON, H. B.: Small, Lightweight Ionization Gauge Control Circuit. Rev. Sci. Instr., vol. 30, 887, 1959.
75. FEAKES, F.; TORNEY, F. L., JR.; AND BROCK, F. J.: Gauge Calibration Study in Extreme High Vacuum. Nat. Res. Corp., NASA CR–167, 1965.
76. KREISMAN, W.: Extension of the Low Pressure Limit of McLeod Gauges. Geophysics Corp. of America, Final Rept., NASA CR–52877, 1963.
77. NASA Tech Brief 65–10224, Heater Decomposes Oil Backstreaming From High-Vacuum Pumps. Aug. 1965.
78. MURACA, R. F.; ET AL.: Investigation of the Space Storability of Pressurizing Gases. Stanford Res. Inst., NASA Contract NAS7–105, Rept. No. 2, Aug. 1962.
79. CARUSO, S. V.: Calibration of Diatron-20 Residual Gas Analyzer for Use in High Vacuum. NASA TMX–51927, 1962.
80. MURACA, R. F.; ET AL.: Polymers for Spacecraft Hardware—Materials Specifications and Engineering Information. Stanford Res. Inst., NASA Contract JPL–950745, Interim Rept. No. 2, Mar. 15, 1966.
81. LEVIN, G. V.; ET AL.: Gulliver, an Experiment for Extraterrestrial Life Detection and Analysis. Presented at COSPAR, Space Science Symposium, Warsaw, Poland, June 1963, NASA CR–55511.
82. LEVIN, G. V.; ET AL.: Radioisotopic Biochemical Probe for Extraterrestrial Life. Resources Res., Inc., 2d Ann. Rept., NASA CR–55318, 1963.
83. LEVIN, G. V.; ET AL.: Radioisotopic Biochemical Probe for Extraterrestrial Life. Hazleton Lab., Inc., Prog. Rept., NASA CR–60709, 1964.
84. ELLIS, G. E.: Study of Extraterrestrial Life Detection Concept. The Marquardt Corp., NASA CR–62003, 1964.
85. LEDERBERG, J.; AND LEVENTHAL, E.: Cytochemical Studies of Planetary Microorganisms, Explorations in Exobiology. Stanford Univ. School of Med., Status Rept., NASA CR–51096, 1963.
86. HOCHSTEIN, L.: The Fluorometric Assay of Soil Enzymes. Stanford Univ. School of Med., NASA CR–50919, 1962.
87. VISHNIAC, W.: Extraterrestrial Microbiology. J. Aerospace Med., vol. 31, 678, 1960.
88. VISHNIAC, W.: Development of a Life Detector for Planetary Soils. Univ. of Rochester, Final Rept., NASA CR–56528, 1961.
89. Detection of Extraterrestrial Life, Method II, Optical Rotatory Dispersion. Melpar, Inc., Final Rept., NASA CR–55657.
90. WEETALL, H.; WELIKY, W.; AND VANGO, S. P.: Detection of Micro-organisms in Soil by Their Catalatic Activity. Nature, vol. 206, 1019, 1965.
91. OYAMA, V. I.: Ames Research Center, Private communication, Dec. 1965.

☆ U.S. GOVERNMENT PRINTING OFFICE: 1967—O 263-200